THE EUROPEAN
PHYSICAL JOURNAL C

Measurement of K_S^0 and Λ^0 production in $t\bar{t}$ dileptonic events in pp collisions at $\sqrt{s} = 7$ TeV with the ATLAS detector

ATLAS Collaboration[*]

CERN, 1211 Geneva 23, Switzerland

Abstract Measurements of K_S^0 and Λ^0 production in $t\bar{t}$ final states have been performed. They are based on a data sample with integrated luminosity of 4.6 fb^{-1} from proton–proton collisions at a centre-of-mass energy of 7 TeV, collected in 2011 with the ATLAS detector at the Large Hadron Collider. Neutral strange particles are separated into three classes, depending on whether they are contained in a jet, with or without a b-tag, or not associated with a selected jet. The aim is to look for differences in their main kinematic distributions. A comparison of data with several Monte Carlo simulations using different hadronisation and fragmentation schemes, colour reconnection models and different tunes for the underlying event has been made. The production of neutral strange particles in $t\bar{t}$ dileptonic events is found to be well described by current Monte Carlo models for K_S^0 and Λ^0 production within jets, but not for those produced outside jets.

Contents

[*] e-mail: atlas.publications@cern.ch

1 Introduction and motivation

Neutral strange particle production has been studied in collider experiments using e^+e^- [1–11], pp [12–19], $p\bar{p}$ [20–22], ep [23,24] and heavy-ion collisions [25,26], as well as in fixed-target experiments [27–40]. These measurements provide interesting tests of theoretical jet fragmentation functions [41] and can be used to validate and tune the values of empirical parameters used in the parton shower and fragmentation parts of the Monte Carlo (MC) models. Since the mass of the strange quark is comparable to the QCD scale parameter Λ_{QCD}, perturbative calculations cannot be performed. These models must be highly accurate to constrain the underlying event (UE) effects in the high transverse momentum (p_T) production investigated at the Large Hadron Collider (LHC). In particular the ratio $\gamma_s = s/u$, giving the suppression factor of strange to non-strange meson production in the hadronic final states, is measured to be larger in pp collisions than in e^+e^- annihilation. A review is given in Ref. [42].

It was suggested [43] that the suppression factor γ_s would be significantly larger, or even tend to unity, in nucleus–nucleus collisions because the many strings produced within the Lund fragmentation scheme in a limited phase space may interact, giving rise to the formation of 'colour ropes'. Recent data from RHIC [25,44] tend to support these ideas and show that neutral strange particle production is enhanced. In pp collisions at LHC energies, many overlapping strings due to multi-parton interactions are also expected to come into play, so that higher rates of strange meson and baryon production are expected [42]. This effect was confirmed recently by the ALICE [16] and CMS [15] collaborations.

The measurements presented in this paper are useful contributions for future determinations of $|V_{ts}|$. The prospects for directly measuring the CKM matrix element $|V_{ts}|$ are discussed in Refs. [45,46]. The idea is to measure the fraction of $pp \rightarrow t\bar{t} \rightarrow W^+bW^-\bar{s}(W^+sW^-\bar{b})$ in $t\bar{t}$ decays. Since this is small compared with the dominant background $pp \rightarrow t\bar{t} \rightarrow W^+bW^-\bar{b}$, a good understanding of neutral strange particle production inside b-jets in $t\bar{t}$ final states is needed for a future direct measurement of this matrix element.

Studies of neutral strange particle production at the LHC have been carried out using minimum-bias events at low luminosities [12–18]. The aim of this paper is to extend the studies to $t\bar{t}$ production, which is known to be a copious source of high-p_T jets, especially b-jets. In doing so, three cases are considered depending on whether the neutral strange particles are embedded in jets, with or without a b-tag, or not associated with any selected jet.

In current MC generators the production of neutral strange particles within jets in top quark decays exhibits little sensitivity to initial-state radiation effects, different choices of parton distribution functions (PDF) or UE effects. In contrast, neutral strange particle production outside jets is more sensitive to details of the parton shower's initial- and final-state radiation, the fragmentation scheme and multi-parton interactions (MPI). They are also very sensitive to the ratio γ_s of strange to up quarks.

This analysis was performed using a $t\bar{t}$ event sample collected with the ATLAS detector in the 2011 running period with pp collisions at $\sqrt{s} = 7$ TeV. These data are less affected by multiple pp interactions within the same (in time) or nearby (out of time) bunch crossings, or pile-up, than data collected later.

This paper is organised as follows. Section 2 gives a brief description of the ATLAS detector. Section 3 is devoted to the MC samples used. Section 4 explains the data sample and the event selection criteria. Section 5 is dedicated to the reconstruction and selection of neutral strange particles, as well as the background subtraction procedure. Section 6 shows the results at the detector level compared with MC generator simulations. Neutral strange particle production is studied in terms of distributions of transverse momentum, pseudorapidity, energy and multiplicity for the three cases stated above. Section 7 discusses the efficiency correction calculations and the statistical error propagation. Section 8 gives details of the main systematic uncertainties. Section 9 shows the results corrected to the particle level compared with the predictions of different MC models, thus checking the model-dependence of neutral strange particle production in these events. Finally, Sect. 10 presents a summary and conclusions.

2 The ATLAS detector

The ATLAS detector is described in detail in Ref. [47]. All of its subsystems are relevant for this analysis, including the inner detector (ID), the electromagnetic and hadronic calorimeters and the muon spectrometer.

The inner detector, located within a 2 T axial magnetic field, is used to measure the momentum of charged particles. Its η–ϕ coverage includes the full azimuthal range $-\pi \leq \phi \leq \pi$ and the pseudorapidity range $|\eta| < 2.5$.[1] The inner detector includes a silicon pixel detector (Pixel), a silicon microstrip tracker (SCT) and a transition radiation tracker (TRT). The calorimeter system covers the pseudorapidity range $|\eta| < 4.9$. The electromagnetic section, covering the region $|\eta| < 3.2$, uses liquid argon as the active material in barrel and endcap calorimeters with accordion-shaped electrodes and lead absorbers. The hadronic calorimeter system consists of a steel/scintillator-tile barrel calorimeter ($|\eta| < 1.7$) and a copper liquid-argon endcap ($1.7 < |\eta| < 3.2$). In addition, a forward calorimeter consisting of liquid argon with copper and tungsten for the absorbers extends the pseudorapidity coverage to $|\eta| = 4.9$. The muon spectrometer, located inside a toroidal magnetic field, provides triggering and muon tracking capabilities in the ranges $|\eta| < 2.4$ and $|\eta| < 2.7$ respectively. This allows identification of muons with momenta above 3 GeV and precision determination of the muon transverse momentum up to 1 TeV. In this analysis muons reconstructed in the muon spectrometer are matched with well-measured tracks from the inner detector.

The trigger system [48] uses three consecutive levels: level 1 (L1), level 2 (L2) and the event filter (EF). The L1 triggers are hardware-based and use coarse detector information to identify regions of interest, whereas the L2 triggers are based on fast online data reconstruction algorithms. Finally, the EF triggers use offline data reconstruction algorithms. For this analysis, events are required to pass a single-electron or single-muon trigger.

3 Monte Carlo event simulation

The MC generators used to describe particle production in pp collisions differ in the approximations used to calculate the underlying short-distance QCD process, in the manner parton showers are used to take into account higher-order

---

[1] ATLAS uses a right-handed coordinate system with its origin at the nominal interaction point (IP) in the centre of the detector and the z-axis along the beam pipe. The x-axis points from the IP to the centre of the LHC ring, and the y-axis points upward. Cylindrical coordinates (r, ϕ) are used in the transverse plane, ϕ being the azimuthal angle around the beam pipe. The pseudorapidity is defined in terms of the polar angle θ as $\eta = -\ln\tan(\theta/2)$.

effects and in the fragmentation scheme responsible for long-distance effects. The generated events were passed through a detailed GEANT 4 simulation [49] of the ATLAS detector [50].

The baseline $t\bar{t}$ MC sample was produced with the next-to-leading-order (NLO) generator POWHEGBOX (referred to hereafter as POWHEG) [51–53] for the matrix element calculation with the CTEQ66 NLO PDF. The parton shower and hadronisation processes were implemented using PYTHIA6 [54] with the CTEQ6L PDF [55]. PYTHIA6 orders the parton shower by p_T and uses the Lund string fragmentation scheme [56]. The parton shower and UE effects were modelled using a set of tuned parameters called the PERUGIA2011C tune [57]. Pile-up contributions were accounted for by generating events with PYTHIA6, using the AMBT2B minimum bias (MB) tune. These were then overlaid onto the signal events at detector level. The strangeness suppression factor γ_s was taken at its default value $\gamma_s = 0.3$ in the AMBT2B tune, while $\gamma_s = 0.2$ was used in the PERUGIA2011C tune. The latter was tuned to LEP data.

Additional MC samples are used to estimate the hadronisation model dependence of K_S^0 and Λ production. They are based on MC@NLO + HERWIG [58,59], which orders the parton showers by angular separation and uses the cluster hadronisation model [60] and CT10 NLO [61] PDFs. Multi-parton interactions were simulated using JIMMY [62] with the AUET2 tune, while pile-up effects were taken into account as in POWHEG+PYTHIA6. The parameter governing strangeness suppression in HERWIG is not γ_s, but the probability of producing an $s\bar{s}$-pair when the clusters are fragmented. This parameter was set at its default value, which is equal to that for the other light quarks. The suppression is then given by the s-quark mass in the non-perturbative gluon splitting $g \rightarrow s\bar{s}$.

The data, corrected for detector effects, are also compared with events from other MC generators at particle level, without detector MC simulation:

- SHERPA 2.1.1 [63], which uses a different approach than previous generators for the matrix element calculation up to NLO accuracy with the CT10 PDFs, as well as for the parton shower implementation, with cluster hadronisation. SHERPA uses $\gamma_s = 0.4$.
- POWHEG with the NNPDF3.0 NLO PDF set [64], interfaced to Pythia8 [65] with the NNPDF2.3 LO PDF set and the A14 tune [66] for the parton shower, hadronisation and UE modelling.
- POWHEG interfaced to HERWIG7 (v7.1) [67] with the NNPDF3.0 NLO PDF set and H7UE tune, as default, for the parton shower, hadronisation and UE modelling.
- MADGRAPH5 aMC@NLO generator (referred to hereafter as aMC@NLO) [68] interfaced to HERWIG7 as before.

Table 1 Summary of basic generator settings used to simulate the $t\bar{t}$ events

MC generator	ME order	PDF	UE tune
POWHEG + PYTHIA6	NLO	CTEQ66 NLO	PERUGIA2011C
MC@NLO + HERWIG	NLO	CT10 NLO	JIMMY-AUET2
SHERPA 2.1.1	NLO	CT10 NLO	SHERPA
POWHEG + PYTHIA8	NLO	NNPDF3.0 NLO	A14
POWHEG + HERWIG7	NLO	NNPDF3.0 NLO	H7UE
aMC@NLO + HERWIG7	NLO	NNPDF3.0 NLO	H7UE
ACERMC + PYTHIA6	LO	CTEQ6L	PERUGIA/ TUNEAPRO (with and w/o CR)

- The leading-order (LO) ACERMC generator [69] interfaced to PYTHIA6, with different tunes such as PERUGIA2011C or TUNEAPRO [70] for parton showering and hadronisation, as well as with different colour reconnection (CR) schemes.

Table 1 presents a summary of the different signal MC sample tunes used in this analysis.

Background samples were generated for the production of Z boson in association with jets, including heavy flavours, using the ALPGEN [71] generator with the CTEQ6L PDFs [55], and interfaced with HERWIG and JIMMY. The same generator was used for the diboson backgrounds, WW, WZ and ZZ, while MC@NLO was used for the simulation of the single-top-quark background in the Wt final state.

The MC simulated samples are normalised to their corresponding cross-sections, as described in the following. The $t\bar{t}$ signal is normalised to the cross-section calculated at approximate next-to-next-to-leading order (NNLO) using the HATHOR package [72], while for the single-top-quark production cross-section, the calculations in Ref. [73] were used. The Z plus jets cross-sections are taken from ALPGEN [71] with additional NNLO K-factors as given in Ref. [74].

The simulated events are weighted such that the distribution of the number of interactions per bunch crossing in the simulated samples matches that of the data. The size of the MC samples considered in this analysis exceeds that of the data sample by more than an order of magnitude.

4 Data sample and event selection

The data sample used in this analysis corresponds to an integrated luminosity of 4.6 fb^{-1}, collected in 2011. The uncertainty in the integrated luminosity is 1.8% [75]. The sample consists of data taken while all relevant subdetector systems were operating under stable beam conditions.

In order to reduce the jet activity from hadronic $W^\pm$ decay channels, the dileptonic $t\bar{t}$ decay mode is used in this analysis. Events in this decay mode were selected as described in Refs. [76,77], using a trigger based upon a high-p_T electron with a threshold of either 20 or 22 GeV, or a muon with $p_T(\mu) > 18$ GeV. Events are required to have at least one primary vertex, with five or more tracks with $p_T^{track} \geq 400$ MeV. If there is more than one primary vertex, the one with the largest $\sum p_T^2$ is chosen, where the sum is over the transverse momenta of tracks from the vertex.

Electron candidates are reconstructed from energy deposits in the calorimeter that are associated with tracks reconstructed in the ID. The candidates must pass a tight selection [78], which uses calorimeter and tracking variables as well as TRT information for $|\eta| < 2.0$, and are required to have transverse momentum $p_T(e) > 25$ GeV and $|\eta| < 2.47$. Electrons in the transition region between the barrel and endcap calorimeters are not considered. Muon candidates are reconstructed by searching for track segments in different layers of the muon spectrometer. These segments are combined and matched with tracks found in the ID. The candidates are re-fitted using the complete track information from both detector systems and are required to have a good fit for muons with $p_T(\mu) > 20$ GeV and $|\eta| < 2.5$.

The selected events are required to have exactly two isolated charged leptons (e or μ). At least one of them must match with the corresponding trigger object. For electron candidates, the isolation criterion requires that the transverse energy deposited around the electron in the calorimeter in a cone of size[2] $\Delta R = 0.2$ is below 3.5 GeV, excluding the electron energy cluster itself. For muon candidates, both the transverse energy in the calorimeter and the transverse momentum in the tracking detector around the muon in a cone of size $\Delta R = 0.3$ must be below 4 GeV. The track isolation is calculated from the scalar sum of the transverse momenta of tracks with $p_T > 1$ GeV, excluding the muon. Cosmic-ray muons are rejected by a veto on muon candidate pairs back-to-back in the transverse plane and with transverse impact parameter $|d_0| > 0.5$ mm relative to the beam axis [79]. The two isolated leptons are required to have opposite charges. For the ee and $\mu\mu$ channels, the invariant mass of the two leptons must be greater than 15 GeV, to reject background from low-mass resonances decaying into lepton pairs, and at least 10 GeV away from the Z boson mass.

Jets are reconstructed with the anti-k_t algorithm [80] with radius parameter $R = 0.4$. The input objects to the jet algorithm, for both data and detector-level simulation, are topological clusters of energy in the calorimeter [81]. These clusters are seeded by calorimeter cells with $|E_{cell}| > 4\sigma$, with

σ the RMS of the noise. Neighbouring cells are added and clusters are formed following an iterative procedure.

The baseline calibration of these clusters corrects their energy to the electromagnetic energy scale, which is established using test beam measurements for electrons, pions and muons in the electromagnetic and hadronic calorimeters [82–84]. Effects due to non-compensating calorimeter response, energy losses in dead material, shower leakage, and inefficiencies in energy clustering and jet reconstruction are taken into account. This is done by matching calorimeter jets with MC particle jets in bins of $|\eta|$ and p_T. The result is called the jet energy scale (JES), thoroughly discussed in Ref. [85]. It is different for b-jets and light-flavour jets since they have different particle compositions. More details and a discussion of JES uncertainties are given in Ref. [86]. The jet energy resolution (JER) and its uncertainties are discussed in Ref. [87].

The selected events are required to have at least two jets with $|\eta| < 2.5$ and $p_T > 25$ GeV. In addition, jets are required to have a jet vertex fraction [88], defined as the scalar transverse momentum sum of the tracks that are associated with the jet and originate from the hard-scatter vertex divided by the scalar sum of all associated tracks, greater than 0.75 in order to minimise pile-up effects. At least one of the jets must be identified as a b-tagged jet, using the multivariate MV1 algorithm [89] based on the reconstruction of secondary vertices and three-dimensional impact parameter information. The MV1 working point corresponds to a b-tagging efficiency of 70%, calculated using $t\bar{t}$ MC events with an average light-flavour mistag rate of 2%. Jets overlapping with an accepted electron are removed if the separation is $\Delta R < 0.2$. Electrons are removed if $0.2 < \Delta R < 0.4$. Muons are removed if their separation from a jet is $\Delta R < 0.4$.

The reconstruction of the direction and magnitude of the missing transverse momentum (E_T^{miss}) is described in Ref. [90] and begins with the vector sum of the transverse momenta of all jets with $p_T > 20$ GeV and $|\eta| < 4.5$. The transverse momenta of electron candidates are added. The contributions from all muon candidates and from all calorimeter clusters not belonging to a reconstructed object are also included. The missing transverse momentum is required to be $E_T^{miss} > 60$ GeV for the ee and $\mu\mu$ channels, and for the $e\mu$ channel the requirement is $H_T > 130$ GeV, where H_T is the scalar sum of the transverse momenta of the two leptons and the selected jets.

After applying these selection criteria, which are summarised in Table 2, a sample of 6926 $t\bar{t}$ candidate events is selected. MC studies indicate that the background contamination in the sample after event selection is $\sim 6\%$, dominated by single-top-quark events. The background contribution from Z boson production with the Z boson decaying leptonically, in association with jets (including heavy flavours $b\bar{b}$), is at the level of 1%. An additional source of

---

[2] Angular distance in the η–ϕ plane is defined as $\Delta R = \sqrt{(\Delta\eta)^2 + (\Delta\phi)^2}$.

Table 2 Summary of the event selection criteria for the analysis

Selection	ee	$\mu\mu$	$e\mu$
Leptons	Exactly 2 leptons, opposite-sign charge, isolated		
Electrons	$E_T > 25$ GeV, $|\eta| < 2.47$, excluding $1.37 < |\eta| < 1.52$		
Muons	$p_T > 20$ GeV, $|\eta| < 2.5$		
Jets	≥ 2 jets, $p_T > 25$ GeV, $|\eta| < 2.5$		
b-tagging	≥ 1 b-tagged jet at $\epsilon_b = 70\%$ with MV1		
m_{ll}	$|m_{ll} - 91$ GeV$| > 10$ GeV, $m_{ll} > 15$ GeV		None
E_T^{miss} or H_T	$E_T^{\mathrm{miss}} > 60$ GeV		$H_T > 130$ GeV

Table 3 Expected composition of the selected sample in terms of number of events (N_{evt}) and fractions (%) of different processes. Uncertainties are statistical only

Process	N_{evt}	Percentage [%]
$t\bar{t}$ dileptonic	6860 ± 80	93.9
Single top	300 ± 20	4.1
Z + jets	77 ± 9	1.1
Diboson	61 ± 8	0.9
Predicted	7300 ± 90	
Observed	6926	

background where one or more of the reconstructed lepton candidates are non-prompt or misidentified is found to be at the 1% level with a very large (50%) statistical uncertainty [76,91], and is not considered in this analysis. The expected composition of the sample is summarised in Table 3, where 'Diboson' includes the WW, WZ and ZZ contributions. The percentages for signal and background processes quoted in Table 3 are in agreement with those quoted in Ref. [91].

Figure 1 shows the distribution of jet multiplicity and the p_T spectra of all jets, b-tagged jets and non-b-tagged jets. The jet activity is indeed limited, as 94% of the selected events contain at most four jets. The shapes of the normalised distributions in data are in good agreement with the prediction given by the $t\bar{t}$ POWHEG + PYTHIA6 simulation only. The small contributions from processes other than $t\bar{t}$ are neglected in the following analysis.

MC studies show that 99% of the selected b-tagged jets correspond to particle level b-jets, while 28% of jets in the non-b-tagged sample are b-jets which are not tagged by the MV1 algorithm. These fractions are calculated by matching detector-level jets, b-tagged or not, to their corresponding particle-level jets, which are defined in Sect. 7. These fractions are found to be largely independent of whether non-$t\bar{t}$ backgrounds are considered or not. Furthermore, the purity of b-tagged jets is rather independent of jet p_T as shown in Figure 1(c).

5 K_S^0 and Λ reconstruction

5.1 Neutral strange particle reconstruction

Neutral strange hadrons are reconstructed in the $K_S^0 \rightarrow \pi^+\pi^-$ ($\Lambda \rightarrow p\pi^-$, $\bar{\Lambda} \rightarrow \bar{p}\pi^+$) decay mode by identifying two tracks originating from a displaced vertex, thus profiting from the long lifetimes of neutral K mesons (Λ baryons) with $c\tau_0 \approx 2.7$ cm ($c\tau_0 \approx 7.9$ cm).

Tracks are reconstructed within the $|\eta| < 2.5$ acceptance of the ID, as described in Refs. [92,93]. The K_S^0 (Λ) candidates are oppositely charged track pairs with the transverse momentum of the two-track system $p_T > 100$ (500) MeV. The tracks must have at least two hits in the Pixel or SCT detectors, and are fitted to a common vertex. For K_S^0 reconstruction, the pion mass is assumed for both tracks, while the proton and pion masses are assumed for the Λ case.[3] Further requirements on these candidates are given below, and Ref. [12] provides more details:

- The χ^2 of the two-track vertex fit is required to be less than 15 (with 1 degree of freedom).
- The transverse flight distance (R_{xy}) is defined to be the distance between the K_S^0 (Λ) decay point and either the secondary b-tagged vertex, when the K_S^0 (Λ) is contained in a jet with a b-tag, or the reconstructed primary vertex when the K_S^0 (Λ) is contained in a jet without a b-tag or is not associated with any selected jet. A requirement 4 mm $< R_{xy} < 450$ mm (17 mm $< R_{xy} < 450$ mm) ensures that the tracks are reconstructed inside the Pixel+SCT part of the ID tracker.
- The angle between the K_S^0 (Λ) momentum vector and the K_S^0 (Λ) flight direction (obtained from the line connecting the decay vertex to the primary vertex, or to the secondary vertex if the K_S^0 (Λ) is inside a b-jet) has to satisfy $\cos\theta_K > 0.999$ ($\cos\theta_\Lambda > 0.9998$).

---

[3] For Λ and $\bar{\Lambda}$ decays, the track with the higher p_T is assigned the proton mass and the other track is assigned the pion mass. In the following and due to the sample size, Λ refers to the sum of Λ and $\bar{\Lambda}$ particles.
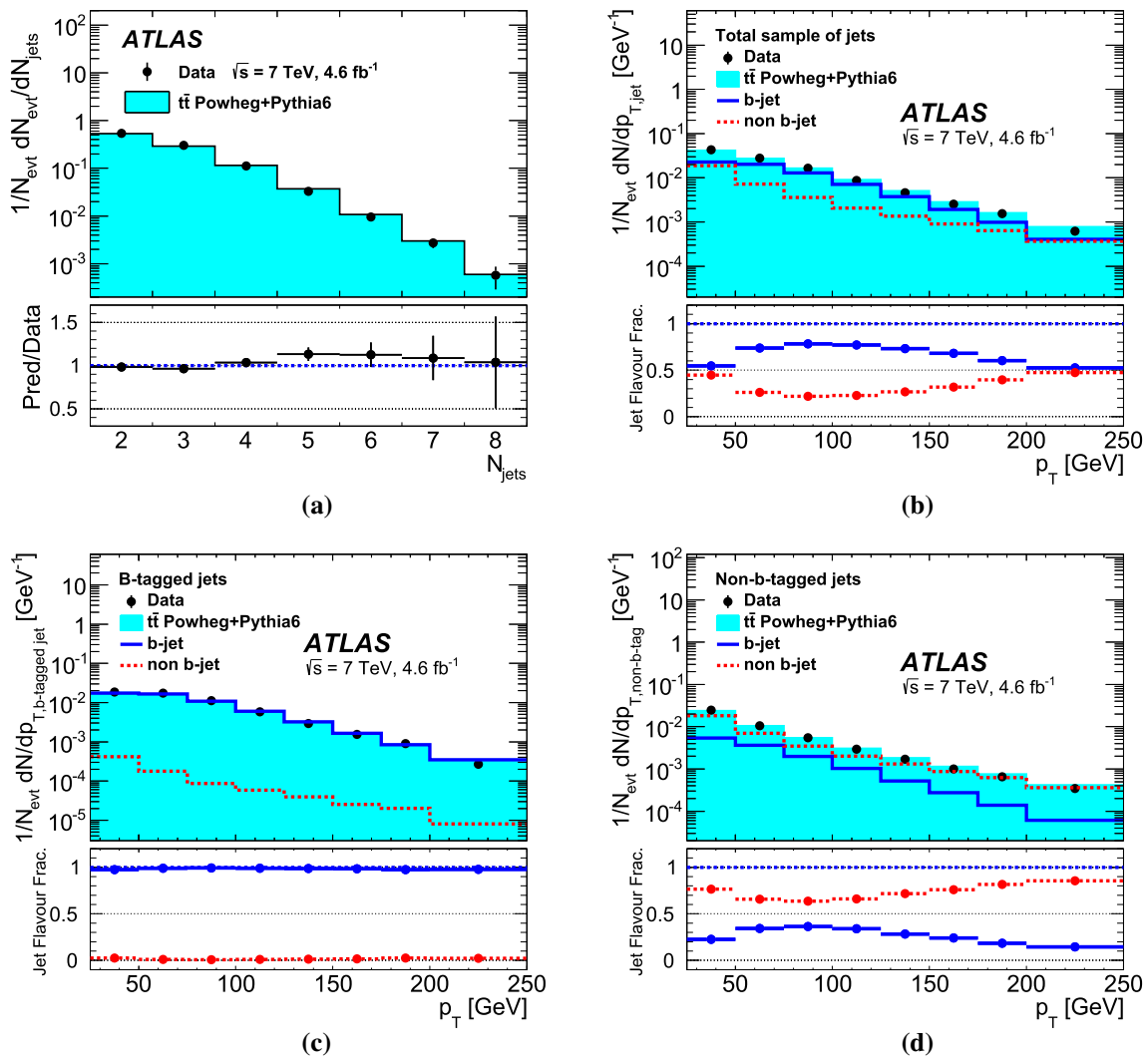
Fig. 1 Spectra of **a** jet multiplicity N_{jets} and **b** jet p_{T} in data compared with $t\bar{t}$ POWHEG + PYTHIA6 predictions at detector level. The expected b-jet flavour fractions for **c** b-tagged and **d** non-b-tagged jets as a function of jet p_{T} are also compared with data. These distributions are normalised to the total number of selected events in data or MC predictions

The K_S^0 (Λ) candidates that fulfil these conditions are then separated into three classes: candidates inside a b-tagged jet, inside a non-b-tagged jet and outside any jet. To this end the separation ΔR between the K_S^0 (Λ) line of flight and the jet axis in the η–ϕ plane is calculated. If $\Delta R < 0.4$, a K_S^0 (Λ) is associated with a jet. Otherwise it is classified as being outside any jet. There are no cases of a single K_S^0 (Λ) being inside two different jets.

The mass distributions for three classes of K_S^0 and the total sample of Λ candidates in data are shown in Fig. 2 compared with the POWHEG + PYTHIA6 predictions scaled to the total number of events in the data sample. The three K_S^0 mass distributions exhibit a resonance structure, centred around the nominal K_S^0 mass, with constant tails extending on both sides, indicating the presence of fake candidates, i.e.

track pairs which not being K_S^0 or Λ decay products have a mass in the signal mass ranges considered. The K_S^0 mass distributions are fairly well described by the nominal $t\bar{t}$ MC simulation except for the K_S^0 candidates not associated with jets, in which case the MC prediction underestimates the data by roughly 30%. Similar features are exhibited by the mass distribution of Λ candidates.

5.2 Background subtraction

In order to take into account the background due to fake candidates in the K_S^0 (Λ) mass distributions, a simple sideband subtraction in the reconstructed mass distribution is used. The signal range [480–520] MeV ([1106–1126] MeV) is considered for K_S^0 (Λ) production. The background sidebands are
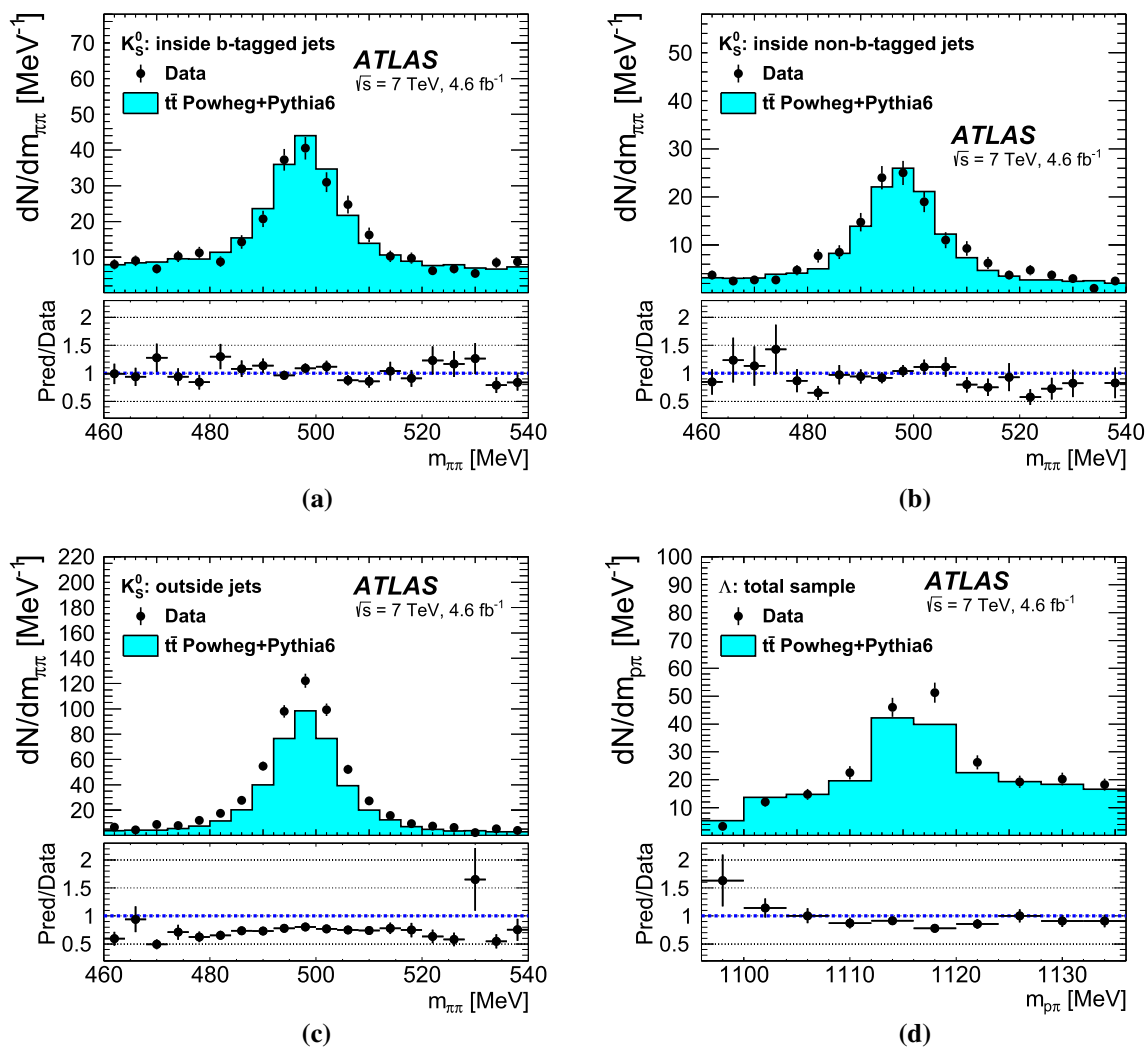
Fig. 2 K_S^0 and Λ candidate mass distributions in data compared with POWHEG + PYTHIA6 simulation. Three classes are presented for K_S^0: **a** inside b-tagged jets, **b** inside non-b-tagged jets, and **c** outside any jet. The total sample is shown for **d** Λ candidates

taken to be [460–480] and [520–540] MeV ([1096–1106] and [1126–1136] MeV) for K_S^0 (Λ) production. Candidates in the signal (sideband) region are given positive (negative) weights when filling histograms for neutral strange particle spectra such as the transverse momentum, pseudorapidity or energy. The sideband subtraction is applied to both data and detector-level MC samples. It relies on the assumption that the kinematic distributions for fake candidates in the signal region are similar to those in the sidebands. The validity of this assumption was checked with MC studies. The number of reconstructed events is shown in Table 4. It was checked that after unfolding for detector effects, the results of the analysis are independent of sensible variations of the signal and sideband region widths.

The results of this simple sideband subtraction procedure, used as a baseline, is cross-checked by fitting the mass distributions to a Gaussian function centred at the nom-

inal mass plus a constant (linear) shape for the K_S^0 (Λ) background. Choosing a different background shape (constant/linear) changes the results by less than 10% of the statistical uncertainties. The estimated numbers of signal and background events obtained using the two background methods agree within statistical uncertainties. The limited sample size precludes extending this fitting procedure for signal extraction as a function of the neutral strange particle kinematic variables under study.

The resulting K_S^0 and Λ masses from fits to the total $\pi\pi$ and $p\pi$ mass distributions are 497.8 ± 0.2 MeV and 1115.8 ± 0.3 MeV, in agreement with the PDG values [94]. The K_S^0 (Λ) widths from the fits are 6.83 ± 0.03 MeV (4.16 ± 0.04 MeV). The signal mass range includes 99% (95%) of the K_S^0 (Λ) signal, which ensures that the sidebands for the background subtraction are not contaminated by signal.

Table 4 The numbers of K_S^0 and Λ particles (N_K and N_Λ) reconstructed in the data after sideband background subtraction for each class and for the total sample with their statistical uncertainties

Class	N_K	N_Λ
Inside b-tagged jets	530 ± 34	115 ± 19
Inside non-b-tagged jets	391 ± 25	65 ± 14
Outside any jet	1837 ± 49	183 ± 18
Total sample	2758 ± 69	363 ± 31

As previously noted in Refs. [12–14,16,17], fitting to a double-Gaussian function with a common mean value improves the quality of the fits. This was also tried in this analysis. The resulting Gaussian mean values coincide with those obtained from a single-Gaussian fit and the numbers of signal and background events are stable within statistical uncertainties.

6 Results at detector level

Neutral strange particle production is studied as a function of the transverse momentum p_T, the energy E, the pseudorapidity η, the transverse flight distance R_{xy} and the multiplicity N. For K_S^0 and Λ production inside jets, the energy fraction, $x_{K,\Lambda} = E_{K,\Lambda}/E_{\text{jet}}$, is also considered.

For this purpose, the reconstructed K_S^0 and Λ mass distributions are obtained in different bins of the variables under study, and the numbers of signal events after proper sideband subtraction are determined, as discussed in Sect. 5.2. They are normalised to the total number of events in data or MC generator fulfilling the dileptonic $t\bar{t}$ selection criteria presented in Table 3. No attempt is made to subtract the non-$t\bar{t}$ background because the normalised K_S^0 spectra for the $t\bar{t}$ signal are found in MC predictions to be compatible with those for single-top-quark events, which form the main background.

6.1 K_S^0 production at detector level

The kinematic distributions for K_S^0 production are displayed in Figs. 3, 4, 5. They are separated into the three different classes defined in Sect. 5 and compared with two different MC models, namely POWHEG + PYTHIA6 + PERUGIA2011C and MC@NLO + HERWIG + JIMMY. The data show both the statistical as well as the total systematic uncertainties. The total uncertainties are obtained as the sum in quadrature of the statistical and detector level systematic uncertainties, namely those due to tracking, JES and JER. The systematic uncertainties are discussed in detail in Sect. 8.

As shown in Table 4, approximately two-thirds of the total K_S^0 sample are not associated with jets, the remaining one-third being roughly equally distributed between b-tagged and non-b-tagged jets. For those inside jets, the K_S^0 spectra do not show a strong dependence on whether the jets are b-tagged or not. On the other hand, K_S^0 candidates not associated with jets are softer in p_T or energy than those embedded in jets and their pseudorapidity distribution is constant over a wider central plateau. The K_S^0 multiplicity inside b-tagged jets, Fig. 3f, is similar to that inside non-b-tagged jets, Fig. 4f, while that outside any jet falls off less steeply, Fig. 5e.

The gross features of the data are described fairly well by both MC simulations, except for K_S^0 production not associated with any jet. Here the MC simulations predict roughly 30% fewer K_S^0 than observed in data, while the shapes of the distributions exhibit fair agreement but for the multiplicity distribution.

6.2 Λ production at detector level

Similar distributions for Λ production are also obtained. Due to the limited number of events, only distributions for the total sample are shown in Fig. 6.

The gross features exhibited by the Λ baryons are similar to those of the K_S^0 mesons. The quality of the MC description of the data is also similar to that discussed in the previous subsection.

7 Unfolding to particle level

In order to take into account detector effects, the data are unfolded to the particle level. This allows a direct comparison with theoretical calculations as well as with measurements from other experiments. For kinematic quantities such as the transverse momentum and pseudorapidity, for which migrations are negligible, this is done by computing the reconstruction efficiencies on a bin-by-bin basis (as also in Refs. [1–11,23,24]). For the multiplicity distributions, however, a Bayesian unfolding procedure is applied because the bin-to-bin migrations are relevant.

7.1 Efficiency correction

The reconstruction efficiencies (ϵ) are calculated by dividing bin-by-bin each of the distributions (p_T, $|\eta|$, energy and energy fraction) at detector level by the one at particle level for each of the three classes of candidates considered:

$$\epsilon_i = \frac{\frac{1}{N_{\text{evt}}^{\text{det}}} \frac{dN_{K,\Lambda}^{\text{det}}}{dx_i}}{\frac{1}{N_{\text{evt}}^{\text{particle}}} \frac{dN_{K,\Lambda}^{\text{particle}}}{dx_i}}$$

where x_i stands for the i-th bin in the variable x which denotes any of the kinematic variables mentioned above.

Fig. 3 Kinematic characteristics for K_S^0 production inside b-tagged jets, for data and detector-level MC events simulated with the POWHEG + PYTHIA6 and MC@NLO + HERWIG generators. Total uncertainties are represented by the shaded area. Statistical uncertainties for MC samples are negligible in comparison with data
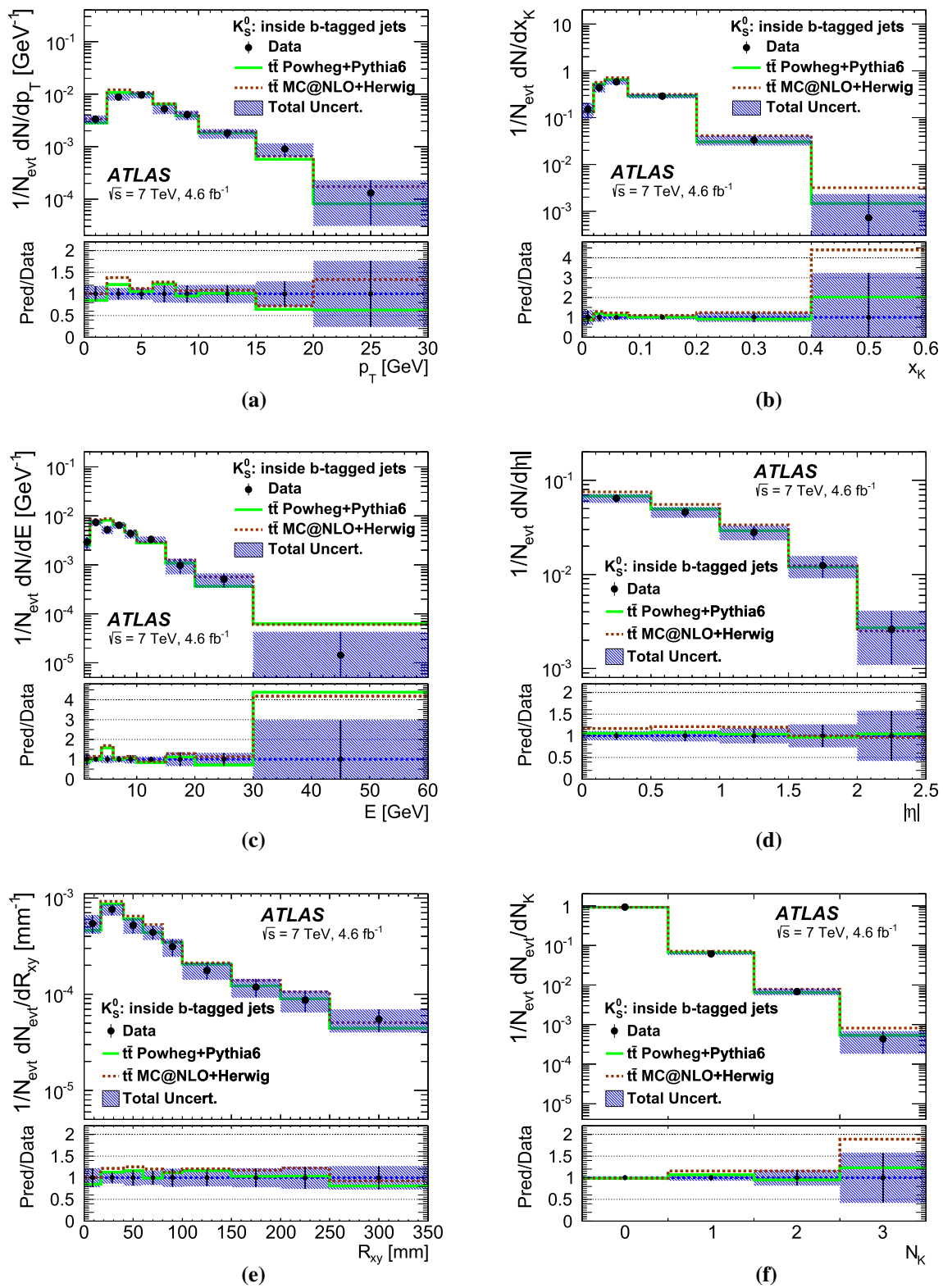
Fig. 4 Kinematic characteristics for K_S^0 production inside non-b-tagged jets, for data and detector-level MC events simulated with the POWHEG + PYTHIA6 and MC@NLO + HERWIG generators. Total uncer- tainties are represented by the shaded area. Statistical uncertainties for MC samples are negligible in comparison with data

(a)

(b)

(c)

(d)

(e)
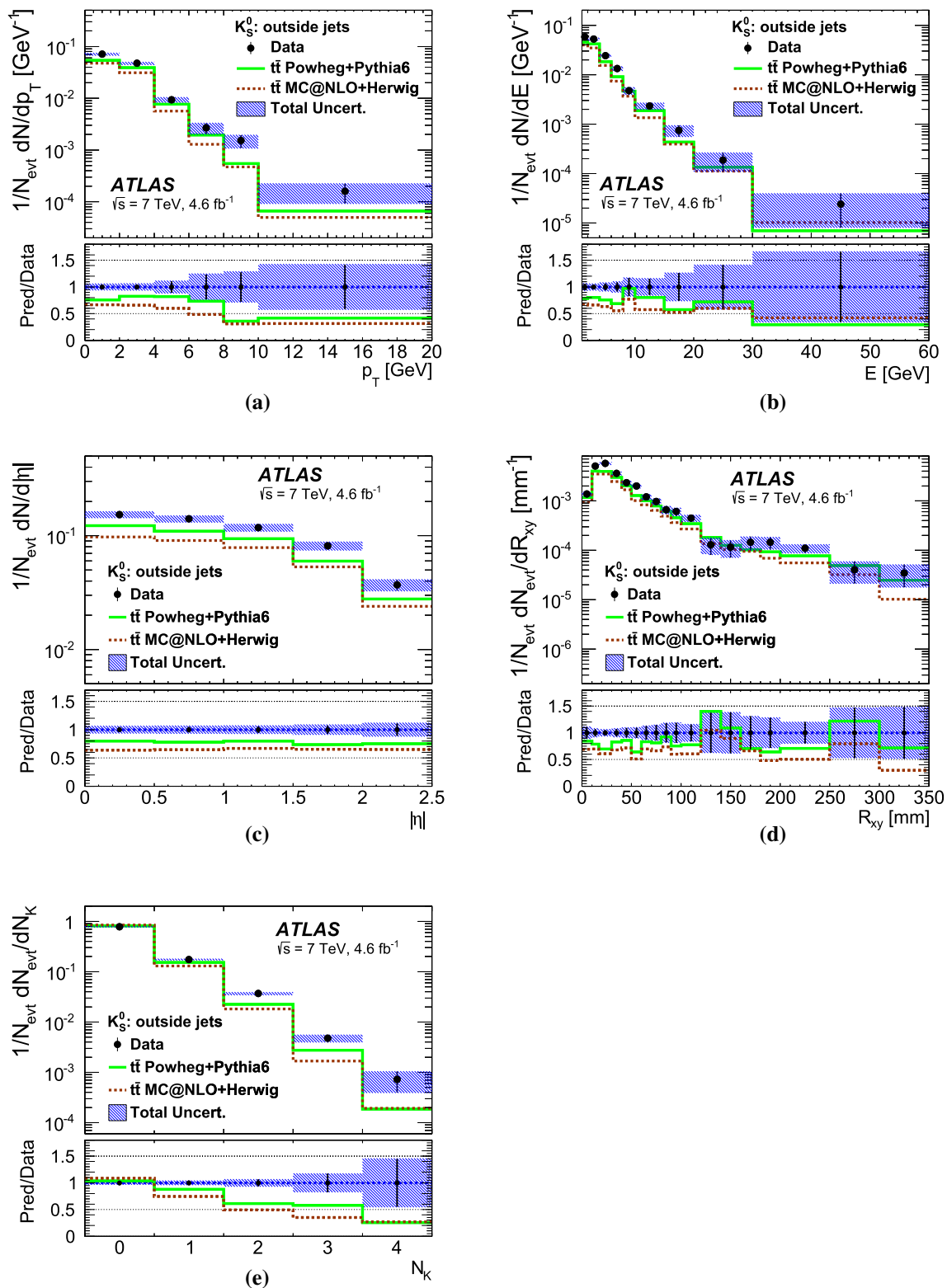
Fig. 5 Kinematic characteristics for K_S^0 production not associated with jets, for data and detector-level MC events simulated with the POWHEG + PYTHIA6 and MC@NLO + HERWIG generators. Total uncertainties are represented by the shaded area. Statistical uncertainties for MC samples are negligible in comparison with data
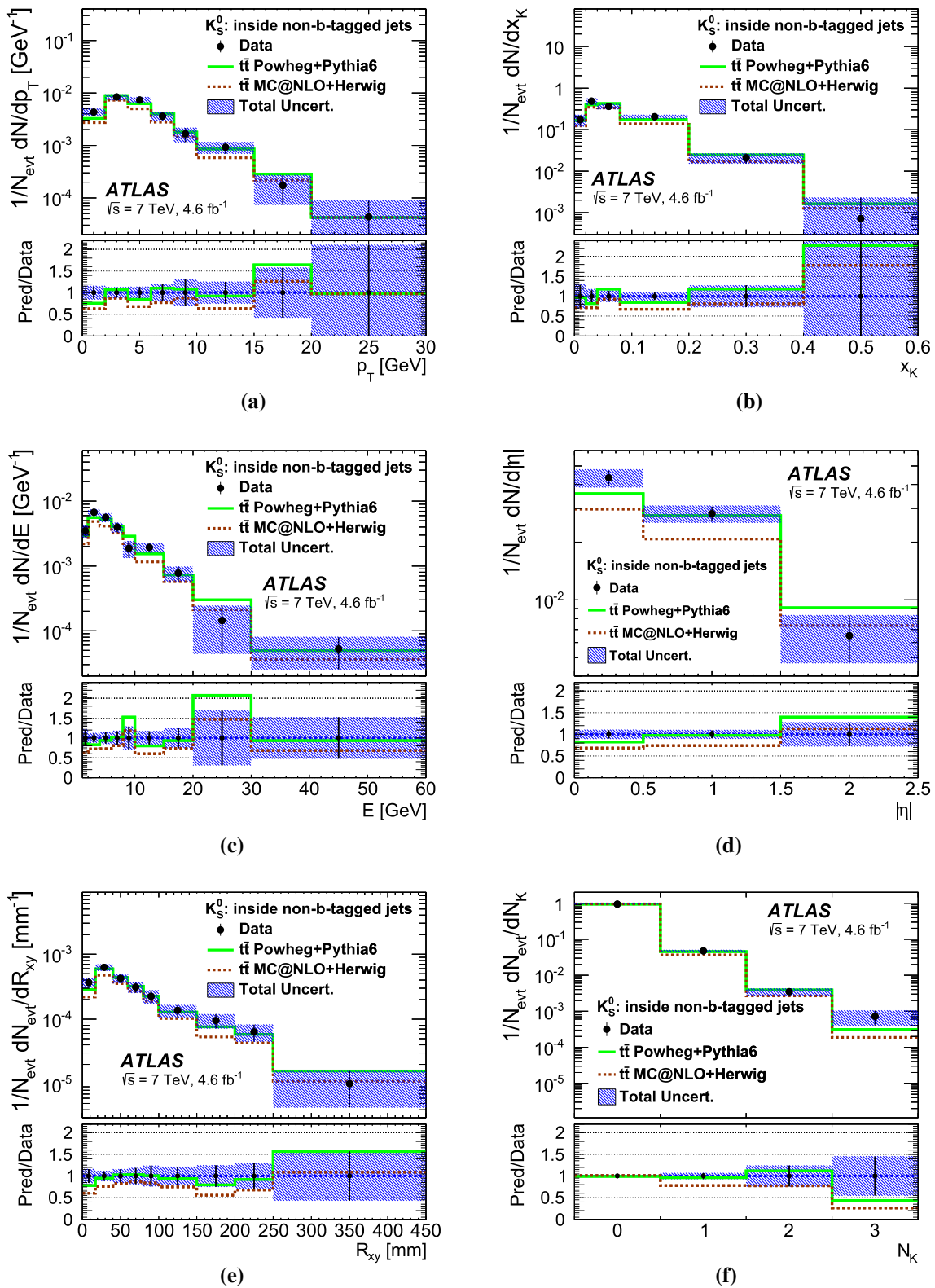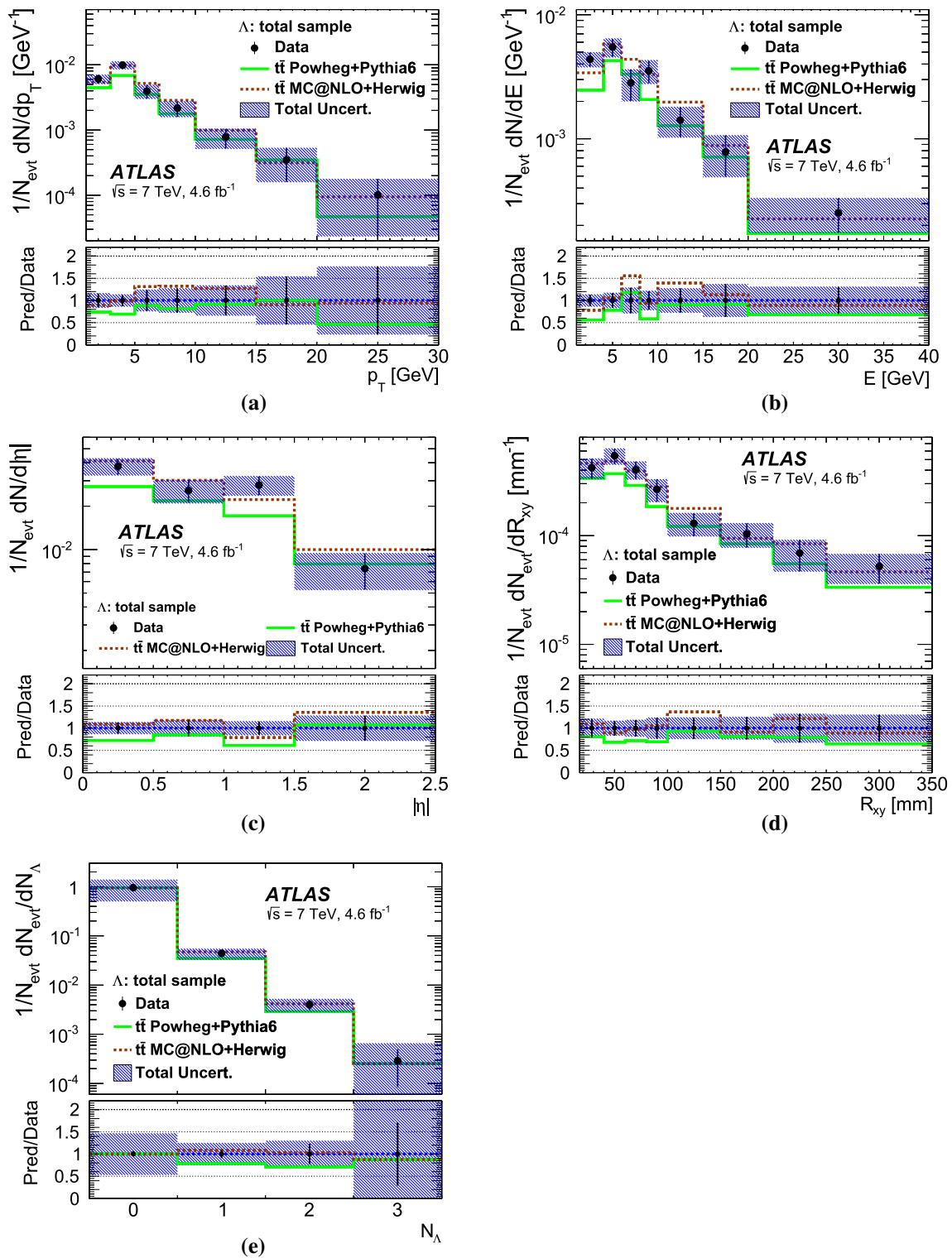
Fig. 6 Kinematic characteristics for the total Λ production, for data and detector-level MC events simulated with the POWHEG + PYTHIA6 and MC@NLO + HERWIG generators. Total uncertainties are represented by the shaded area. Statistical uncertainties for MC samples are negligible in comparison with data

They are shown in Fig. 7, for each of the classes, as well as for the total sample. For neutral strange particles embedded in *b*-tagged jets, this efficiency correction also includes the

b-tagging efficiency. The small size of the MC sample prevents the use of a multidimensional binning for the correction procedure.

Fig. 7 The K_S^0 reconstruction efficiency as a function of **a** p_T, **b** energy, **c** $|\eta|$ and **d** energy fraction for POWHEG + PYTHIA6 and four classes of K_S^0: inside b-tagged jets (triangle), inside non-b-tagged jets (inverted triangle), outside any jet (circle), and the total sample (square)
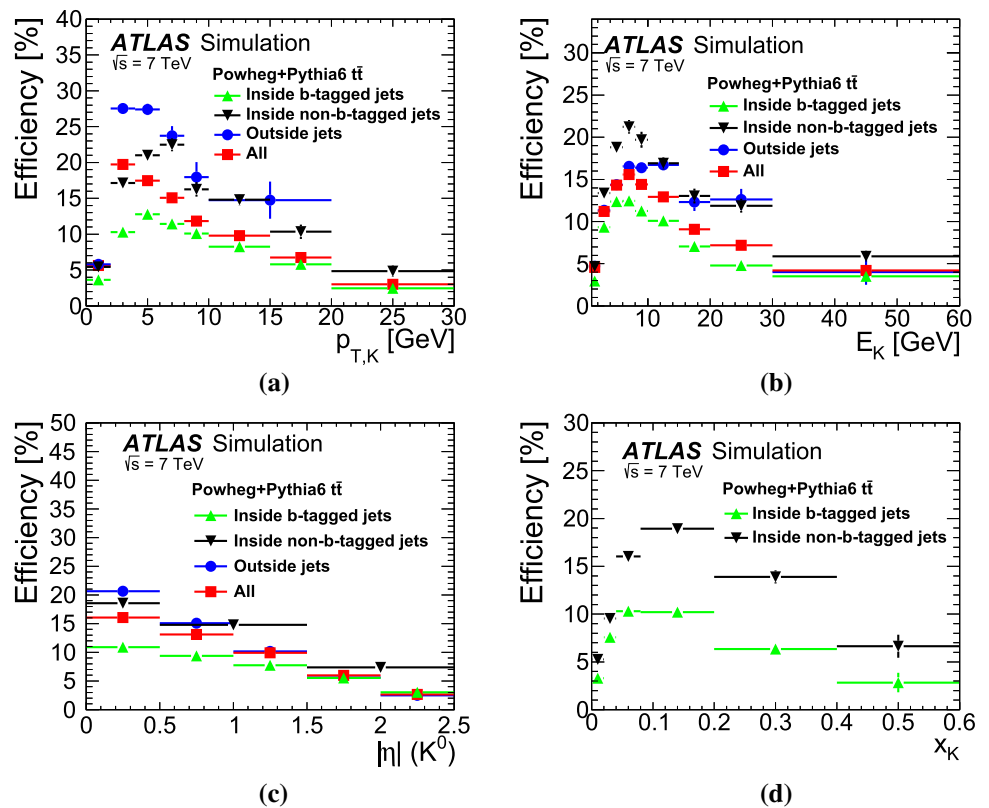
The particle-level distributions are obtained using leptons (from W decays), jets and neutral strange particles (K_S^0 and Λ) in the events selected at detector level. Particle-level jets are built using all particles in MC simulation with a lifetime above 10^{-11} s, excluding muons and neutrinos. The kinematic criteria for jets at particle and detector level are the same, namely $p_T > 25$ GeV and $|\eta| < 2.5$. The particle-level b-jets are defined as those containing a b-hadron, with $p_T > 5$ GeV and $\Delta R < 0.3$ from the jet axis. Particle-level K_S^0 and Λ candidates, including those decaying to neutral particles, are required to be within $|\eta| < 2.5$ and have an energy $E > 1$ GeV, as no K_S^0 candidates are reconstructed below that energy at detector level. Similar to the detector level, the K_S^0 (Λ) candidates at particle level which fulfil these conditions are separated into three classes using the same ΔR criteria with respect to a particle-level jet.

MC studies show that migrations between classes when going from detector to particle level are generally smaller than 5%. For example, K_S^0 candidates which are not associated with any jet at detector level, have a 1% (3%) probability to be classified as embedded in a b-jet (non-b-jet) at particle level. A notable exception is that of K_S^0 candidates inside non-b-tagged jets at detector level, which have a 32% probability to be classified as embedded in a b-jet at particle level. This is due to the b-tagging efficiency, which is included in the reconstruction efficiency as defined above.

The contribution of non-fiducial events, i.e. events which pass the detector-level selection but are not present at the

particle level, introduces a small bias which is taken into account as a systematic uncertainty. More details are given in Sect. 8.

The reconstructed distributions of K_S^0 (Λ) are corrected with a weight given by $1/\epsilon_i$, depending on their class. The POWHEG + PYTHIA6 MC sample was used to derive efficiencies. Since the MC simulation does not include pile-up at the particle level, the efficiency calculation effectively corrects for the pile-up effects present at the detector level. This is further discussed in Sect. 8.

Figure 7 shows that the reconstruction efficiency inside b-tagged jets is lower than inside non-b-tagged jets, due to the fact that the average b-tagging efficiency is 70% and the b-jet contamination in the non-b-tagged sample is around 30%. It was checked that the efficiency for K_S^0 reconstruction inside b-jets is independent of whether they are b-tagged or not at detector level. The efficiency for K_S^0 (Λ) outside jets peaks at lower p_T values than for those inside, and falls more sharply in the distributions' tails. This can be attributed to the differences in their transverse momentum spectra.

The efficiency for K_S^0 (Λ) outside jets is lower than that reported in Ref. [12] for a minimum-bias sample with less pile-up and restricted to lower transverse momenta.

In order to investigate the dependence of the efficiency corrections on the jet multiplicity, these efficiencies are derived for events with more than or at most four jets. They are found to agree within statistical errors. This is expected since each

additional jet with $R = 0.4$ represents only about 1.5% of the total available phase space in the η–ϕ plane.

7.2 Bayesian unfolding

The unfolding based on the efficiency calculations discussed so far relies on the assumption that the neutral strange particles, once reconstructed, are measured to a precision which is much smaller than the bin widths. As an alternative an iterative Bayesian unfolding [95] as implemented in the RooUnfold program [96] was tried. The method numerically calculates the inverse of the migration matrices for each of the distributions under study. The POWHEG + PYTHIA6 MC sample is used to determine these migration matrices by matching detector-level and particle-level K_S^0 that are in the same class and have an angular separation $\Delta R < 0.01$. The resulting matrices exhibit a very pronounced diagonal correlation. The number of iterations is chosen such that the residual bias, evaluated through a closure test as discussed in Sect. 8, is within a tolerance of 1% for the statistically significant bins as in Ref. [97]. The Bayesian unfolded distributions and the bin-by-bin corrected ones agree with each other with a precision which is much smaller than the statistical uncertainties.

The K_S^0 multiplicity distributions cannot be unfolded using a bin-by-bin efficiency correction due to the large migrations between the particle multiplicity bins at the detector and particle levels. For the multiplicity unfolding, only the visible decays, $K_S^0 \to \pi^+\pi^-$, are considered at particle level. This reduces the size of the non-diagonal terms in the migration matrices. For the calculation of average multiplicities, a correction factor accounting for the invisible decays, $K_S^0 \to \pi^0\pi^0$, is applied a posteriori when necessary.

The results ($N^{\text{part},i}$) of this Bayesian unfolding procedure are given by:

$$N^{\text{part},i} = \sum_j N_{\text{detec},j} \times \epsilon_{\text{detec},j} A_{\text{detec},j}^{\text{part},i} / \epsilon^{\text{part},i}$$

where i and j are the particle and detector level bin indices, respectively, $N_{\text{detec},j}$ is the data result at detector level, $A_{\text{detec},j}^{\text{part},i}$ is the migration matrix refined through iteration as explained above, and $\epsilon_{\text{detec},j}$ and $\epsilon^{\text{part},i}$ the matching efficiencies for detector and particle level neutral strange particles.

The statistical uncertainties in data and MC simulation are propagated simultaneously through the unfolding procedure by using pseudo-experiments. A set of 10^3 replicas is created for each measured distribution by applying a Poisson-distributed fluctuation. Each replica is then unfolded using a statistically independent fluctuated migration matrix. The statistical uncertainty of the unfolded distribution is defined as the standard deviation of the 10^3 unfolded replicas. As a cross-check, pulls are obtained from these replicas and found to follow a normal distribution, as expected.

8 Systematic uncertainties

Since the present analysis is concerned with the measurement of normalised distributions, many systematic uncertainty sources considered in top quark cross-section measurements [76], particularly those related to the lepton and b-tagging efficiency scale factors, cancel out. Similarly, the systematic uncertainty due to non-$t\bar{t}$ processes is expected to be very small and therefore not taken into account. The following systematic uncertainties are considered in this analysis:

- The systematic uncertainties due to tracking inefficiencies: they are taken from minimum-bias events [12] in bins of the track transverse momentum and pseudorapidity and found to be below 2% and dominated by the uncertainties in the modelling of the detector material. They result in an estimated 4–5% uncertainty for two-body decays, which is the case for K_S^0 and Λ production. This relies on the assumption that the uncertainties from minimum-bias events are also valid in a dense environment as given by a jet. It was checked that there are no systematic effects in the MC description of the neutral strange particle production as a function of the angular separation to the jet-axis.

- The systematic uncertainty related to the choice of MC generator used in the unfolding: the systematic uncertainties due to modelling are calculated as the relative differences between the unfolded distributions obtained with the nominal POWHEG + PYTHIA6 MC samples and those obtained with the alternative MC@NLO + HERWIG samples. For kinematic quantities such as the transverse momentum and pseudorapidity, they can be expressed as the deviation of the efficiency ratios from unity. These systematic uncertainties range up to 20–25%, or even to 50% for the tails of the multiplicity distributions, and thus represent the dominant source of systematic uncertainty. The choice of parton shower (PS) and hadronisation scheme plays the predominant role, as tested by comparing the efficiencies calculated with POWHEG + PYTHIA6 and POWHEG + HERWIG samples. The matrix element (ME) calculation method plays a minor role, as seen when comparing the efficiencies calculated with POWHEG + HERWIG and MC@NLO + HERWIG samples.

- The systematic uncertainty related to pile-up: as a first attempt to check how well the MC pile-up modelling describes the data, mass distributions for K_S^0 and Λ candidates are obtained for two samples of events depending on whether the average number of interactions per bunch crossing, $\langle\mu\rangle$, is higher or lower than the median ($\langle\mu\rangle = 8.36$). This exercise shows that neutral strange particles embedded in jets, with or without a b-tag, are not at all affected by pile-up. This is not the case for neu-

Table 5 Summary table of systematic uncertainty sources: MC generator choice for the unfolding, pile-up (PU) mismodelling, tracking inefficiency, JES and JER, non-fiducial events, and non-closure test

Systematic uncertainty	MC choice	PU	Tracking	JES	JER	Fiducial	Non-closure
Relative values	< 20–25%	∼ 8%	∼ 4–5%	< 5%	< 5%	< 5%	< 1 %

tral strange particles outside jets, for which a clear linear dependence on $\langle\mu\rangle$ is observed. In order to estimate the systematic uncertainty associated with this class, a data-driven procedure is developed, which compares the $\langle\mu\rangle$ dependence of the K_S^0 multiplicity observed in data and MC events at high longitudinal impact parameter values. The resulting systematic uncertainty is found to be of the order of 8%.

- The systematic uncertainty related to the JES and JER: the propagation of the JES [85] and JER [87] uncertainties is taken into account. They affect most of the distributions indirectly through changes in the number of jets satisfying the selection criteria. The only distribution directly affected by these uncertainties is the energy fraction. The resulting uncertainties from both the JES and JER are found to be well below 5%.

- The b-tagging efficiency: in order to study the systematic uncertainty due to the choice of b-tagging efficiency, the analysis was repeated using two alternative b-tagging efficiencies of 60% and 85%. The obvious effect of this is that the number of jets classified as b-tagged (or not) changes. However, as shown in Figs. 3 and 4, the distributions for K_S^0 production inside b-tagged jets are very similar to those for K_S^0 production inside non-b-tagged jets, so the uncertainties for normalised distributions are expected to be small. The average multiplicity for K_S^0 production per b-tagged jet (or non-b-tagged jet) is found to be independent of the choice of b-tagging working point within the statistical uncertainty. Thus the systematic uncertainty due to the choice of b-tagging efficiency is negligible.

- The unfolding non-closure uncertainty, which is calculated in two steps. In the first step, the particle-level MC distributions are reweighted such that the reweighted detector-level distributions match the data. Then, these reweighted detector-level MC distributions are unfolded to the particle level using the same procedure as for the data, and compared with the reweighted particle-level MC distributions. The relative difference seen in this comparison is taken as the systematic uncertainty and is typically below 1%.

- Non-fiducial events uncertainty: it is calculated as the difference between two sets of POWHEG + PYTHIA6 K_S^0 and Λ particle level distributions, normalised to the total number of selected events. One set comes from an event sample selected using detector-level criteria and the other

Table 6 K_S^0 and Λ unfolded (particle-level) average multiplicities per event ($\langle n_{K,\Lambda}\rangle$), including statistical and systematic uncertainties, for each class and for the total sample, along with the ones obtained from the POWHEG + PYTHIA6 MC generator at particle level

Class	Unfolded data from p_T $\langle n_{K,\Lambda}\rangle \pm$ (stat) $\pm$ (syst)	MC PYTHIA6 particle $\langle n_{K,\Lambda}\rangle \pm$ (stat)
K_S^0 inside b-jets	$0.91 \pm 0.07 \pm 0.03$	0.917 ± 0.003
K_S^0 inside non-b-jets	$0.43 \pm 0.03 \pm 0.04$	0.397 ± 0.002
K_S^0 outside any jet	$2.91 \pm 0.10 \pm 0.57$	2.248 ± 0.004
K_S^0 total sample	$4.26 \pm 0.14 \pm 0.59$	3.563 ± 0.005
Λ total sample	$0.65 \pm 0.07 \pm 0.05$	0.499 ± 0.014

set is selected using particle-level criteria. The same kinematic requirements are applied to leptons and jets at the detector and particle levels. Typically, these systematic uncertainties are below 5%.

Table 5 summarises the approximate magnitude of the systematic uncertainties considered. The total systematic uncertainties are then calculated as the sum in quadrature of the systematic uncertainties due to the sources discussed above.

9 Results at the particle level

The K_S^0 and Λ average multiplicities per event for corrected data and POWHEG + PYTHIA6 MC events at particle level are shown in Table 6. They are obtained from the unfolded transverse momentum (p_T) spectra.

It was checked that the average multiplicities obtained from the iterative Bayesian unfolded multiplicity distributions are in good agreement within statistical uncertainties with the values in Table 6. Since the migration matrices were obtained considering only visible decays at particle level, the resulting multiplicities are corrected for the branching ratio of $K_S^0 \to \pi^0 \pi^0$.

A complete set of results at particle level can be found in Ref. [98].

9.1 K_S^0 unfolded distributions

The unfolded distributions in p_T, E, $|\eta|$ and N_K for K_S^0 production inside b-jets, inside non-b-jets and outside any jet are shown in Figs. 8, 9, 10. Furthermore, for K_S^0 production

(a)

(b)

(c)

(d)

(e)

Fig. 8 Kinematic characteristics for K^0_S production inside b-jets, for corrected data and particle-level MC events simulated with the POWHEG + PYTHIA6, MC@NLO + HERWIG, SHERPA, POWHEG + PYTHIA8, POWHEG + HERWIG7 and aMC@NLO + HERWIG7 generators. Total uncertainties are represented by the shaded area. Statistical uncertainties for MC samples are negligible in comparison with data
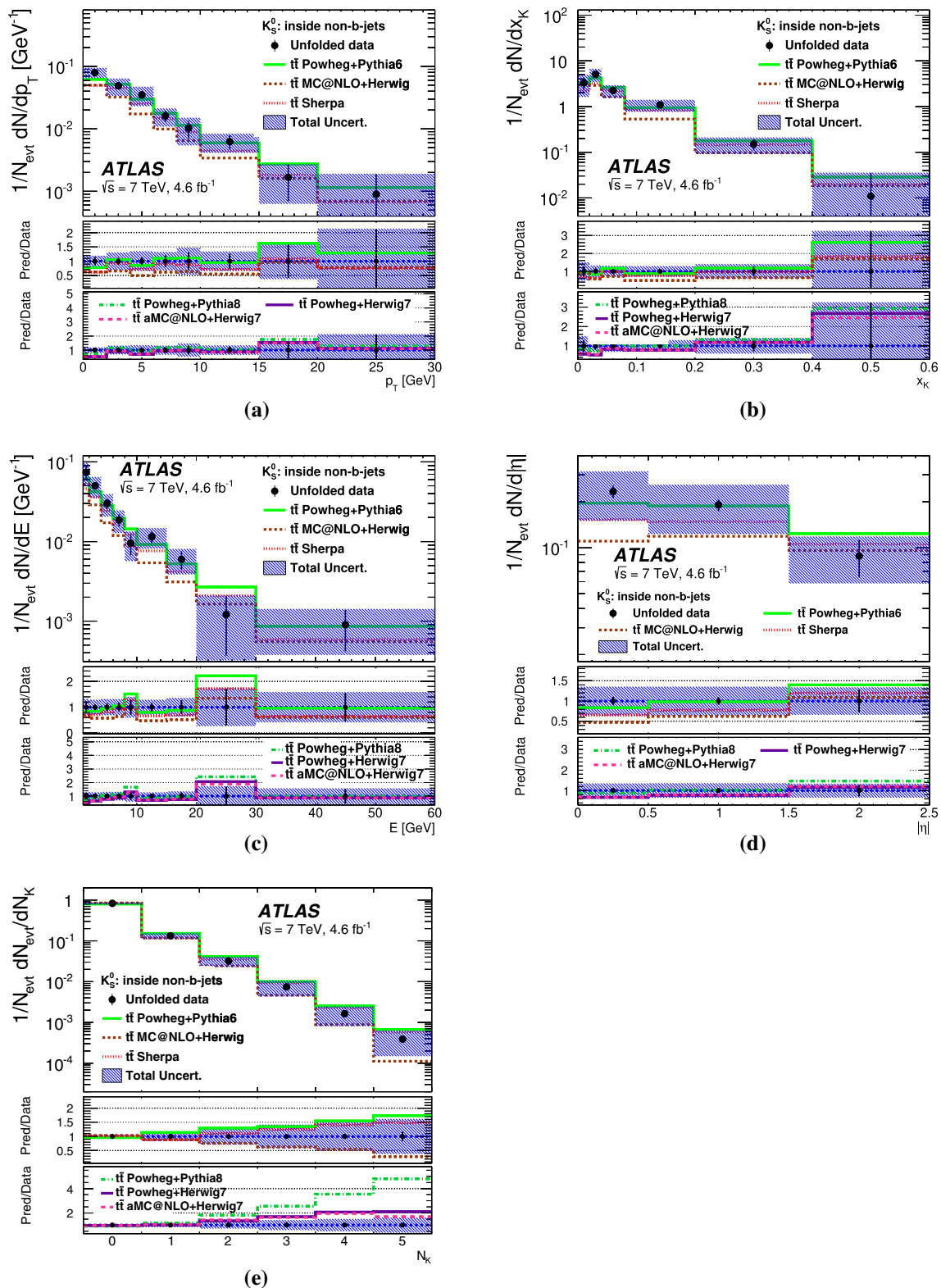
Fig. 9 Kinematic characteristics for K^0_S production inside non-*b*-jets, for corrected data and particle-level MC events simulated with the Powheg + Pythia6, MC@NLO + Herwig, Sherpa, Powheg + Pythia8, Powheg + Herwig7 generators. Total uncertainties are represented by the shaded area. Statistical uncertainties for MC samples are negligible in comparison with data
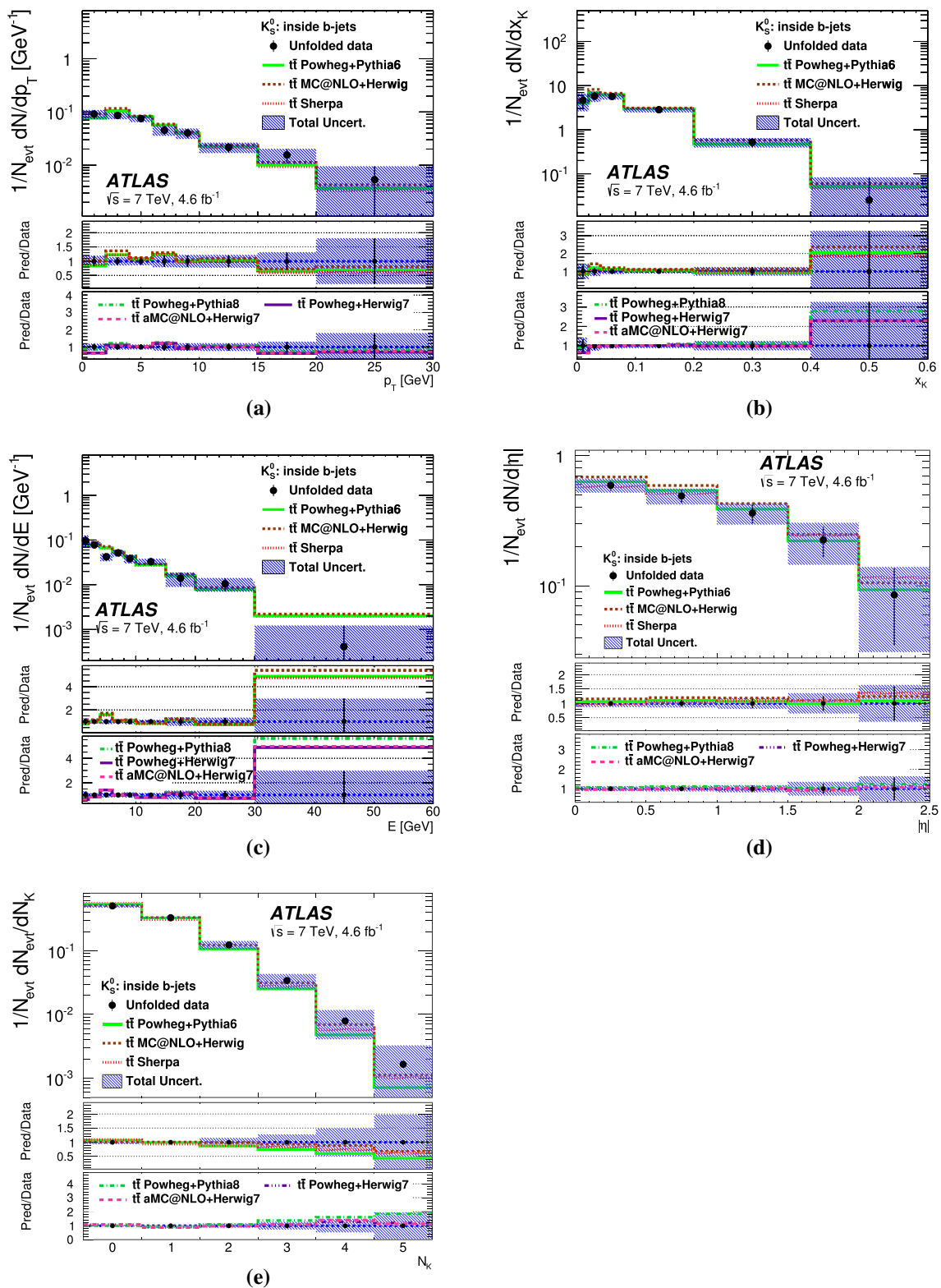
Fig. 10 Kinematic characteristics for K_S^0 production not associated with jets, for corrected data and particle-level MC events simulated with the POWHEG + PYTHIA6, MC@NLO + HERWIG, SHERPA, POWHEG + PYTHIA8, POWHEG + HERWIG7 and aMC@NLO + HERWIG7 generators. Total uncertainties are represented by the shaded area. Statistical uncertainties for MC samples are negligible in comparison with data
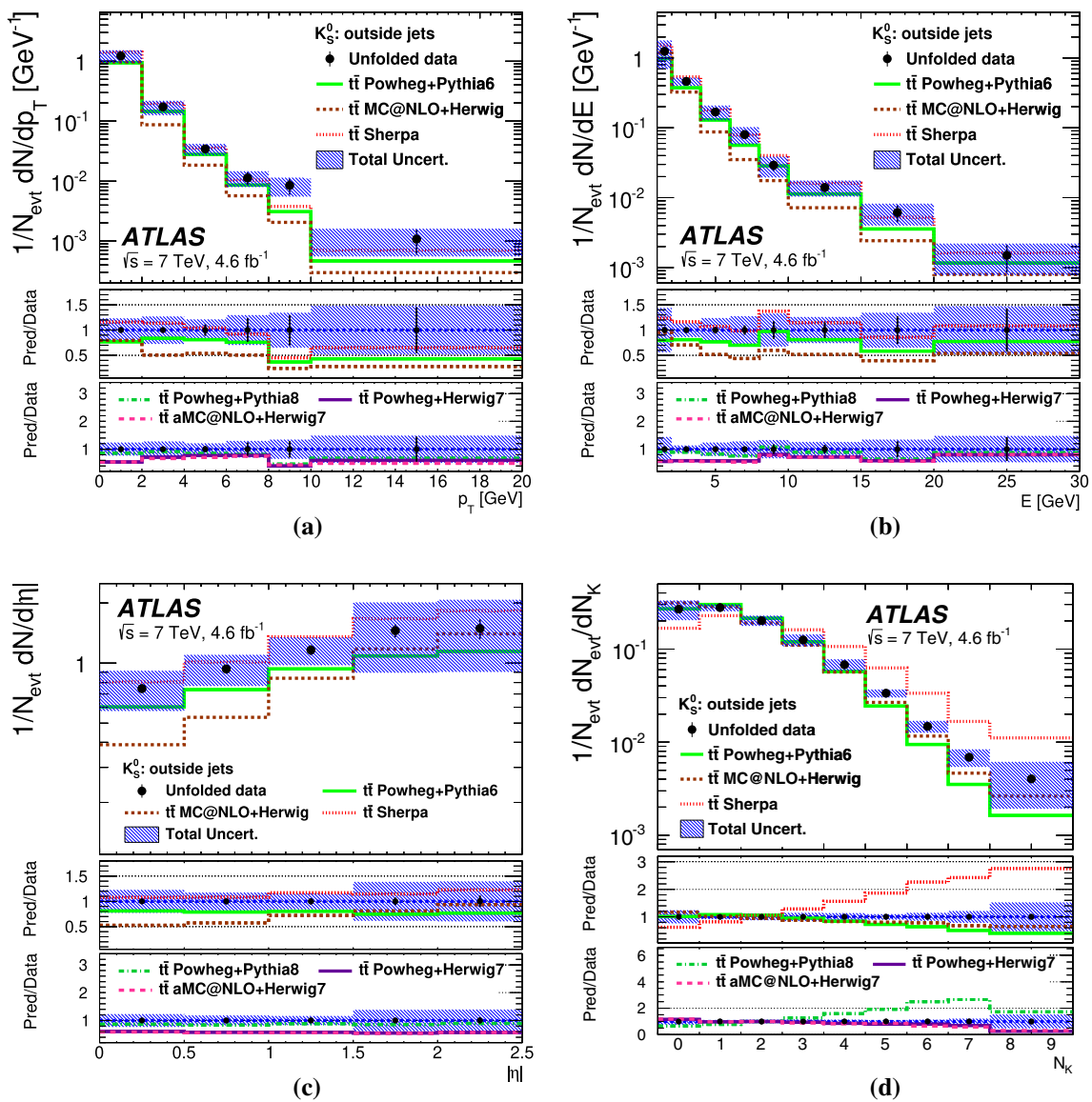
inside jets, the distribution of the energy fraction, x_K, is also shown. Numerical results are summarised in the Appendix. The unfolded data are compared with the expectations from six different MC models: POWHEG + PYTHIA6, MC@NLO + HERWIG, SHERPA, POWHEG + PYTHIA8, POWHEG + HERWIG7 and aMC@NLO + HERWIG7.

To be more quantitative in the comparison between data and MC predictions, a χ^2 test is performed for the distributions shown in Figs. 8, 9, 10 prior to normalisation. The MC samples are then scaled to the same number of $t\bar{t}$ dileptonic events as in the data. The χ^2 is defined as:

$$\chi^2 = V^{\mathrm{T}} \cdot Cov^{-1} \cdot V$$

where V is the vector of differences between MC predictions and unfolded data, and Cov^{-1} denotes the inverse of the covariance matrix.

The covariance matrix is obtained by using pseudo-experiments. A set of 10^3 replicas of the corresponding unfolded data distributions is created. In order to include systematic effects, these replicas are smeared with Gaussian functions whose widths are given by the systematic errors considered as uncorrelated. The results of the χ^2 test are summarised in Tables 7, 8, 9, including the associated p-values. They are used to assess the significance of the differences between the various generators and the data for each observ-

Table 7 Values of the χ^2 per degree of freedom and their corresponding p-values, for K_S^0 production inside b-jets, for POWHEG + PYTHIA6, MC@NLO + HERWIG, SHERPA, POWHEG + PYTHIA8, POWHEG + HERWIG7 and aMC@NLO + HERWIG7 predictions

| | $\chi^2/n.d.f.$ (p-value) K_S^0 inside b-jets | | | | | |
	PW+PYTHIA6	MC+HERWIG	SHERPA	PW+PYTHIA8	PW+HERWIG7	aMC+HERWIG7
p_T	0.77 (0.63)	1.31 (0.23)	0.80 (0.61)	0.59 (0.79)	0.64 (0.74)	0.66 (0.73)
E	1.81 (0.06)	2.54 (0.007)	1.67 (0.09)	1.80 (0.06)	1.54 (0.13)	1.53 (0.13)
$|\eta|$	0.56 (0.73)	1.44 (0.21)	0.33 (0.90)	0.61 (0.69)	0.25 (0.64)	0.23 (0.65)
x_K	0.40 (0.88)	1.08 (0.37)	0.19 (0.98)	0.25 (0.96)	0.14 (0.99)	0.15 (0.99)
N_K	1.25 (0.28)	0.62 (0.68)	1.94 (0.08)	2.15 (0.06)	3.72 (0.002)	5.18 (0.00)

Table 8 Values of the χ^2 per degree of freedom and their corresponding p-values, for K_S^0 production inside non-b-jets, for POWHEG + PYTHIA6, MC@NLO + HERWIG, SHERPA, POWHEG + PYTHIA8, POWHEG + HERWIG7 and aMC@NLO + HERWIG7 predictions

| | $\chi^2/n.d.f.$ (p-value) K_S^0 inside non-b-jets | | | | | |
	PW+PYTHIA6	MC+HERWIG	SHERPA	PW+PYTHIA8	PW+HERWIG7	aMC+HERWIG7
p_T	0.42 (0.91)	1.32 (0.23)	0.71 (0.69)	0.60 (0.78)	0.92 (0.50)	0.88 (0.53)
E	1.25 (0.26)	1.58 (0.11)	1.12 (0.34)	1.51 (0.14)	1.44 (0.16)	1.16 (0.31)
$|\eta|$	0.90 (0.44)	0.64 (0.59)	0.43 (0.73)	1.20 (0.30)	0.37 (0.78)	0.43 (0.73)
x_K	0.82 (0.55)	1.51 (0.17)	0.78 (0.58)	0.72 (0.64)	0.98 (0.44)	0.93 (0.48)
N_K	1.50 (0.19)	1.21 (0.30)	0.70 (0.62)	14.29 (0.00)	2.28 (0.04)	2.14 (0.06)

Table 9 Values of the χ^2 per degree of freedom and their corresponding p-values, for K_S^0 production outside jets, for POWHEG + PYTHIA6, MC@NLO + HERWIG, SHERPA, POWHEG + PYTHIA8, POWHEG + HERWIG7 and aMC@NLO + HERWIG7 predictions

| | $\chi^2/n.d.f.$ (p-value) K_S^0 outside jets | | | | | |
	PW+PYTHIA6	MC+HERWIG	SHERPA	PW+PYTHIA8	PW+HERWIG7	aMC+HERWIG7
p_T	0.98 (0.44)	2.64 (0.015)	0.93 (0.47)	0.60 (0.73)	1.22 (0.29)	1.44 (0.19)
E	1.05 (0.40)	2.67 (0.004)	1.14 (0.33)	0.80 (0.61)	2.25 (0.02)	2.47 (0.008)
$|\eta|$	0.94 (0.45)	2.30 (0.04)	1.36 (0.24)	0.57 (0.71)	3.28 (0.006)	3.55 (0.003)
N_K	2.77 (0.005)	1.85 (0.06)	30.5 (0.00)	34.59 (0.00)	1.41 (0.18)	1.76 (0.08)

able. For the kinematic distributions, which are normalised to the average multiplicities, the number of degrees of freedom has been taken as the number of bins. While for the N_K distributions, which are normalised to unit area, the number of degrees of freedom has been reduced by one.

The unfolded distributions in Figs. 8, 9, 10 and the χ^2 and p-values in Tables 7, 8, 9 show that:

- On average, the POWHEG + PYTHIA6 or PYTHIA8 and SHERPA generators give a very similar description of the data, while MC@NLO + HERWIG, aMC@NLO + HERWIG7 and POWHEG + HERWIG7 are slightly disfavoured.
- In general, the MC distributions reproduce the K_S^0 particle spectra inside jets rather well. This is expected since jet fragmentation functions are studied from $S p \bar{p} S$ to Tevatron energies, so the MC simulations are tuned fairly well.
- The spectra for K_S^0 production outside jets are reproduced in shape, but are underestimated by approximately

30%. This observation is consistent with a CMS study of strange particle production in the UE [14]. These data could be used to improve the simulation of the UE, especially to tune the $\gamma_s = s/u$ parameter. This parameter needs to be larger than 0.2, the value used in the PYTHIA6 + PERUGIA2011C tune [57]. The PYTHIA8 + A14 predictions come closer to the data than the PYTHIA6 + PERUGIA2011C ones. This is attributed to the fact that the A14 tune uses γ_s value equal to 0.217, as in the MONASH tune [99], which is 10 % larger than that in the default PYTHIA6 + PERUGIA2011C tune. HERWIG + JIMMY and HERWIG7 + H7UE gives a somewhat worse description than PYTHIA6 + PERUGIA2011C, which indicates the need to also tune the strangeness suppression here or even to use an improved colour reconnection scheme for MPI as suggested in Ref. [100]. SHERPA, which uses strangeness suppression of $\gamma_s = 0.4$, tends to overestimate the K_S^0 yields outside jets.
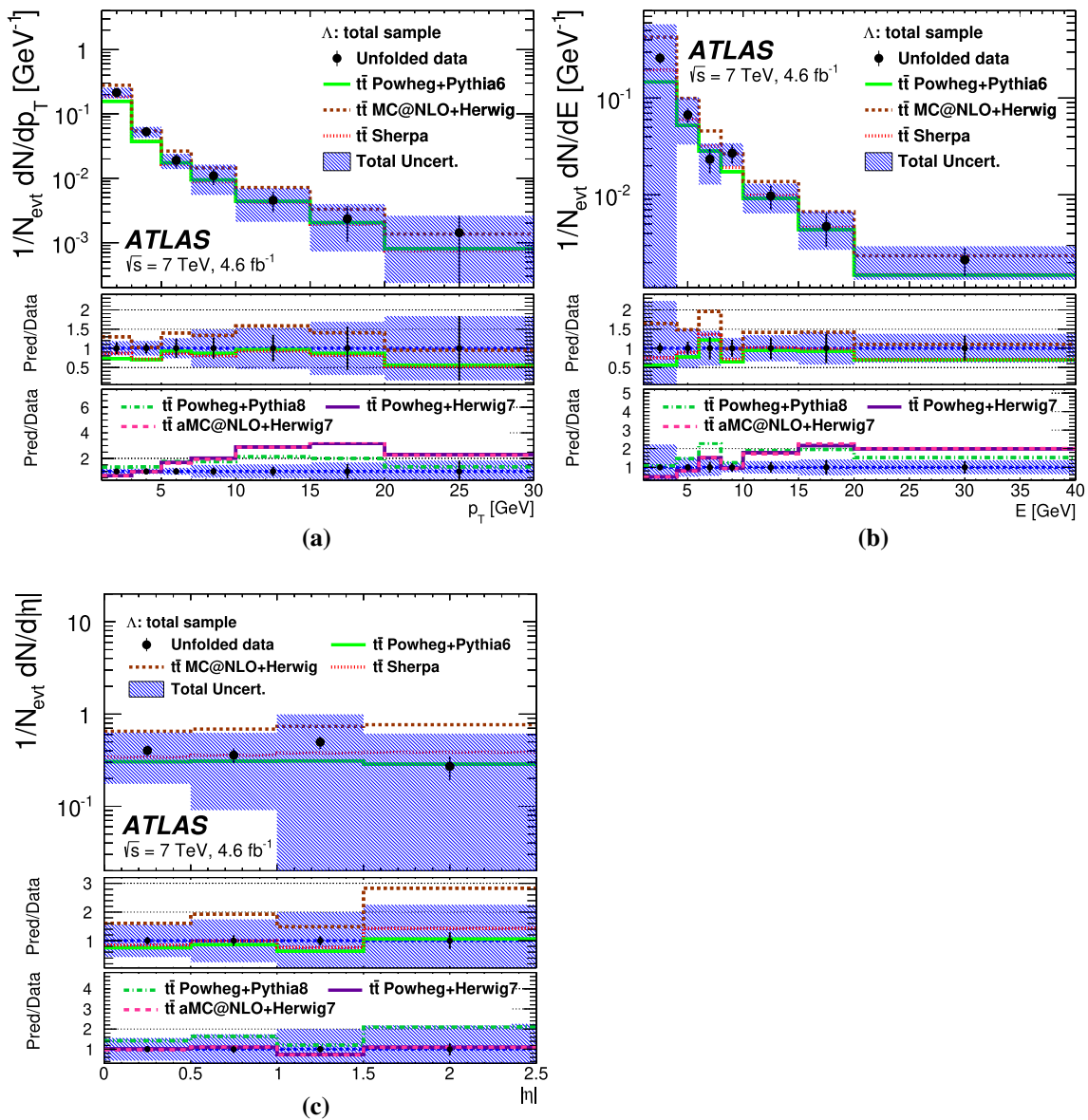
Fig. 11 Kinematic characteristics for the total Λ production, for corrected data and particle-level MC events simulated with the POWHEG + PYTHIA6, MC@NLO + HERWIG, SHERPA, POWHEG + PYTHIA8, POWHEG + HERWIG7 and aMC@NLO + HERWIG7 generators. Total uncertainties are represented by the shaded area. Statistical uncertainties for MC samples are negligible in comparison with data

Table 10 Values of the χ^2 per degree of freedom and their corresponding p-values, for the total Λ sample, for POWHEG + PYTHIA6, MC@NLO + HERWIG, SHERPA, POWHEG + PYTHIA8, POWHEG + HERWIG7 and aMC@NLO + HERWIG7 predictions

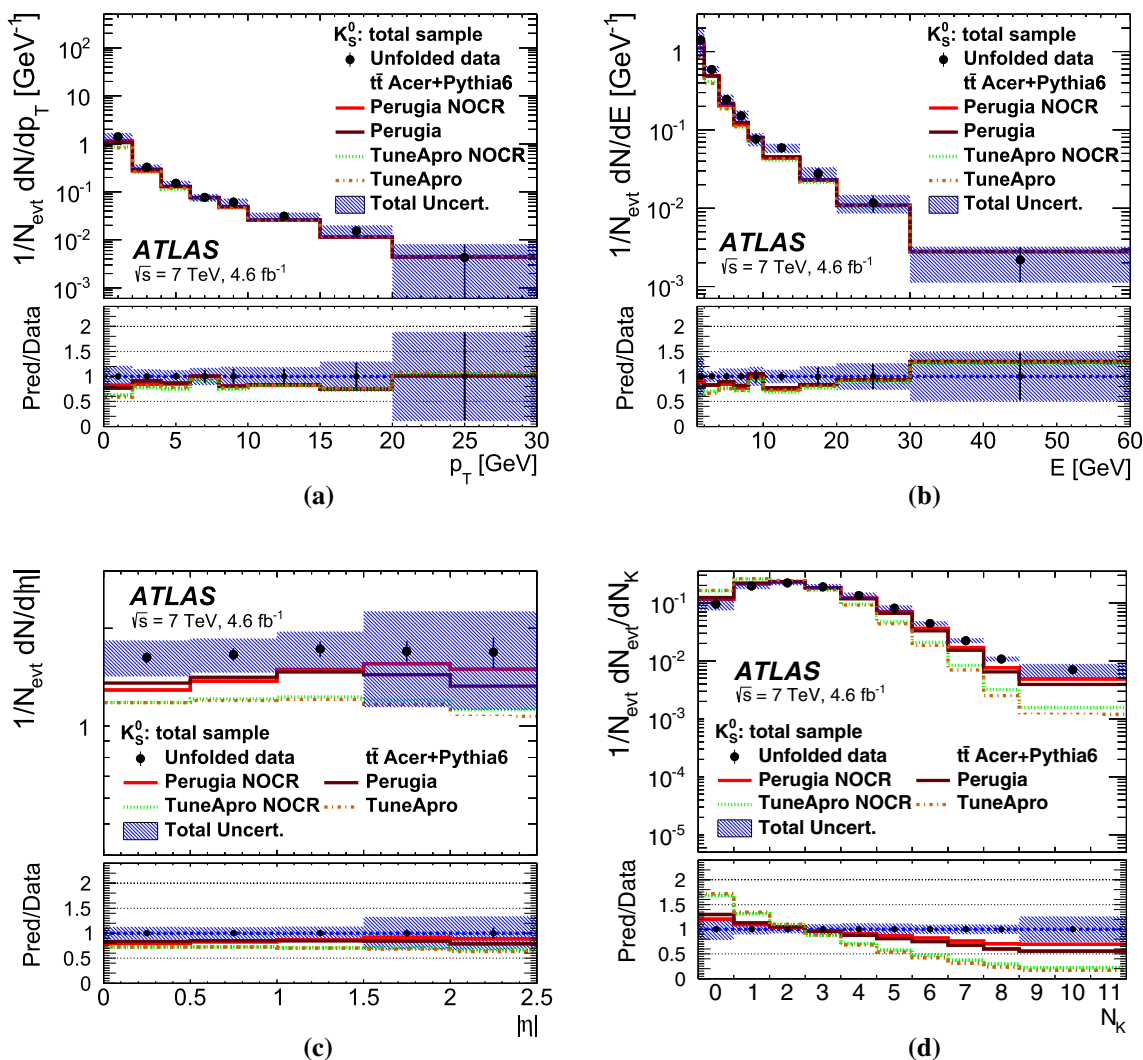|	$\chi^2/n.d.f.$ (p-value) Λ total sample					
	PW+PYTHIA6	MC+HERWIG	SHERPA	PW+PYTHIA8	PW+HERWIG7	aMC+HERWIG7
p_T	0.50 (0.83)	0.93 (0.48)	0.52 (0.82)	3.87 (0.0003)	5.56 (0.00)	5.36 (0.00)
E	0.89 (0.51)	1.90 (0.06)	0.89 (0.51)	3.97 (0.0002)	3.18 (0.002)	3.28 (0.002)
$|\eta|$	0.33 (0.86)	1.62 (0.17)	0.25 (0.91)	0.96 (0.43)	0.44 (0.78)	0.43 (0.79)

Fig. 12 Kinematic characteristics for the total K_S^0 production, for corrected data and particle-level events from the ACER + PYTHIA6 generator with two different tunes: PERUGIA and TUNEAPRO, with and without colour reconnection (CR). Total uncertainties are represented by the shaded area. Statistical uncertainties for MC samples are negligible in comparison with data

Table 11 Values of the χ^2 per degree of freedom and their corresponding p-values, for the total K_S^0 production, along with the ACERMC + PYTHIA6 predictions with the following tunes: PERUGIA and TUNEAPRO (with and without colour reconnection)

$\chi^2/n.d.f.$	(p-value) K_S^0 total sample		
	PERUGIA	PERUGIA (no CR)	TUNEAPRO	TUNEAPRO (no CR)
p_T	0.42 (0.91)	0.50 (0.85)	1.12 (0.35)	1.36 (0.21)
E	1.54 (0.13)	1.90 (0.05)	3.55 (0.0002)	3.37 (0.0004)
$|\eta|$	1.15 (0.33)	1.34 (0.24)	4.18 (0.0008)	3.90 (0.002)

- The energy and transverse momentum spectra for K_S^0 mesons inside b-jets are similar to the spectra for those inside non-b-jets. The spectra for K_S^0 mesons produced outside jets are much softer than for those produced in association with a jet.
- The pseudorapidity distributions for K_S^0 mesons produced outside jets are constant over a wider central plateau than for those produced in association with a jet.

9.2 Λ unfolded distributions

The same distributions studied for K_S^0 production are now presented for the total Λ production. Numerical results are summarised in the Appendix. Comparisons with MC predictions are made in Fig. 11. The Λ production is suppressed relative to K_S^0 production as expected. Due to poor statistics, Λ production cannot be divided into classes.

The results of a χ^2 test for the comparison between unfolded data and MC predictions are summarised in Table 10. POWHEG + PYTHIA6 and SHERPA generators give a similar fair description of the data, while MC@NLO + HERWIG is somewhat disfavoured. POWHEG + PYTHIA8, POWHEG + HERWIG7 and aMC@NLO + HERWIG7 are even more disfavoured.

9.3 Comparison with other MC generators

Following Ref. [77], the sensitivity of the total neutral strange particle production to different underlying-event tunes and colour reconnection schemes was studied. A comparison with the ACER + PYTHIA6 MC generator, with two different underlying-event tunes with and without colour reconnection, is presented in Fig. 12. The results of a χ^2 test, similar to that described in the previous subsection, are summarised in Table 11. The study shows that:

- Colour reconnection effects are very small, and therefore difficult to tune with present statistics.
- TUNEAPRO is slightly disfavoured relative to the PERUGIA tune.

10 Summary

Measurements of K_S^0 and Λ production in $t\bar{t}$ dileptonic final states are reported. They use a data sample with integrated luminosity of 4.6 fb^{-1} from proton–proton collisions at a centre-of-mass energy of 7 TeV, collected in 2011 with the ATLAS detector at the LHC. The K_S^0 distributions in energy, p_T and $|\eta|$ are presented for three subsamples depending on whether the K_S^0 is associated with a jet, with or without a b-tag, or is outside any selected jet. The corresponding K_S^0 multiplicities are also measured. The small sample size precludes such a detailed analysis for Λ production, for which distributions are shown only for the total sample, which includes the sum of Λ and $\bar{\Lambda}$. The results are unfolded to the particle level using the neutral strange particle reconstruction efficiencies in each distribution within the kinematic region given by $E > 1$ GeV and $|\eta| < 2.5$. The measurements are compared with current MC predictions where the $t\bar{t}$ matrix elements are calculated at NLO accuracy with POWHEG, MC@NLO, SHERPA and aMC@NLO, or at LO with ACERMC. Several variations of the MC generators are considered:

- Fragmentation scheme and UE: PYTHIA6 + PERUGIA2011C, PYTHIA8 + A14, PYTHIA6 + TUNEAPRO, HERWIG + JIMMY, HERWIG7 + H7UE or SHERPA.
- Colour reconnection effects.

The main conclusions to be drawn from the analysis are the following:

- Strange baryon production is suppressed relative to strange meson production both inside and outside jets.
- Neutral strange particle production outside jets is much softer than inside jets, and the pseudorapidity distributions are constant over a wider region.
- Neutral strange particle multiplicities outside jets are larger than inside.
- Current MC models give a fair description of the gross features exhibited by K_S^0 and Λ produced inside jets, while the observed yields for neutral strange particles outside jets lie roughly 30% above the PYTHIA6 + PERUGIA2011C and HERWIG + JIMMY or HERWIG7 + H7UE MC predictions, with PYTHIA8 + A14 falling short of the data by 15–20%.

A better description of the yields for K_S^0 and Λ outside jets in $t\bar{t}$ final states would require further tuning of the current MC models, particularly the strangeness suppression mechanisms, and/or more elaborate models for MPI and colour reconnection schemes. For this purpose a Rivet analysis routine and HEPData tables are provided.

Data Availability Statement This manuscript has no associated data or the data will not be deposited. [Authors' comment: "All ATLAS scientific output is published in journals, and preliminary results are made

available in Conference Notes. All are openly available, without restriction on use by external parties beyond copyright law and the standard conditions agreed by CERN. Data associated with journal publications are also made available: tables and data from plots (e.g. cross section values, likelihood profiles, selection efficiencies, cross section limits, ...) are stored in appropriate repositories such as HEPDATA (http://hepdata.cedar.ac.uk/). ATLAS also strives to make additional material related to the paper available that allows a reinterpretation of the data in the context of new theoretical models. For example, an extended encapsulation of the analysis is often provided for measurements in the framework of RIVET (http://rivet.hepforge.org/)." This information is taken from the ATLAS Data Access Policy, which is a public document that can be downloaded from http://opendata.cern.ch/record/413 [opendata.cern.ch].]

Appendix: Numerical results

Numerical values for p_T and $|\eta|$ K_S^0 unfolded distributions are presented in Tables 12, 13, 14, 15, 16, 17, along with statistical uncertainties and a breakdown of systematic uncertainties.

Table 12 Transverse momentum distribution unfolded to particle level for K_S^0 not associated with jets, and including invisible decays, along with the statistical and systematic uncertainties

p_T[GeV]	$\frac{1}{N_{evt}}\frac{dN}{dp_T}$	Stat.	Model	Track	JES	JER	Pile-up	Fiducial	Unfold
(0.0, 2.0)	1.22	0.04	0.25	0.06	$^{+0.02}_{-0.02}$	0.003	0.10	0.03	0.002
(2.0, 4.0)	0.172	0.008	0.042	0.009	$^{+0.002}_{-0.002}$	0.001	0.014	0.01	$< 10^{-3}$
(4.0, 6.0)	0.034	0.004	0.005	0.002	$^{+0.0008}_{-0.0006}$	$< 10^{-3}$	0.003	0.002	$< 10^{-3}$
(6.0, 8.0)	0.011	0.003	0.001	0.0006	$^{+0.0008}_{-0.0006}$	$< 10^{-3}$	0.001	0.001	$< 10^{-3}$
(8.0, 10.0)	0.0084	0.0025	0.0007	0.0004	$^{+0.0006}_{-0.0004}$	$< 10^{-3}$	0.0007	0.0006	$< 10^{-3}$
(10.0, 20.0)	0.0011	0.0005	0.0001	0.0001	$^{+0.0001}_{-0.0001}$	$< 10^{-3}$	0.0001	0.0001	$< 10^{-4}$

Table 13 Transverse momentum distribution unfolded to the particle level for K_S^0 associated with b-jets, and including invisible decays, along with the statistical and systematic uncertainties

p_T[GeV]	$\frac{1}{N_{evt}}\frac{dN}{dp_T}$	Stat.	Model	Track	JES	JER	Pile-up	Fiducial	Unfold
(0.0, 2.0)	0.091	0.017	0.003	0.005	$^{+0.002}_{-0.002}$	0.001	$< 10^{-3}$	0.001	0.001
(2.0, 4.0)	0.086	0.011	0.003	0.004	$^{+0.003}_{-0.003}$	0.001	$< 10^{-3}$	0.001	0.001
(4.0, 6.0)	0.075	0.010	0.002	0.004	$^{+0.002}_{-0.002}$	0.001	$< 10^{-3}$	0.001	0.001
(6.0, 8.0)	0.045	0.009	0.002	0.002	$^{+0.001}_{-0.001}$	0.001	$< 10^{-3}$	0.001	0.001
(8.0, 10.0)	0.040	0.008	0.002	0.002	$^{+0.001}_{-<10^{-3}}$	$< 10^{-3}$	$< 10^{-3}$	0.001	0.001
(10.0, 15.0)	0.022	0.005	0.002	0.001	$^{+0.001}_{-<10^{-3}}$	$< 10^{-3}$	$< 10^{-3}$	$< 10^{-3}$	$< 10^{-3}$
(15.0, 20.0)	0.0155	0.005	0.001	0.0008	$^{+<10^{-3}}_{-<10^{-3}}$	$< 10^{-3}$	$< 10^{-3}$	$< 10^{-3}$	$< 10^{-3}$
(20.0, 30.0)	0.0053	0.004	0.0003	0.0003	$^{+<10^{-3}}_{-<10^{-3}}$	$< 10^{-4}$	$< 10^{-3}$	$< 10^{-4}$	$< 10^{-3}$

Table 14 Transverse momentum distribution unfolded to the particle level for K_S^0 associated with non-b-jets, and including invisible decays, along with the statistical and systematic uncertainties

p_T[GeV]	$\frac{1}{N_{\text{evt}}}\frac{dN}{dp_T}$	Stat.	Model	Track	JES	JER	Pile-up	Fiducial	Unfold
(0.0, 2.0)	0.080	0.012	0.003	0.003	$+0.004$ -0.005	0.002	$< 10^{-3}$	0.006	0.002
(2.0, 4.0)	0.049	0.006	0.013	0.002	$+0.002$ -0.002	0.001	$< 10^{-3}$	0.004	0.001
(4.0, 6.0)	0.035	0.005	0.011	0.002	$+0.001$ -0.001	0.001	$< 10^{-3}$	0.003	0.001
(6.0, 8.0)	0.016	0.003	0.004	0.001	$+0.001$ -0.0005	0.001	$< 10^{-3}$	$< 10^{-3}$	$< 10^{-3}$
(8.0, 10.0)	0.010	0.003	0.004	0.0004	$+0.0003$ -0.0002	$< 10^{-3}$	$< 10^{-3}$	$< 10^{-3}$	$< 10^{-3}$
(10.0, 15.0)	0.0062	0.002	0.0013	0.0003	$+0.0001$ -0.0001	$< 10^{-4}$	$< 10^{-3}$	$< 10^{-3}$	$< 10^{-3}$
(15.0, 20.0)	0.0017	0.001	0.0004	0.0001	$+<10^{-4}$ $-<10^{-4}$	$< 10^{-4}$	$< 10^{-3}$	$< 10^{-4}$	$< 10^{-4}$
(20.0, 30.0)	0.0009	0.001	0.0002	$< 10^{-4}$	$+<10^{-4}$ $-<10^{-4}$	$< 10^{-4}$	$< 10^{-3}$	$< 10^{-4}$	$< 10^{-4}$

Table 15 Pseudorapidity distribution unfolded to the particle level for K_S^0 not associated with jets, and including invisible decays, along with the statistical and systematic uncertainties

$|\eta|$	$\frac{1}{N_{\text{evt}}}\frac{dN}{d|\eta|}$	Stat.	Model	Track	JES	JER	Pile-up	Fiducial	Unfold
(0.0, 0.5)	0.744	0.036	0.141	0.038	$+0.007$ -0.007	0.004	0.062	0.046	$< 10^{-3}$
(0.5, 1.0)	0.933	0.048	0.120	0.048	$+0.007$ -0.009	0.008	0.077	0.047	$< 10^{-3}$
(1.0, 1.5)	1.161	0.068	0.122	0.059	$+0.010$ -0.008	0.004	0.097	0.041	$< 10^{-3}$
(1.5, 2.0)	1.454	0.108	0.529	0.074	$+0.021$ -0.018	0.021	0.1200	0.030	$< 10^{-3}$
(2.0, 2.5)	1.490	0.167	0.542	0.076	$+0.022$ -0.019	0.022	0.125	0.031	$< 10^{-3}$

Table 16 Pseudorapidity distribution unfolded to the particle level for K_S^0 associated with b-jets, and including invisible decays, along with the statistical and systematic uncertainties

$|\eta|$	$\frac{1}{N_{\text{evt}}}\frac{dN}{d|\eta|}$	Stat.	Model	Track	JES	JER	Pile-up	Fiducial	Unfold
(0.0, 0.5)	0.592	0.055	0.015	0.029	$+0.012$ -0.012	0.009	$< 10^{-3}$	0.032	$< 10^{-3}$
(0.5, 1.0)	0.490	0.059	0.011	0.024	$+0.009$ -0.007	0.007	$< 10^{-3}$	0.019	$< 10^{-3}$
(1.0, 1.5)	0.363	0.062	0.015	0.018	$+0.010$ -0.009	0.007	$< 10^{-3}$	0.002	$< 10^{-3}$
(1.5, 2.0)	0.225	0.059	0.049	0.011	$+0.005$ -0.008	0.002	$< 10^{-3}$	0.016	$< 10^{-3}$
(2.0, 2.5)	0.085	0.051	0.018	0.004	$+0.002$ -0.003	$< 10^{-3}$	$< 10^{-3}$	0.006	$< 10^{-3}$

Table 17 Pseudorapidity distribution unfolded to the particle level for K_S^0 associated with non-b-jets, and including invisible decays, along with the statistical and systematic uncertainties

$|\eta|$	$\frac{1}{N_{\text{evt}}}\frac{dN}{d|\eta|}$	Stat.	Model	Track	JES	JER	Pile-up	Fiducial	Unfold
(0.0, 0.5)	0.233	0.023	0.077	0.010	$+0.007$ -0.009	0.002	$< 10^{-3}$	0.013	$< 10^{-3}$
(0.5, 1.5)	0.191	0.017	0.063	0.008	$+0.006$ -0.006	0.001	$< 10^{-3}$	0.014	$< 10^{-3}$
(1.5, 2.5)	0.088	0.024	0.016	0.004	$+0.003$ -0.004	0.003	$< 10^{-3}$	0.005	$< 10^{-3}$

Numerical values for the p_T and $|\eta|$ Λ unfolded distributions are presented in Tables 18 and 19, along with statistical uncertainties and a breakdown of systematic uncertainties.

Table 18 Transverse momentum distribution unfolded to the particle level for the Λ total sample, and including invisible decays, along with the statistical and systematic uncertainties

p_T[GeV]	$\frac{1}{N_{evt}}\frac{dN}{dp_T}$	Stat.	Model	Track	JES	JER	Pile-up	Fiducial	Unfold
(1.0, 3.0)	0.215	0.034	0.114	0.011	$^{+0.003}_{-0.004}$	0.002	0.017	0.004	$< 10^{-3}$
(3.0, 5.0)	0.053	0.007	0.004	0.003	$^{+0.001}_{-0.001}$	0.001	0.004	0.001	$< 10^{-3}$
(5.0, 7.0)	0.019	0.005	0.002	0.001	$^{+<10^{-3}}_{-<10^{-3}}$	0.001	0.002	0.001	$< 10^{-3}$
(7.0, 10.0)	0.011	0.003	0.001	0.001	$^{+<10^{-3}}_{-<10^{-3}}$	$< 10^{-3}$	0.001	$< 10^{-3}$	$< 10^{-3}$
(10.0, 15.0)	0.0045	0.002	0.002	$< 10^{-3}$	$^{+<10^{-3}}_{-<10^{-3}}$	$< 10^{-3}$	$< 10^{-3}$	$< 10^{-3}$	$< 10^{-3}$
(15.0, 20.0)	0.0024	0.001	0.001	$< 10^{-3}$	$^{+<10^{-4}}_{-<10^{-4}}$	$< 10^{-3}$	$< 10^{-3}$	$< 10^{-4}$	$< 10^{-3}$
(20.0, 30.0)	0.0014	0.001	0.001	$< 10^{-3}$	$^{+<10^{-4}}_{-<10^{-}}$	$< 10^{-4}$	$< 10^{-3}$	$< 10^{-4}$	$< 10^{-4}$

Table 19 Pseudorapidity distribution unfolded to the particle level for the Λ total sample, and including invisible decays, along with the statistical and systematic uncertainties

$|\eta|$	$\frac{1}{N_{evt}}\frac{dN}{d|\eta|}$	Stat.	Model	Track	JES	JER	Pile-up	Fiducial	Unfold
(0.0, 0.5)	0.403	0.053	0.220	0.020	$^{+0.009}_{-0.006}$	0.006	0.032	0.006	$< 10^{-3}$
(0.5, 1.0)	0.358	0.066	0.258	0.018	$^{+0.006}_{-0.008}$	0.003	0.029	0.004	$< 10^{-3}$
(1.0, 1.5)	0.494	0.077	0.488	0.024	$^{+0.011}_{-0.011}$	0.008	0.040	0.011	$< 10^{-3}$
(1.5, 2.5)	0.271	0.077	0.331	0.013	$^{+0.003}_{-0.006}$	0.007	0.022	0.003	$< 10^{-3}$

References

1. PLUTO Collaboration, Inclusive K^0 production in e^+e^- annihilation for $9.3 < \sqrt{s} < 31.6\,GeV$. Phys. Lett. B **104**, 79 (1981)
2. JADE Collaboration, Charged particle and neutral kaon production in e^+e^- annihilation at PETRA. Z. Phys. C **20**, 1594 (1983)
3. TPC Collaboration, K^{*0} and K_S^0 Meson Production in e^+e^- Annihilations at 29 GeV. Phys. Rev. Lett. **53**, 2378 (1984)
4. MARK II Collaboration, Measurement of K^* and K^0 inclusive rates in e^+e^- annihilation at 29 GeV. Phys. Rev. D **31**, 3013 (1985)
5. HRS Collaboration, Hadron production in e^+e^- annihilation at 29 GeV. Phys. Rev. D **35**, 2639 (1987)
6. CELLO Collaboration, Inclusive strange particle production in e^+e^- annihilation. Z. Phys. C **46**, 397 (1990)
7. TASSO Collaboration, Strange meson production in e^+e^- annihilation. Z. Phys. C **47**, 183 (1990)
8. ALEPH Collaboration, Production of K^0 and Λ in hadronic Z decays. Z. Phys. C **64**, 361 (1994)
9. DELPHI Collaboration, Production characteristics of K^0 and light meson resonances in hadronic decays of the Z^0. Z. Phys. C **65**, 587 (1995)
10. OPAL Collaboration, The production of neutral kaons in Z^0 decays and their Bose–Einstein correlations. Z. Phys. C **67**, 389 (1995)
11. L3 Collaboration, Measurement of inclusive production of neutral hadrons from Z decays. Phys. Lett. B **328**, 223 (1994)
12. ATLAS Collaboration, K_S^0 and Λ production in pp interactions at $\sqrt{s} = 0.9$ and $7\,TeV$ measured with the ATLAS detector at the LHC. Phys. Rev. D **85**, 012001 (2012). arXiv:1111.1297 [hep-ex]
13. ATLAS Collaboration, Measurement of the transverse polarization of Λ and $\bar{\Lambda}$ hyperons produced in proton–proton collisions at $\sqrt{s} = 7\,TeV$ using the ATLAS detector. Phys. Rev.D **91**, 032004 (2015). arXiv:1412.1692 [hep-ex]
14. CMS Collaboration, Measurement of neutral strange particle production in the underlying event in proton–proton collisions at $\sqrt{s} = 7\,TeV$. Phys. Rev. D **88**, 052001 (2013). arXiv:1305.6016 [hep-ex]
15. CMS Collaboration, Strange particle production in pp collisions at $\sqrt{s} = 0.9$ and $7\,TeV$. JHEP **05**, 064 (2011). arXiv:1102.4282 [hep-ex]
16. ALICE Collaboration, Strange particle production in proton–proton collisions at $\sqrt{s} = 0.9\,TeV$ with ALICE at the LHC. Eur. Phys. J. C **71**, 1594 (2011). arXiv:1012.3257 [hep-ex]
17. LHCb Collaboration, Prompt K_S^0 production in pp collisions at $\sqrt{s} = 0.9\,TeV$. Phys. Lett. B **693**, 69 (2010). arXiv:1008.3105 [hep-ex]
18. LHCb Collaboration, Measurement of V^0 production ratios in pp collisions at $\sqrt{s} = 0.9$ and $7\,TeV$. JHEP **08**, 034 (2011). arXiv:1107.0882 [hep-ex]
19. STAR Collaboration, Strange particle production in $p + p$ collisions at $\sqrt{s} = 200\,GeV$. Phys. Rev. C **75**, 064901 (2007). arXiv:nucl-ex/0607033
20. UA5 Collaboration, Kaon production in $\bar{p}p$ interactions at c.m. energies from 200 to 900 GeV. Z. Phys. C **41**, 179 (1988)
21. G. Bocquet et al., Inclusive production of strange particles in $p\bar{p}$ collisions at $\sqrt{s} = 630\,GeV$ with UA1. Phys. Lett. B **366**, 441 (1996)
22. CDF Collaboration, K_S^0 and Λ^0 production studies in $p\bar{p}$ collisions at $\sqrt{s} = 1800$ and 630 GeV. Phys. Rev. D **72**, 052001 (2005). arXiv:hep-ex/0504048
23. ZEUS Collaboration, Neutral strange particle production in deep inelastic scattering at HERA. Z. Phys. C **68**, 29 (1995). arXiv:hep-ex/9505011
24. H1 Collaboration, Strangeness production in deep-inelastic positron-proton scattering at HERA. Nucl. Phys. B **480**(480), 3 (1996). arXiv:hep-ex/9607010

25. STAR Collaboration, Enhanced strange baryon production in $Au + Au$ collisions compared to $p + p$ at $\sqrt{s_{NN}} = 200\,GeV$. Phys. Rev. C **77**, 044908 (2008). arXiv:0705.2511

26. STAR Collaboration, Midrapidity Λ and $\bar{\Lambda}$ Production in $Au+Au$ Collisions at $\sqrt{s_{NN}} = 130\,GeV$. Phys. Rev. Lett. **89**, 092301 (2002). arXiv:nucl-ex/0203016 [nucl-ex]

27. P.H. Stuntebeck et al., Inclusive production of K_1^0, Λ^0 and $\bar{\Lambda}_0$ in $18.5 - \frac{GeV}{c}\pi^\pm p$ interactions. Phys. Rev. D **9**, 608 (1974)

28. R. Sugahara et al., Inclusive strange particle production in $\pi^- p$ interactions at 6 GeV/c. Nucl. Phys. B **156**, 237 (1979)

29. V. Blobel et al., Bonn–Hamburg–Munich Collaboration, Multiplicities, topological cross sections, and single particle inclusive distributions from pp interactions at 12 and 24 GeV/c. Nucl. Phys. B **69**, 454 (1974)

30. P. Bosetti et al., Aachen–Bonn–CERN–Cracow Collaboration, Inclusive strange particle production in $\pi^+ p$ interactions at 16 GeV/c. Nucl. Phys. B **94**, 21 (1975)

31. D. Bogert et al., Inclusive production of neutral strange particles in $250\,GeV/c\,\pi^- p$ interactions. Phys. Rev. D **16**, 2098 (1977)

32. F. Barreiro et al., Inclusive neutral-strange-particle production in $\pi^- p$ interactions at 15 GeV/c. Phys. Rev. D **17**, 669 (1978)

33. D. Brick et al., Inclusive production of neutral strange particles by $147\,GeV/c\,\pi^+/K^+/p$ interactions in hydrogen. Nucl. Phys. B **164**, 1 (1980)

34. H. Kichimi et al., Inclusive study of strange-particle production in pp interactions at 405 GeV/c. Phys. Rev. D **20**, 37 (1979)

35. F. Lopinto et al., Inclusive K^0, Λ, $K^{*\pm}(890)$, and $\Sigma^{*\pm}(1385)$ production in pp collisions at 300 GeV/c. Phys. Rev. D **22**, 573 (1980)

36. K. Abe et al., SLAC Hybrid Facility Photon Collaboration, Inclusive photoproduction of neutral strange particles at 20 GeV. Phys. Rev. D **29**, 1877 (1984)

37. I. Cohen et al., Inclusive K_S^0 and Λ Electroproduction. Phys. Rev. Lett. **40**, 1614 (1978)

38. R.G. Hicks et al., Muoproduction of neutral strange hadrons at 225 GeV. Phys. Rev. Lett. **45**, 765 (1980)

39. H. Grassler et al., Aachen–Bonn–CERN–Munich–Oxford Collaboration, Inclusive neutral strange particle production in νp interactions. Nucl. Phys. B **194**, 1 (1992)

40. V.V. Ammosov et al., Charged current events with neutral strange particles in high-energy antineutrino interactions. Nucl. Phys. B **177**, 365 (1981)

41. J. Binnewies, B.A. Kniehl, G. Kramer, Neutral kaon production in e^+e^-, ep and $p\bar{p}$ collisions at next-to-leading order. Phys. Rev. D **53**, 3573 (1996). arXiv:hep-ph/9506437

42. Ch. Bierlich, G. Gustafson, L. Loennblad, A. Tarasov, Effects of overlapping strings in pp collisions. JHEP **03**, 148 (2015). arXiv:1412.6259 [hep-ex]

43. T.S. Biro, H.B. Nielsen, J. Knoll, Color rope model for extreme relativistic heavy ion collisions. Nucl. Phys. B **245**, 449 (1984)

44. STAR Collaboration, Identified particle distributions in pp and Au–Au collisions at $\sqrt{s_{NN}} = 200\,GeV$. Phys. Rev. Lett. **92**, 112301 (2004). arXiv:nucl-ex/0310004

45. A. Ali, F. Barreiro, Th Lagouri, Prospects of measuring the CKM matrix element $|V_{ts}|$ at the LHC. Phys. Lett. B **693**, 44 (2010). arXiv:1005.4647

46. S. Calvente, J. LLorente, F. Barreiro, The importance of jet shapes for tagging purposes. Nucl. Phys. B Proc. **273-275**, 2761 (2016)

47. ATLAS Collaboration, The ATLAS experiment at the CERN LHC. JINST **3**, S08003 (2008)

48. ATLAS Collaboration, Performance of the ATLAS trigger system in, Eur. Phys. J. C **72**(2012), 1849 (2010). arXiv:1110.1530 [hep-ex]

49. S. Agostinelli et al., GEANT4-a simulation toolkit. Nucl. Instr. Methods A **506**, 250 (2008)

50. ATLAS Collaboration, The ATLAS simulation infrastructure. Eur. Phys. J. C **70**, 823 (2010). arXiv:1005.4568 [physics.ins-det]

51. S. Frixione, P. Nason, C. Oleari, Matching NLO QCD computations with parton shower simulations: the POWHEG method. JHEP **11**, 070 (2007). arXiv:0709.2092 [hep-ph]

52. S. Alioli, P. Nason, C. Oleari, E. Re, A general framework for implementing NLO calculations in shower Monte Carlo programs: the POWHEG BOX. JHEP **06**, 043 (2010). arXiv:1002.2581 [hep-ph]

53. S. Frixione, G. Ridolfi, P. Nason, A positive-weight next-to-leading-order Monte Carlo for heavy flavour hadroproduction. JHEP **09**, 126 (2007). arXiv:0707.3088 [hep-ph]

54. T. Sjöstrand et al., High-energy-physics event generation with PYTHIA 6.1. Comput. Phys. Commun. **135**, 238 (2001). arXiv:hep-ph/0010017

55. J. Pumplin et al., New generation of parton distributions with uncertainties from global QCD analysis. JHEP **07**, 012 (2002).

56. B. Andersson., G. Gustafson, G. Ingelman, T. Sjöstrand, Parton fragmentation and string dynamics. Phys. Rep. **97**, 31 (1983)

57. P.Z. Skands, Tuning Monte Carlo generators: the Perugia tunes. Phys. Rev. D **82**, 074018 (1996). arXiv:1005.3457 [hep-ex]

58. S. Frixione, F. Stoeckli, P. Torrielli, B.R. Webber, NLO QCD corrections in Herwig++ with MC@NLO. JHEP **01**, 053 (2011). arXiv:1010.0568 [hep-ex]

59. G. Corcella et al., HERWIG 6: an event generator for hadron emission reactions with interfering gluons (including supersymmetric processes). JHEP **01**, 010 (2001). arXiv:hep-ph/0011363

60. R.D. Field, S. Wolfram, A QCD model for e^+e^- annihilation. Nucl. Phys. B **711**, 65 (1983)

61. H.L. Lai et al., New parton distributions for collider physics. Phys. Rev. D **82**, 074024 (2010). arXiv:1007.2241 [hep-ex]

62. J. Butterworth, J. Forshaw, M. Seymour, Multiparton interactions in photoproduction at HERA. Z. Phys. C **72**, 637 (1996). arXiv:hep-ph/9601371

63. T. Gleisberg et al., Event generator with Sherpa 1.1. JHEP **02**, 007 (2009). arXiv:0811.4622 [hep-ex]

64. R.D. Ball et al., Parton distributions for the LHC Run II. JHEP **04**, 040 (2015). arXiv:1410.8849 [hep-ph]

65. T. Sjöstrand, S. Mrenna, P. Skands, A brief introduction to PYTHIA 8.1. Comput. Phys. Commun. **178**, 852 (2008). arXiv:0710.3820

66. ATLAS Collaboration, ATLAS Pythia 8 tunes to 7 TeV data, ATL-PHYS-PUB-2014-021 (2014). http://cds.cern.ch/record/1966419

67. J. Bellm et al., Herwig 7.0/Herwig++ 3.0 release note. Eur. Phys. J. C **76** 196, (2016). arXiv:1512.01178 [hep-ph]

68. J. Alwall et al., The automated computation of tree-level and next-to-leading order differential cross sections, and their matching to parton shower simulations. JHEP **07**, 079 (2014). arXiv:1405.0301 [hep-ph]

69. B. Kersevan, E. Richter-Was, The Monte Carlo events generator Acer-MC version 1.0 with interfaces to Phythia 6.2 and Herwig 6.3. Comput. Phys. Commun. **149**, 142 (2003). arXiv:hep-ph/0201302

70. A. Buckley et al., Systematic event generator tuning for the LHC. Eur. Phys. J. C **65**, 331 (2010). arXiv:0907.2973 [hep-ph]

71. M.L. Mangano, M. Moretti, F. Piccinini, R. Pittau, A.D. Polosa, ALPGEN, a generator for hard multiparton processes in hadronic collisions. JHEP **0307**, 001 (2003). arXiv:hep-ph/0206293v2 [hep-ph]

72. M. Aliev, H. Lacker, U. Langenfeld, S. Moch, P. Uwer, M. Wiedermann, HATHOR - HAdronic Top and Heavy quarks crOss section calculatoR. Comput. Phys. Commun. **182**, 1034 (2011). arXiv:1007.1327 [hep-ex]

73. N. Kidonakis, Two-loop soft anomalous dimensions for single top quark associated production with a W^- or H^-. Phys. Rev. D **82**, 054018 (2010). arXiv:1005.4451 [hep-ex]

74. R. Gavin, Y. Li, F. Petriello, S. Quackenbush, FEWZ 2.0: a code for hadronic Z production at next-to-next-to-leading order. Comput. Phys. Commun. **182**, 2388 (2011). arXiv:1011.3540 [hep-ex]
75. ATLAS Collaboration, Improved luminosity determination in pp collisions at $\sqrt{s} = 7\,TeV$ using the ATLAS detector at the LHC. Eur. Phys. J. C **73**, 2518 (2013). arXiv:1302.4393 [hep-ex]
76. ATLAS Collaboration, Measurement of the cross-section for top-quark pair production in pp collisions at $\sqrt{s} = 7\,TeV$ with the ATLAS detector using final states with two high-pT leptons. JHEP **05**, 059 (2012). arXiv:1202.4892 [hep-ex]
77. ATLAS Collaboration, Measurement of jet shapes in top pair events at $\sqrt{s} = 7\,TeV$ using the ATLAS detector. Eur. Phys. J. C **72**, 2676 (2013). arXiv:1307.5749 [hep-ex]
78. ATLAS Collaboration, Electron performance measurements with the ATLAS detector using the 2010 LHC proton–proton collision data. Eur. Phys. J. C **72**, 1909 (2012). arXiv:1110.3174 [hep-ex]
79. ATLAS Collaboration, Studies of the performance of the ATLAS detector using cosmic-ray muons. Eur. Phys. J. C **71**, 1593 (2011). arXiv:1011.6665 [physics.ins-det]
80. M. Cacciari, G.P. Salam, G. Soyez, The anti-k_t jet clustering algorithm. JHEP **04**, 063 (2008). arXiv:0802.1189 [hep-ex]
81. ATLAS Collaboration, Topological cell clustering in the ATLAS calorimeters and its performance in LHC Run 1. Eur. Phys. J. C **77**, 490 (2017). arXiv:1603.02934 [hep-ex]
82. W. Lampl et al., Calorimeter clustering algorithms: description and performance, ATLAS-LARGPUB-2008-002 (2008). http://cds.cern.ch/record/1099735
83. M. Aleksa et al., ATLAS combined test beam: computation and validation of the electronic calibration constants for the electromagnetic calorimeter, ATL-LARG-PUB-2006-003 (2006). http://cds.cern.ch/record/942528
84. ATLAS Collaboration, Readiness of the ATLAS Tile Calorimeter for LHC collisions. Eur. Phys. J. C **70**, 1193 (2010). arXiv:1007.5423 [hep-ex]
85. ATLAS Collaboration, Jet energy measurement with the ATLAS detector in proton-proton collisions at $\sqrt{s} = 7\,TeV$. Eur. Phys. J. C **73**, 2304 (2013). arXiv:1112.6426 [hep-ex]
86. ATLAS Collaboration, Measurement of inclusive jet and dijet production in pp collisions at $\sqrt{s} = 7\,TeV$ using the ATLAS detector. Phys. Rev. D **86**, 014022 (2012). arXiv:1112.6297 [hep-ex]
87. ATLAS Collaboration, Jet energy resolution in proton-proton collisions at $\sqrt{s} = 7\,TeV$ recorded in 2010 with the ATLAS detector. Eur. Phys. J. C **73**, 2306 (2013). arXiv:1210.6210 [hep-ex]
88. ATLAS Collaboration, Performance of pile-up mitigation techniques for jets in pp collisions at $\sqrt{s} = 8\,TeV$ using the ATLAS detector. Eur. Phys. J. C **76**, 581 (2016). arXiv:1510.03823 [hep-ex]
89. ATLAS Collaboration, Performance of b-jet identification in the ATLAS experiment. JINST **11**, P04008 (2016). arXiv:1512.01094 [hep-ex]
90. ATLAS Collaboration, Performance of missing transverse momentum reconstruction in proton–proton collisions at $\sqrt{s} = 7\,TeV$ with ATLAS. Eur. Phys. J. C **72**, 1844 (2012). arXiv:1108.5602 [hep-ex]
91. ATLAS Collaboration, Measurement of top quark pair differential cross-sections in the dilepton channel in pp collisions at $\sqrt{s} = 7$ and 8 TeV with ATLAS. Phys. Rev. D **94**, 092003 (2016). arXiv:1607.07281 [hep-ex]
92. ATLAS Collaboration, Charged particle multiplicities in pp interactions measured with the ATLAS detector at the LHC. New J. Phys. **13**, 053033 (2011). arXiv:1012.5104 [hep-ex]
93. ATLAS Collaboration, Performance of the ATLAS silicon pattern recognition algorithm in data and simulation at $\sqrt{s} = 7\,TeV$. ATLAS-CONF-2010-072 (2010). https://cds.cern.ch/record/1281363
94. M. Tanabashi et al., PDG Collaboration, Review of Particle Physics. Phys. Rev. D **98**, 030001 (2018)
95. G. D'Agostini, A multidimensional unfolding method based on Bayes' theorem. Nucl. Instrum. Methods A **362**, 487 (1995)
96. T. Adye, Unfolding algorithms and tests using RooUnfold, PHYSTAT 2011 Proc. (2011). arXiv:1105.1160 [hep-ex]
97. ATLAS Collaboration, Measurement of the inclusive jet cross-sections in proton–proton collisions at $\sqrt{s} = 8\,TeV$ with the ATLAS detector. JHEP **09**, 020 (2017). arXiv:1706.03192 [hep-ex]
98. HepData. www.hepdata.net/record/ins1746286. Accessed 14 Dec 2019
99. P. Skands, S. Carrazza, J. Rojo, Tuning PYTHIA 8.1: the Monash 2013 tune. Eur. Phys. J. C **74**, 3024 (2014). arXiv:1404.5630 [hep-ph]
100. S. Gieseke, P. Kirchgaeßer, S. Plätzer, Baryon production from cluster hadronisation. Eur. Phys. J. C **78**, 99 (2018). arXiv:1710.10906 [hep-ex]

ATLAS Collaboration

G. Aad[101], B. Abbott[128], D. C. Abbott[102], O. Abdinov[13,*], A. Abed Abud[70a,70b], K. Abeling[53], D. K. Abhayasinghe[93], S. H. Abidi[167], O. S. AbouZeid[40], N. L. Abraham[156], H. Abramowicz[161], H. Abreu[160], Y. Abulaiti[6], B. S. Acharya[66a,66b,q], B. Achkar[53], S. Adachi[163], L. Adam[99], C. Adam Bourdarios[132], L. Adamczyk[83a], L. Adamek[167], J. Adelman[120], M. Adersberger[113], A. Adiguzel[12c,al], S. Adorni[54], T. Adye[144], A. A. Affolder[146], Y. Afik[160], C. Agapopoulou[132], M. N. Agaras[38], A. Aggarwal[118], C. Agheorghiesei[27c], J. A. Aguilar-Saavedra[140a,140f,ak], F. Ahmadov[79], W. S. Ahmed[103], X. Ai[15a], G. Aielli[73a,73b], S. Akatsuka[85], T. P. A. Åkesson[96], E. Akilli[54], A. V. Akimov[110], K. Al Khoury[132], G. L. Alberghi[23a,23b], J. Albert[176], M. J. Alconada Verzini[161], S. Alderweireldt[36], M. Aleksa[36], I. N. Aleksandrov[79], C. Alexa[27b], D. Alexandre[19], T. Alexopoulos[10], A. Alfonsi[119], M. Alhroob[128], B. Ali[142], G. Alimonti[68a], J. Alison[37], S. P. Alkire[148], C. Allaire[132], B. M. M. Allbrooke[156], B. W. Allen[131], P. P. Allport[21], A. Aloisio[69a,69b], A. Alonso[40], F. Alonso[88], C. Alpigiani[148], A. A. Alshehri[57], M. Alvarez Estevez[98], D. Álvarez Piqueras[174], M. G. Alviggi[69a,69b], Y. Amaral Coutinho[80b], A. Ambler[103], L. Ambroz[135], C. Amelung[26], D. Amidei[105], S. P. Amor Dos Santos[140a], S. Amoroso[46], C. S. Amrouche[54], F. An[78], C. Anastopoulos[149], N. Andari[145], T. Andeen[11], C. F. Anders[61b], J. K. Anders[20], A. Andreazza[68a,68b], V. Andrei[61a], C. R. Anelli[176], S. Angelidakis[38], A. Angerami[39], A. V. Anisenkov[121a,121b], A. Annovi[71a], C. Antel[61a], M. T. Anthony[149], M. Antonelli[51], D. J. A. Antrim[171], F. Anulli[72a], M. Aoki[81], J. A. Aparisi Pozo[174], L. Aperio Bella[36], G. Arabidze[106], J. P. Araque[140a], V. Araujo Ferraz[80b], R. Araujo Pereira[80b], C. Arcangeletti[51], A. T. H. Arce[49], F. A. Arduh[88], J-F. Arguin[109], S. Argyropoulos[77], J.-H. Arling[46], A. J. Armbruster[36], L. J. Armitage[92], A. Armstrong[171], O. Arnaez[167], H. Arnold[119], A. Artamonov[122,*], G. Artoni[135], S. Artz[99], S. Asai[163], N. Asbah[59], E. M. Asimakopoulou[172], L. Asquith[156], K. Assamagan[29], R. Astalos[28a], R. J. Atkin[33a], M. Atkinson[173], N. B. Atlay[151], H. Atmani[132], K. Augsten[142], G. Avolio[36], R. Avramidou[60a], M. K. Ayoub[15a], A. M. Azoulay[168b], G. Azuelos[109,ba], M. J. Baca[21], H. Bachacou[145], K. Bachas[67a,67b], M. Backes[135], F. Backman[45a,45b], P. Bagnaia[72a,72b], M. Bahmani[84], H. Bahrasemani[152], A. J. Bailey[174], V. R. Bailey[173], J. T. Baines[144], M. Bajic[40], C. Bakalis[10], O. K. Baker[183], P. J. Bakker[119], D. Bakshi Gupta[8], S. Balaji[157], E. M. Baldin[121a,121b], P. Balek[180], F. Balli[145], W. K. Balunas[135], J. Balz[99], E. Banas[84], A. Bandyopadhyay[24], S. Banerjee[181,k], A. A. E. Bannoura[182], L. Barak[161], W. M. Barbe[38], E. L. Barberio[104], D. Barberis[55a,55b], M. Barbero[101], T. Barillari[114], M-S. Barisits[36], J. Barkeloo[131], T. Barklow[153], R. Barnea[160], S. L. Barnes[60c], B. M. Barnett[144], R. M. Barnett[18], Z. Barnovska-Blenessy[60a], A. Baroncelli[60a], G. Barone[29], A. J. Barr[135], L. Barranco Navarro[45a,45b], F. Barreiro[98], J. Barreiro Guimarães da Costa[15a], S. Barsov[138], R. Bartoldus[153], G. Bartolini[101], A. E. Barton[89], P. Bartos[28a], A. Basalaev[46], A. Bassalat[132,at], R. L. Bates[57], S. J. Batista[167], S. Batlamous[35e], J. R. Batley[32], B. Batool[151], M. Battaglia[146], M. Bauce[72a,72b], F. Bauer[145], K. T. Bauer[171], H. S. Bawa[31,o], J. B. Beacham[49], T. Beau[136], P. H. Beauchemin[170], F. Becherer[52], P. Bechtle[24], H. C. Beck[53], H. P. Beck[20,u], K. Becker[52], M. Becker[99], C. Becot[46], A. Beddall[12d], A. J. Beddall[12a], V. A. Bednyakov[79], M. Bedognetti[119], C. P. Bee[155], T. A. Beermann[76], M. Begalli[80b], M. Begel[29], A. Behera[155], J. K. Behr[46], F. Beisiegel[24], A. S. Bell[94], G. Bella[161], L. Bellagamba[23b], A. Bellerive[34], P. Bellos[9], K. Beloborodov[121a,121b], K. Belotskiy[111], N. L. Belyaev[111], D. Benchekroun[35a], N. Benekos[10], Y. Benhammou[161], D. P. Benjamin[6], M. Benoit[54], J. R. Bensinger[26], S. Bentvelsen[119], L. Beresford[135], M. Beretta[51], D. Berge[46], E. Bergeaas Kuutmann[172], N. Berger[5], B. Bergmann[142], L. J. Bergsten[26], J. Beringer[18], S. Berlendis[7], N. R. Bernard[102], G. Bernardi[136], C. Bernius[153], T. Berry[93], P. Berta[99], C. Bertella[15a], I. A. Bertram[89], G. J. Besjes[40], O. Bessidskaia Bylund[182], N. Besson[145], A. Bethani[100], S. Bethke[114], A. Betti[24], A. J. Bevan[92], J. Beyer[114], R. Bi[139], R. M. Bianchi[139], O. Biebel[113], D. Biedermann[19], R. Bielski[36], K. Bierwagen[99], N. V. Biesuz[71a,71b], M. Biglietti[74a], T. R. V. Billoud[109], M. Bindi[53], A. Bingul[12d], C. Bini[72a,72b], S. Biondi[23a,23b], M. Birman[180], T. Bisanz[53], J. P. Biswal[161], A. Bitadze[100], C. Bittrich[48], K. Bjørke[134], K. M. Black[25], T. Blazek[28a], I. Bloch[46], C. Blocker[26], A. Blue[57], U. Blumenschein[92], G. J. Bobbink[119], V. S. Bobrovnikov[121a,121b], S. S. Bocchetta[96], A. Bocci[49], D. Boerner[46], D. Bogavac[14], A. G. Bogdanchikov[121a,121b], C. Bohm[45a], V. Boisvert[93], P. Bokan[53,172], T. Bold[83a], A. S. Boldyrev[112], A. E. Bolz[61b], M. Bomben[136], M. Bona[92], J. S. Bonilla[131], M. Boonekamp[145], H. M. Borecka-Bielska[90], A. Borisov[123], G. Borissov[89], J. Bortfeldt[36], D. Bortoletto[135], V. Bortolotto[73a,73b], D. Boscherini[23b], M. Bosman[14], J. D. Bossio Sola[103], K. Bouaouda[35a], J. Boudreau[139], E. V. Bouhova-Thacker[89], D. Boumediene[38], S. K. Boutle[57], A. Boveia[126], J. Boyd[36], D. Boye[33b,au], I. R. Boyko[79], A. J. Bozson[93], J. Bracinik[21], N. Brahimi[101], G. Brandt[182], O. Brandt[61a], F. Braren[46], B. Brau[102], J. E. Brau[131], W. D. Breaden Madden[57], K. Brendlinger[46], L. Brenner[46], R. Brenner[172], S. Bressler[180], B. Brickwedde[99], D. L. Briglin[21], D. Britton[57], D. Britzger[114], I. Brock[24], R. Brock[106], G. Brooijmans[39], W. K. Brooks[147c], E. Brost[120], J.H Broughton[21], P. A. Bruckman de Renstrom[84], D. Bruncko[28b], A. Bruni[23b], G. Bruni[23b], L. S. Bruni[119], S. Bruno[73a,73b], B. H. Brunt[32], M. Bruschi[23b], N. Bruscino[139], P. Bryant[37], L. Bryngemark[96], T. Buanes[17], Q. Buat[36], P. Buchholz[151], A. G. Buckley[57], I. A. Budagov[79], M. K. Bugge[134], F. Bührer[52], O. Bulekov[111], T. J. Burch[120], S. Burdin[90], C. D. Burgard[119], A. M. Burger[129], B. Burghgrave[8], J. T. P. Burr[46],

J. C. Burzynski[102], V. Büscher[99], E. Buschmann[53], P. J. Bussey[57], J. M. Butler[25], C. M. Buttar[57], J. M. Butterworth[94], P. Butti[36], W. Buttinger[36], A. Buzatu[158], A. R. Buzykaev[121a,121b], G. Cabras[23a,23b], S. Cabrera Urbán[174], D. Caforio[56], H. Cai[173], V. M. M. Cairo[153], O. Cakir[4a], N. Calace[36], P. Calafiura[18], A. Calandri[101], G. Calderini[136], P. Calfayan[65], G. Callea[57], L. P. Caloba[80b], S. Calvente Lopez[98], D. Calvet[38], S. Calvet[38], T. P. Calvet[155], M. Calvetti[71a,71b], R. Camacho Toro[136], S. Camarda[36], D. Camarero Munoz[98], P. Camarri[73a,73b], D. Cameron[134], R. Caminal Armadans[102], C. Camincher[36], S. Campana[36], M. Campanelli[94], A. Camplani[40], A. Campoverde[151], V. Canale[69a,69b], A. Canesse[103], M. Cano Bret[60c], J. Cantero[129], T. Cao[161], Y. Cao[173], M. D. M. Capeans Garrido[36], M. Capua[41a,41b], R. Cardarelli[73a], F. Cardillo[149], G. Carducci[41a,41b], I. Carli[143], T. Carli[36], G. Carlino[69a], B. T. Carlson[139], L. Carminati[68a,68b], R. M. D. Carney[45a,45b], S. Caron[118], E. Carquin[147c], S. Carrá[46], J. W. S. Carter[167], M. P. Casado[14,f], A. F. Casha[167], D. W. Casper[171], R. Castelijn[119], F. L. Castillo[174], V. Castillo Gimenez[174], N. F. Castro[140a,140e], A. Catinaccio[36], J. R. Catmore[134], A. Cattai[36], J. Caudron[24], V. Cavaliere[29], E. Cavallaro[14], M. Cavalli-Sforza[14], V. Cavasinni[71a,71b], E. Celebi[12b], F. Ceradini[74a,74b], L. Cerda Alberich[174], K. Cerny[130], A. S. Cerqueira[80a], A. Cerri[156], L. Cerrito[73a,73b], F. Cerutti[18], A. Cervelli[23a,23b], S. A. Cetin[12b], D. Chakraborty[120], S. K. Chan[59], W. S. Chan[119], W. Y. Chan[90], J. D. Chapman[32], B. Chargeishvili[159b], D. G. Charlton[21], T. P. Charman[92], C. C. Chau[34], S. Che[126], A. Chegwidden[106], S. Chekanov[6], S. V. Chekulaev[168a], G. A. Chelkov[79,az], M. A. Chelstowska[36], B. Chen[78], C. Chen[60a], C. H. Chen[78], H. Chen[29], J. Chen[60a], J. Chen[39], S. Chen[137], S. J. Chen[15c], X. Chen[15b,ay], Y. Chen[82], Y-H. Chen[46], H. C. Cheng[63a], H. J. Cheng[15a,15d], A. Cheplakov[79], E. Cheremushkina[123], R. Cherkaoui El Moursli[35e], E. Cheu[7], K. Cheung[64], T. J. A. Chevalérias[145], L. Chevalier[145], V. Chiarella[51], G. Chiarelli[71a], G. Chiodini[67a], A. S. Chisholm[36,21], A. Chitan[27b], I. Chiu[163], Y. H. Chiu[176], M. V. Chizhov[79], K. Choi[65], A. R. Chomont[72a,72b], S. Chouridou[162], Y. S. Chow[119], M. C. Chu[63a], X. Chu[15a], J. Chudoba[141], A. J. Chuinard[103], J. J. Chwastowski[84], L. Chytka[130], K. M. Ciesla[84], D. Cinca[47], V. Cindro[91], I. A. Cioară[27b], A. Ciocio[18], F. Cirotto[69a,69b], Z. H. Citron[180,m], M. Citterio[68a], D. A. Ciubotaru[27b], B. M. Ciungu[167], A. Clark[54], M. R. Clark[39], P. J. Clark[50], C. Clement[45a,45b], Y. Coadou[101], M. Cobal[66a,66c], A. Coccaro[55b], J. Cochran[78], H. Cohen[161], A. E. C. Coimbra[36], L. Colasurdo[118], B. Cole[39], A. P. Colijn[119], J. Collot[58], P. Conde Muiño[140a,g], E. Coniavitis[52], S. H. Connell[33b], I. A. Connelly[57], S. Constantinescu[27b], F. Conventi[69a,bb], A. M. Cooper-Sarkar[135], F. Cormier[175], K. J. R. Cormier[167], L. D. Corpe[94], M. Corradi[72a,72b], E. E. Corrigan[96], F. Corriveau[103,ag], A. Cortes-Gonzalez[36], M. J. Costa[174], F. Costanza[5], D. Costanzo[149], G. Cowan[93], J. W. Cowley[32], J. Crane[100], K. Cranmer[124], S. J. Crawley[57], R. A. Creager[137], S. Crépé-Renaudin[58], F. Crescioli[136], M. Cristinziani[24], V. Croft[119], G. Crosetti[41a,41b], A. Cueto[5], T. Cuhadar Donszelmann[149], A. R. Cukierman[153], S. Czekierda[84], P. Czodrowski[36], M. J. Da Cunha Sargedas De Sousa[60b], J. V. Da Fonseca Pinto[80b], C. Da Via[100], W. Dabrowski[83a], T. Dado[28a], S. Dahbi[35e], T. Dai[105], C. Dallapiccola[102], M. Dam[40], G. D'amen[23a,23b], V. D'Amico[74a,74b], J. Damp[99], J. R. Dandoy[137], M. F. Daneri[30], N. P. Dang[181,k], N. S. Dann[100], M. Danninger[175], V. Dao[36], G. Darbo[55b], O. Dartsi[5], A. Dattagupta[131], T. Daubney[46], S. D'Auria[68a,68b], W. Davey[24], C. David[46], T. Davidek[143], D. R. Davis[49], I. Dawson[149], K. De[8], R. De Asmundis[69a], M. De Beurs[119], S. De Castro[23a,23b], S. De Cecco[72a,72b], N. De Groot[118], P. de Jong[119], H. De la Torre[106], A. De Maria[15c], D. De Pedis[72a], A. De Salvo[72a], U. De Sanctis[73a,73b], M. De Santis[73a,73b], A. De Santo[156], K. De Vasconcelos Corga[101], J. B. De Vivie De Regie[132], C. Debenedetti[146], D. V. Dedovich[79], A. M. Deiana[42], M. Del Gaudio[41a,41b], J. Del Peso[98], Y. Delabat Diaz[46], D. Delgove[132], F. Deliot[145,t], C. M. Delitzsch[7], M. Della Pietra[69a,69b], D. Della Volpe[54], A. Dell'Acqua[36], L. Dell'Asta[73a,73b], M. Delmastro[5], C. Delporte[132], P. A. Delsart[58], D. A. DeMarco[167], S. Demers[183], M. Demichev[79], G. Demontigny[109], S. P. Denisov[123], D. Denysiuk[119], L. D'Eramo[136], D. Derendarz[84], J. E. Derkaoui[35d], F. Derue[136], P. Dervan[90], K. Desch[24], C. Deterre[46], K. Dette[167], C. Deutsch[24], M. R. Devesa[30], P. O. Deviveiros[36], A. Dewhurst[144], S. Dhaliwal[26], F. A. Di Bello[54], A. Di Ciaccio[73a,73b], L. Di Ciaccio[5], W. K. Di Clemente[137], C. Di Donato[69a,69b], A. Di Girolamo[36], G. Di Gregorio[71a,71b], B. Di Micco[74a,74b], R. Di Nardo[102], K. F. Di Petrillo[59], R. Di Sipio[167], D. Di Valentino[34], C. Diaconu[101], F. A. Dias[40], T. Dias Do Vale[140a], M. A. Diaz[147a], J. Dickinson[18], E. B. Diehl[105], J. Dietrich[19], S. Díez Cornell[46], A. Dimitrievska[18], W. Ding[15b], J. Dingfelder[24], F. Dittus[36], F. Djama[101], T. Djobava[159b], J. I. Djuvsland[17], M. A. B. Do Vale[80c], M. Dobre[27b], D. Dodsworth[26], C. Doglioni[96], J. Dolejsi[143], Z. Dolezal[143], M. Donadelli[80d], B. Dong[60c], J. Donini[38], A. D'onofrio[92], M. D'Onofrio[90], J. Dopke[144], A. Doria[69a], M. T. Dova[88], A. T. Doyle[57], E. Drechsler[152], E. Dreyer[152], T. Dreyer[53], A. S. Drobac[170], Y. Duan[60b], F. Dubinin[110], M. Dubovsky[28a], A. Dubreuil[54], E. Duchovni[180], G. Duckeck[113], A. Ducourthial[136], O. A. Ducu[109], D. Duda[114], A. Dudarev[36], A. C. Dudder[99], E. M. Duffield[18], L. Duflot[132], M. Dührssen[36], C. Dülsen[182], M. Dumancic[180], A. E. Dumitriu[27b], A. K. Duncan[57], M. Dunford[61a], A. Duperrin[101], H. Duran Yildiz[4a], M. Düren[56], A. Durglishvili[159b], D. Duschinger[48], B. Dutta[46], D. Duvnjak[1], G. I. Dyckes[137], M. Dyndal[36], S. Dysch[100], B. S. Dziedzic[84], K. M. Ecker[114], R. C. Edgar[105], T. Eifert[36], G. Eigen[17], K. Einsweiler[18], T. Ekelof[172], H. El Jarrari[35e], M. El Kacimi[35c], R. El Kosseifi[101], V. Ellajosyula[172], M. Ellert[172], F. Ellinghaus[182], A. A. Elliot[92], N. Ellis[36], J. Elmsheuser[29], M. Elsing[36], D. Emeliyanov[144], A. Emerman[39], Y. Enari[163], J. S. Ennis[178], M. B. Epland[49], J. Erdmann[47], A. Ereditato[20], M. Errenst[36], M. Escalier[132],

C. Escobar[174], O. Estrada Pastor[174], E. Etzion[161], H. Evans[65], A. Ezhilov[138], F. Fabbri[57], L. Fabbri[23a,23b], V. Fabiani[118], G. Facini[94], R. M. Faisca Rodrigues Pereira[140a], R. M. Fakhrutdinov[123], S. Falciano[72a], P. J. Falke[5], S. Falke[5], J. Faltova[143], Y. Fang[15a], Y. Fang[15a], G. Fanourakis[44], M. Fanti[68a,68b], A. Farbin[8], A. Farilla[74a], E. M. Farina[70a,70b], T. Farooque[106], S. Farrell[18], S. M. Farrington[50], P. Farthouat[36], F. Fassi[35e], P. Fassnacht[36], D. Fassouliotis[9], M. Faucci Giannelli[50], W. J. Fawcett[32], L. Fayard[132], O. L. Fedin[138,r], W. Fedorko[175], M. Feickert[42], S. Feigl[134], L. Feligioni[101], A. Fell[149], C. Feng[60b], E. J. Feng[36], M. Feng[49], M. J. Fenton[57], A. B. Fenyuk[123], J. Ferrando[46], A. Ferrante[173], A. Ferrari[172], P. Ferrari[119], R. Ferrari[70a], D. E. Ferreira de Lima[61b], A. Ferrer[174], D. Ferrere[54], C. Ferretti[105], F. Fiedler[99], A. Filipčič[91], F. Filthaut[118], K. D. Finelli[25], M. C. N. Fiolhais[140a,140c,a], L. Fiorini[174], F. Fischer[113], W. C. Fisher[106], I. Fleck[151], P. Fleischmann[105], R. R. M. Fletcher[137], T. Flick[182], B. M. Flierl[113], L. Flores[137], L. R. Flores Castillo[63a], F. M. Follega[75a,75b], N. Fomin[17], J. H. Foo[167], G. T. Forcolin[75a,75b], A. Formica[145], F. A. Förster[14], A. C. Forti[100], A. G. Foster[21], M. G. Foti[135], D. Fournier[132], H. Fox[89], P. Francavilla[71a,71b], S. Francescato[72a,72b], M. Franchini[23a,23b], S. Franchino[61a], D. Francis[36], L. Franconi[20], M. Franklin[59], A. N. Fray[92], B. Freund[109], W. S. Freund[80b], E. M. Freundlich[47], D. C. Frizzell[128], D. Froidevaux[36], J. A. Frost[135], C. Fukunaga[164], E. Fullana Torregrosa[174], E. Fumagalli[55a,55b], T. Fusayasu[115], J. Fuster[174], A. Gabrielli[23a,23b], A. Gabrielli[18], G. P. Gach[83a], S. Gadatsch[54], P. Gadow[114], G. Gagliardi[55a,55b], L. G. Gagnon[109], C. Galea[27b], B. Galhardo[140a], G. E. Gallardo[135], E. J. Gallas[135], B. J. Gallop[144], P. Gallus[142], G. Galster[40], R. Gamboa Goni[92], K. K. Gan[126], S. Ganguly[180], J. Gao[60a], Y. Gao[90], Y. S. Gao[31,o], C. García[174], J. E. García Navarro[174], J. A. García Pascual[15a], C. Garcia-Argos[52], M. Garcia-Sciveres[18], R. W. Gardner[37], N. Garelli[153], S. Gargiulo[52], V. Garonne[134], A. Gaudiello[55a,55b], G. Gaudio[70a], I. L. Gavrilenko[110], A. Gavrilyuk[122], C. Gay[175], G. Gaycken[24], E. N. Gazis[10], A. A. Geanta[27b], C. N. P. Gee[144], J. Geisen[53], M. Geisen[99], M. P. Geisler[61a], C. Gemme[55b], M. H. Genest[58], C. Geng[105], S. Gentile[72a,72b], S. George[93], T. Geralis[44], L. O. Gerlach[53], P. Gessinger-Befurt[99], G. Gessner[47], S. Ghasemi[151], M. Ghasemi Bostanabad[176], A. Ghosh[132], A. Ghosh[77], B. Giacobbe[23b], S. Giagu[72a,72b], N. Giangiacomi[23a,23b], P. Giannetti[71a], A. Giannini[69a,69b], S. M. Gibson[93], M. Gignac[146], D. Gillberg[34], G. Gilles[182], D. M. Gingrich[3,ba], M. P. Giordani[66a,66c], F. M. Giorgi[23b], P. F. Giraud[145], G. Giugliarelli[66a,66c], D. Giugni[68a], F. Giuli[73a,73b], S. Gkaitatzis[162], I. Gkialas[9,i], E. L. Gkougkousis[14], P. Gkountoumis[10], L. K. Gladilin[112], C. Glasman[98], J. Glatzer[14], P. C. F. Glaysher[46], A. Glazov[46], M. Goblirsch-Kolb[26], S. Goldfarb[104], T. Golling[54], D. Golubkov[123], A. Gomes[140a,140b], R. Goncalves Gama[53], R. Gonçalo[140a,140b], G. Gonella[52], L. Gonella[21], A. Gongadze[79], F. Gonnella[21], J. L. Gonski[59], S. González de la Hoz[174], S. Gonzalez-Sevilla[54], G. R. Gonzalvo Rodriguez[174], L. Goossens[36], P. A. Gorbounov[122], H. A. Gordon[29], B. Gorini[36], E. Gorini[67a,67b], A. Gorišek[91], A. T. Goshaw[49], M. I. Gostkin[79], C. A. Gottardo[24], M. Gouighri[35b], D. Goujdami[35c], A. G. Goussiou[148], N. Govender[33b,b], C. Goy[5], E. Gozani[160], I. Grabowska-Bold[83a], E. C. Graham[90], J. Gramling[171], E. Gramstad[134], S. Grancagnolo[19], M. Grandi[156], V. Gratchev[138], P. M. Gravila[27f], F. G. Gravili[67a,67b], C. Gray[57], H. M. Gray[18], C. Grefe[24], K. Gregersen[96], I. M. Gregor[46], P. Grenier[153], K. Grevtsov[46], C. Grieco[14], N. A. Grieser[128], J. Griffiths[8], A. A. Grillo[146], K. Grimm[31,n], S. Grinstein[14,aa], J.-F. Grivaz[132], S. Groh[99], E. Gross[180], J. Grosse-Knetter[53], Z. J. Grout[94], C. Grud[105], A. Grummer[117], L. Guan[105], W. Guan[181], J. Guenther[36], A. Guerguichon[132], J. G. R. Guerrero Rojas[174], F. Guescini[114], D. Guest[171], R. Gugel[52], T. Guillemin[5], S. Guindon[36], U. Gul[57], J. Guo[60c], W. Guo[105], Y. Guo[60a,v], Z. Guo[101], R. Gupta[46], S. Gurbuz[12c], G. Gustavino[128], P. Gutierrez[128], C. Gutschow[94], C. Guyot[145], M. P. Guzik[83a], C. Gwenlan[135], C. B. Gwilliam[90], A. Haas[124], C. Haber[18], H. K. Hadavand[8], N. Haddad[35e], A. Hadef[60a], S. Hageböck[36], M. Hagihara[169], M. Haleem[177], J. Haley[129], G. Halladjian[106], G. D. Hallewell[101], K. Hamacher[182], P. Hamal[130], K. Hamano[176], H. Hamdaoui[35e], G. N. Hamity[149], K. Han[60a,an], L. Han[60a], S. Han[15a,15d], K. Hanagaki[81,y], M. Hance[146], D. M. Handl[113], B. Haney[137], R. Hankache[136], E. Hansen[96], J. B. Hansen[40], J. D. Hansen[40], M. C. Hansen[24], P. H. Hansen[40], E. C. Hanson[100], K. Hara[169], A. S. Hard[181], T. Harenberg[182], S. Harkusha[107], P. F. Harrison[178], N. M. Hartmann[113], Y. Hasegawa[150], A. Hasib[50], S. Hassani[145], S. Haug[20], R. Hauser[106], L. B. Havener[39], M. Havranek[142], C. M. Hawkes[21], R. J. Hawkings[36], D. Hayden[106], C. Hayes[155], R. L. Hayes[175], C. P. Hays[135], J. M. Hays[92], H. S. Hayward[90], S. J. Haywood[144], F. He[60a], M. P. Heath[50], V. Hedberg[96], L. Heelan[8], S. Heer[24], K. K. Heidegger[52], W. D. Heidorn[78], J. Heilman[34], S. Heim[46], T. Heim[18], B. Heinemann[46,av], J. J. Heinrich[131], L. Heinrich[36], C. Heinz[56], J. Hejbal[141], L. Helary[61b], A. Held[175], S. Hellesund[134], C. M. Helling[146], S. Hellman[45a,45b], C. Helsens[36], R. C. W. Henderson[89], Y. Heng[181], S. Henkelmann[175], A. M. Henriques Correia[36], G. H. Herbert[19], H. Herde[26], V. Herget[177], Y. Hernández Jiménez[33c], H. Herr[99], M. G. Herrmann[113], T. Herrmann[48], G. Herten[52], R. Hertenberger[113], L. Hervas[36], T. C. Herwig[137], G. G. Hesketh[94], N. P. Hessey[168a], A. Higashida[163], S. Higashino[81], E. Higón-Rodriguez[174], K. Hildebrand[37], E. Hill[176], J. C. Hill[32], K. K. Hill[29], K. H. Hiller[46], S. J. Hillier[21], M. Hils[48], I. Hinchliffe[18], F. Hinterkeuser[24], M. Hirose[133], S. Hirose[52], D. Hirschbuehl[182], B. Hiti[91], O. Hladik[141], D. R. Hlaluku[33c], X. Hoad[50], J. Hobbs[155], N. Hod[180], M. C. Hodgkinson[149], A. Hoecker[36], F. Hoenig[113], D. Hohn[52], D. Hohov[132], T. R. Holmes[37], M. Holzbock[113], L. B. A. H Hommels[32], S. Honda[169], T. Honda[81], T. M. Hong[139], A. Hönle[114], B. H. Hooberman[173], W. H. Hopkins[6], Y. Horii[116], P. Horn[48], L. A. Horyn[37], J-Y. Hostachy[58], A. Hostiuc[148],

S. Hou[158], A. Hoummada[35a], J. Howarth[100], J. Hoya[88], M. Hrabovsky[130], J. Hrdinka[76], I. Hristova[19], J. Hrivnac[132], A. Hrynevich[108], T. Hryn'ova[5], P. J. Hsu[64], S.-C. Hsu[148], Q. Hu[29], S. Hu[60c], Y. Huang[15a], Z. Hubacek[142], F. Hubaut[101], M. Huebner[24], F. Huegging[24], T. B. Huffman[135], M. Huhtinen[36], R. F. H. Hunter[34], P. Huo[155], A. M. Hupe[34], N. Huseynov[79,ai], J. Huston[106], J. Huth[59], R. Hyneman[105], S. Hyrych[28a], G. Iacobucci[54], G. Iakovidis[29], I. Ibragimov[151], L. Iconomidou-Fayard[132], Z. Idrissi[35e], P. Iengo[36], R. Ignazzi[40], O. Igonkina[119,ac,*], R. Iguchi[163], T. Iizawa[54], Y. Ikegami[81], M. Ikeno[81], D. Iliadis[162], N. Ilic[118], F. Iltzsche[48], G. Introzzi[70a,70b], M. Iodice[74a], K. Iordanidou[168a], V. Ippolito[72a,72b], M. F. Isacson[172], M. Ishino[163], M. Ishitsuka[165], W. Islam[129], C. Issever[135], S. Istin[160], F. Ito[169], J. M. Iturbe Ponce[63a], R. Iuppa[75a,75b], A. Ivina[180], H. Iwasaki[81], J. M. Izen[43], V. Izzo[69a], P. Jacka[141], P. Jackson[1], R. M. Jacobs[24], B. P. Jaeger[152], V. Jain[2], G. Jäkel[182], K. B. Jakobi[99], K. Jakobs[52], S. Jakobsen[76], T. Jakoubek[141], J. Jamieson[57], K. W. Janas[83a], R. Jansky[54], J. Janssen[24], M. Janus[53], P. A. Janus[83a], G. Jarlskog[96], N. Javadov[79,ai], T. Javůrek[36], M. Javurkova[52], F. Jeanneau[145], L. Jeanty[131], J. Jejelava[159a,aj], A. Jelinskas[178], P. Jenni[52,c], J. Jeong[46], N. Jeong[46], S. Jézéquel[5], H. Ji[181], J. Jia[155], H. Jiang[78], Y. Jiang[60a], Z. Jiang[153,s], S. Jiggins[52], F. A. Jimenez Morales[38], J. Jimenez Pena[174], S. Jin[15c], A. Jinaru[27b], O. Jinnouchi[165], H. Jivan[33c], P. Johansson[149], K. A. Johns[7], C. A. Johnson[65], K. Jon-And[45a,45b], R. W. L. Jones[89], S. D. Jones[156], S. Jones[7], T. J. Jones[90], J. Jongmanns[61a], P. M. Jorge[140a], J. Jovicevic[36], X. Ju[18], J. J. Junggeburth[114], A. Juste Rozas[14,aa], A. Kaczmarska[84], M. Kado[72a,72b], H. Kagan[126], M. Kagan[153], C. Kahra[99], T. Kaji[179], E. Kajomovitz[160], C. W. Kalderon[96], A. Kaluza[99], A. Kamenshchikov[123], L. Kanjir[91], Y. Kano[163], V. A. Kantserov[111], J. Kanzaki[81], L. S. Kaplan[181], D. Kar[33c], M. J. Kareem[168b], E. Karentzos[10], S. N. Karpov[79], Z. M. Karpova[79], V. Kartvelishvili[89], A. N. Karyukhin[123], L. Kashif[181], R. D. Kass[126], A. Kastanas[45a,45b], Y. Kataoka[163], C. Kato[60c,60d], J. Katzy[46], K. Kawade[82], K. Kawagoe[87], T. Kawaguchi[116], T. Kawamoto[163], G. Kawamura[53], E. F. Kay[176], V. F. Kazanin[121a,121b], R. Keeler[176], R. Kehoe[42], J. S. Keller[34], E. Kellermann[96], D. Kelsey[156], J. J. Kempster[21], J. Kendrick[21], O. Kepka[141], S. Kersten[182], B. P. Kerševan[91], S. Ketabchi Haghighat[167], M. Khader[173], F. Khalil-Zada[13], M. Khandoga[145], A. Khanov[129], A. G. Kharlamov[121a,121b], T. Kharlamova[121a,121b], E. E. Khoda[175], A. Khodinov[166], T. J. Khoo[54], E. Khramov[79], J. Khubua[159b], S. Kido[82], M. Kiehn[54], C. R. Kilby[93], Y. K. Kim[37], N. Kimura[66a,66c], O. M. Kind[19], B. T. King[90,*], D. Kirchmeier[48], J. Kirk[144], A. E. Kiryunin[114], T. Kishimoto[163], D. P. Kisliuk[167], V. Kitali[46], O. Kivernyk[5], E. Kladiva[28b,*], T. Klapdor-Kleingrothaus[52], M. Klassen[61a], M. H. Klein[105], M. Klein[90], U. Klein[90], K. Kleinknecht[99], P. Klimek[120], A. Klimentov[29], T. Klingl[24], T. Klioutchnikova[36], F. F. Klitzner[113], P. Kluit[119], S. Kluth[114], E. Kneringer[76], E. B. F. G. Knoops[101], A. Knue[52], D. Kobayashi[87], T. Kobayashi[163], M. Kobel[48], M. Kocian[153], P. Kodys[143], P. T. Koenig[24], T. Koffas[34], N. M. Köhler[114], T. Koi[153], M. Kolb[61b], I. Koletsou[5], T. Komarek[130], T. Kondo[81], N. Kondrashova[60c], K. Köneke[52], A. C. König[118], T. Kono[125], R. Konoplich[124,aq], V. Konstantinides[94], N. Konstantinidis[94], B. Konya[96], R. Kopeliansky[65], S. Koperny[83a], K. Korcyl[84], K. Kordas[162], G. Koren[161], A. Korn[94], I. Korolkov[14], E. V. Korolkova[149], N. Korotkova[112], O. Kortner[114], S. Kortner[114], T. Kosek[143], V. V. Kostyukhin[24], A. Kotwal[49], A. Koulouris[10], A. Kourkoumeli-Charalampidi[70a,70b], C. Kourkoumelis[9], E. Kourlitis[149], V. Kouskoura[29], A. B. Kowalewska[84], R. Kowalewski[176], C. Kozakai[163], W. Kozanecki[145], A. S. Kozhin[123], V. A. Kramarenko[112], G. Kramberger[91], D. Krasnopevtsev[60a], M. W. Krasny[136], A. Krasznahorkay[36], D. Krauss[114], J. A. Kremer[83a], J. Kretzschmar[90], P. Krieger[167], F. Krieter[113], A. Krishnan[61b], K. Krizka[18], K. Kroeninger[47], H. Kroha[114], J. Kroll[141], J. Kroll[137], J. Krstic[16], U. Kruchonak[79], H. Krüger[24], N. Krumnack[78], M. C. Kruse[49], J. A. Krzysiak[84], T. Kubota[104], O. Kuchinskaia[166], S. Kuday[4b], J. T. Kuechler[46], S. Kuehn[36], A. Kugel[61a], T. Kuhl[46], V. Kukhtin[79], R. Kukla[101], Y. Kulchitsky[107,am], S. Kuleshov[147c], Y. P. Kulinich[173], M. Kuna[58], T. Kunigo[85], A. Kupco[141], T. Kupfer[47], O. Kuprash[52], H. Kurashige[82], L. L. Kurchaninov[168a], Y. A. Kurochkin[107], A. Kurova[111], M. G. Kurth[15a,15d], E. S. Kuwertz[36], M. Kuze[165], A. K. Kvam[148], J. Kvita[130], T. Kwan[103], A. La Rosa[114], L. La Rotonda[41a,41b], F. La Ruffa[41a,41b], C. Lacasta[174], F. Lacava[72a,72b], D. P. J. Lack[100], H. Lacker[19], D. Lacour[136], E. Ladygin[79], R. Lafaye[5], B. Laforge[136], T. Lagouri[33c], S. Lai[53], S. Lammers[65], W. Lampl[7], C. Lampoudis[162], E. Lançon[29], U. Landgraf[52], M. P. J. Landon[92], M. C. Lanfermann[54], V. S. Lang[46], J. C. Lange[53], R. J. Langenberg[36], A. J. Lankford[171], F. Lanni[29], K. Lantzsch[24], A. Lanza[70a], A. Lapertosa[55a,55b], S. Laplace[136], J. F. Laporte[145], T. Lari[68a], F. Lasagni Manghi[23a,23b], M. Lassnig[36], T. S. Lau[63a], A. Laudrain[132], A. Laurier[34], M. Lavorgna[69a,69b], M. Lazzaroni[68a,68b], B. Le[104], E. Le Guirriec[101], M. LeBlanc[7], T. LeCompte[6], F. Ledroit-Guillon[58], C. A. Lee[29], G. R. Lee[17], L. Lee[59], S. C. Lee[158], S. J. Lee[34], B. Lefebvre[168a], M. Lefebvre[176], F. Legger[113], C. Leggett[18], K. Lehmann[152], N. Lehmann[182], G. Lehmann Miotto[36], W. A. Leight[46], A. Leisos[162,z], M. A. L. Leite[80d], C. E. Leitgeb[113], R. Leitner[143], D. Lellouch[180,*], K. J. C. Leney[42], T. Lenz[24], B. Lenzi[36], R. Leone[7], S. Leone[71a], C. Leonidopoulos[50], A. Leopold[136], G. Lerner[156], C. Leroy[109], R. Les[167], C. G. Lester[32], M. Levchenko[138], J. Levêque[5], D. Levin[105], L. J. Levinson[180], D. J. Lewis[21], B. Li[15b], B. Li[105], C-Q. Li[60a], F. Li[60c], H. Li[60a], H. Li[60b], J. Li[60c], K. Li[153], L. Li[60c], M. Li[15a], Q. Li[15a,15d], Q. Y. Li[60a], S. Li[60c,60d], X. Li[46], Y. Li[46], Z. Li[60b], Z. Liang[15a], B. Liberti[73a], A. Liblong[167], K. Lie[63c], S. Liem[119], C. Y. Lin[32], K. Lin[106], T. H. Lin[99], R. A. Linck[65], J. H. Lindon[21], A. L. Lionti[54], E. Lipeles[137], A. Lipniacka[17], M. Lisovyi[61b],

T. M. Liss[173,ax], A. Lister[175], A. M. Litke[146], J. D. Little[8], B. Liu[78,af], B.L Liu[6], H. B. Liu[29], H. Liu[105], J. B. Liu[60a], J. K. K. Liu[135], K. Liu[136], M. Liu[60a], P. Liu[18], Y. Liu[15a,15d], Y. L. Liu[105], Y. W. Liu[60a], M. Livan[70a,70b], A. Lleres[58], J. Llorente Merino[15a], S. L. Lloyd[92], C. Y. Lo[63b], F. Lo Sterzo[42], E. M. Lobodzinska[46], P. Loch[7], S. Loffredo[73a,73b], T. Lohse[19], K. Lohwasser[149], M. Lokajicek[141], J. D. Long[173], R. E. Long[89], L. Longo[36], K. A. Looper[126], J. A. Lopez[147c], I. Lopez Paz[100], A. Lopez Solis[149], J. Lorenz[113], N. Lorenzo Martinez[5], M. Losada[22], P. J. Lösel[113], A. Lösle[52], X. Lou[46], X. Lou[15a], A. Lounis[132], P. Love[6], P. A. Love[89], J. J. Lozano Bahilo[174], M. Lu[60a], Y. J. Lu[64], H. J. Lubatti[148], C. Luci[72a,72b], A. Lucotte[58], C. Luedtke[52], F. Luehring[65], I. Luise[136], L. Luminari[72a], B. Lund-Jensen[154], M. S. Lutz[102], D. Lynn[29], R. Lysak[141], E. Lytken[96], F. Lyu[15a], V. Lyubushkin[79], T. Lyubushkina[79], H. Ma[29], L. L. Ma[60b], Y. Ma[60b], G. Maccarrone[51], A. Macchiolo[114], C. M. Macdonald[149], J. Machado Miguens[137], D. Madaffari[174], R. Madar[38], W. F. Mader[48], N. Madysa[48], J. Maeda[82], K. Maekawa[163], S. Maeland[17], T. Maeno[29], M. Maerker[48], A. S. Maevskiy[112], V. Magerl[52], N. Magini[78], D. J. Mahon[39], C. Maidantchik[80b], T. Maier[113], A. Maio[140a,140b,140d], K. Maj[84], O. Majersky[28a], S. Majewski[131], Y. Makida[81], N. Makovec[132], B. Malaescu[136], Pa. Malecki[84], V. P. Maleev[138], F. Malek[58], U. Mallik[77], D. Malon[6], C. Malone[32], S. Maltezos[10], S. Malyukov[79], J. Mamuzic[174], G. Mancini[51], I. Mandić[91], L. Manhaes de Andrade Filho[80a], I. M. Maniatis[162], J. Manjarres Ramos[48], K. H. Mankinen[96], A. Mann[113], A. Manousos[76], B. Mansoulie[145], I. Manthos[162], S. Manzoni[119], A. Marantis[162], G. Marceca[30], L. Marchese[135], G. Marchiori[136], M. Marcisovsky[141], C. Marcon[96], C. A. Marin Tobon[36], M. Marjanovic[38], Z. Marshall[18], M. U. F Martensson[172], S. Marti-Garcia[174], C. B. Martin[126], T. A. Martin[178], V. J. Martin[50], B. Martin dit Latour[17], L. Martinelli[74a,74b], M. Martinez[14,aa], V. I. Martinez Outschoorn[102], S. Martin-Haugh[144], V. S. Martoiu[27b], A. C. Martyniuk[94], A. Marzi n[36], S. R. Maschek[114], L. Masetti[99], T. Mashimo[163], R. Mashinistov[110], J. Masik[100], A. L. Maslennikov[121a,121b], L. H. Mason[104], L. Massa[73a,73b], P. Massarotti[69a,69b], P. Mastrandrea[71a,71b], A. Mastroberardino[41a,41b], T. Masubuchi[163], A. Matic[113], P. Mättig[24], J. Maurer[27b], B. Maček[91], D. A. Maximov[121a,121b], R. Mazini[158], I. Maznas[162], S. M. Mazza[146], S. P. Mc Kee[105], T. G. McCarthy[114], L. I. McClymont[94], W. P. McCormack[18], E. F. McDonald[104], J. A. Mcfayden[36], M. A. McKay[42], K. D. McLean[176], S. J. McMahon[144], P. C. McNamara[104], C. J. McNicol[178], R. A. McPherson[176,ag], J. E. Mdhluli[33c], Z. A. Meadows[102], S. Meehan[148], T. Megy[52], S. Mehlhase[113], A. Mehta[90], T. Meideck[58], B. Meirose[43], D. Melini[174], B. R. Mellado Garcia[33c], J. D. Mellenthin[53], M. Melo[28a], F. Meloni[46], A. Melzer[24], S. B. Menary[100], E. D. Mendes Gouveia[140a,140e], L. Meng[36], X. T. Meng[105], S. Menke[114], E. Meoni[41a,41b], S. Mergelmeyer[19], S. A. M. Merkt[139], C. Merlassino[20], P. Mermod[54], L. Merola[69a,69b], C. Meroni[68a], O. Meshkov[110,112], J. K. R. Meshreki[151], A. Messina[72a,72b], J. Metcalfe[6], A. S. Mete[171], C. Meyer[65], J. Meyer[160], J.-P. Meyer[145], H. Meyer Zu Theenhausen[61a], F. Miano[156], R. P. Middleton[144], L. Mijović[50], G. Mikenberg[180], M. Mikestikova[141], M. Mikuž[91], H. Mildner[149], M. Milesi[104], A. Milic[167], D. A. Millar[92], D. W. Miller[37], A. Milov[180], D. A. Milstead[45a,45b], R. A. Mina[153,s], A. A. Minaenko[123], M. Miñano Moya[174], I. A. Minashvili[159b], A. I. Mincer[124], B. Mindur[83a], M. Mineev[79], Y. Minegishi[163], Y. Ming[181], L. M. Mir[14], A. Mirto[67a,67b], K. P. Mistry[137], T. Mitani[179], J. Mitrevski[113], V. A. Mitsou[174], M. Mittal[60c], A. Miucci[20], P. S. Miyagawa[149], A. Mizukami[81], J. U. Mjörnmark[96], T. Mkrtchyan[184], M. Mlynarikova[143], T. Moa[45a,45b], K. Mochizuki[109], P. Mogg[52], S. Mohapatra[39], R. Moles-Valls[24], M. C. Mondragon[106], K. Mönig[46], J. Monk[40], E. Monnier[101], A. Montalbano[152], J. Montejo Berlingen[36], M. Montella[94], F. Monticelli[88], S. Monzani[68a], N. Morange[132], D. Moreno[22], M. Moreno Llácer[36], C. Moreno Martinez[14], P. Morettini[55b], M. Morgenstern[119], S. Morgenstern[48], D. Mori[152], M. Morii[59], M. Morinaga[179], V. Morisbak[134], A. K. Morley[36], G. Mornacchi[36], A. P. Morris[94], L. Morvaj[155], P. Moschovakos[36], B. Moser[119], M. Mosidze[159b], T. Moskalets[145], H. J. Moss[149], J. Moss[31,p], K. Motohashi[165], E. Mountricha[36], E. J. W. Moyse[102], S. Muanza[101], J. Mueller[139], R. S. P. Mueller[113], D. Muenstermann[89], G. A. Mullier[96], J. L. Munoz Martinez[14], F. J. Munoz Sanchez[100], P. Murin[28b], W. J. Murray[144,178], A. Murrone[68a,68b], M. Muškinja[18], C. Mwewa[33a], A. G. Myagkov[123,ar], J. Myers[131], M. Myska[142], B. P. Nachman[18], O. Nackenhorst[47], A. Nag Nag[48], K. Nagai[135], K. Nagano[81], Y. Nagasaka[62], M. Nagel[52], E. Nagy[101], A. M. Nairz[36], Y. Nakahama[116], K. Nakamura[81], T. Nakamura[163], I. Nakano[127], H. Nanjo[133], F. Napolitano[61a], R. F. Naranjo Garcia[46], R. Narayan[42], D. I. Narrias Villar[61a], I. Naryshkin[138], T. Naumann[46], G. Navarro[22], H. A. Neal[105,*], P. Y. Nechaeva[110], F. Nechansky[46], T. J. Neep[21], A. Negri[70a,70b], M. Negrini[23b], C. Nellist[53], M. E. Nelson[135], S. Nemecek[141], P. Nemethy[124], M. Nessi[36,e], M. S. Neubauer[173], M. Neumann[182], P. R. Newman[21], Y. S. Ng[19], Y. W. Y. Ng[171], H. D. N. Nguyen[101], T. Nguyen Manh[109], E. Nibigira[38], R. B. Nickerson[135], R. Nicolaidou[145], D. S. Nielsen[40], J. Nielsen[146], N. Nikiforou[11], V. Nikolaenko[123,ar], I. Nikolic-Audit[136], K. Nikolopoulos[21], P. Nilsson[29], H. R. Nindhito[54], Y. Ninomiya[81], A. Nisati[72a], N. Nishu[60c], R. Nisius[114], I. Nitsche[47], T. Nitta[179], T. Nobe[163], Y. Noguchi[85], I. Nomidis[136], M. A. Nomura[29], M. Nordberg[36], N. Norjoharuddeen[135], T. Novak[91], O. Novgorodova[48], R. Novotny[142], L. Nozka[130], K. Ntekas[171], E. Nurse[94], F. G. Oakham[34,ba], H. Oberlack[114], J. Ocariz[136], A. Ochi[82], I. Ochoa[39], J. P. Ochoa-Ricoux[147a], K. O'Connor[26], S. Oda[87], S. Odaka[81], S. Oerdek[53], A. Ogrodnik[83a], A. Oh[100], S. H. Oh[49], C. C. Ohm[154], H. Oide[55a,55b], M. L. Ojeda[167], H. Okawa[169], Y. Okazaki[85], Y. Okumura[163], T. Okuyama[81], A. Olariu[27b], L. F. Oleiro Seabra[140a], S. A. Olivares Pino[147a], D. Oliveira Damazio[29], J. L. Oliver[1], M. J. R. Olsson[171],

A. Olszewski[84], J. Olszowska[84], D. C. O'Neil[152], A. Onofre[140a,140e], K. Onogi[116], P. U. E. Onyisi[11], H. Oppen[134], M. J. Oreglia[37], G. E. Orellana[88], D. Orestano[74a,74b], N. Orlando[14], R. S. Orr[167], V. O'Shea[57], R. Ospanov[60a], G. Otero y Garzon[30], H. Otono[87], M. Ouchrif[35d], J. Ouellette[29], F. Ould-Saada[134], A. Ouraou[145], Q. Ouyang[15a], M. Owen[57], R. E. Owen[21], V. E. Ozcan[12c], N. Ozturk[8], J. Pacalt[130], H. A. Pacey[32], K. Pachal[49], A. Pacheco Pages[14], C. Padilla Aranda[14], S. Pagan Griso[18], M. Paganini[183], G. Palacino[65], S. Palazzo[50], S. Palestini[36], M. Palka[83b], D. Pallin[38], I. Panagoulias[10], C. E. Pandini[36], J. G. Panduro Vazquez[93], P. Pani[46], G. Panizzo[66a,66c], L. Paolozzi[54], C. Papadatos[109], K. Papageorgiou[9,i], A. Paramonov[6], D. Paredes Hernandez[63b], S. R. Paredes Saenz[135], B. Parida[166], T. H. Park[167], A. J. Parker[89], M. A. Parker[32], F. Parodi[55a,55b], E. W. P. Parrish[120], J. A. Parsons[39], U. Parzefall[52], L. Pascual Dominguez[136], V. R. Pascuzzi[167], J. M. P. Pasner[146], E. Pasqualucci[72a], S. Passaggio[55b], F. Pastore[93], P. Pasuwan[45a,45b], S. Pataraia[99], J. R. Pater[100], A. Pathak[181], T. Pauly[36], B. Pearson[114], M. Pedersen[134], L. Pedraza Diaz[118], R. Pedro[140a], T. Peiffer[53], S. V. Peleganchuk[121a,121b], O. Penc[141], H. Peng[60a], B. S. Peralva[80a], M. M. Perego[132], A. P. Pereira Peixoto[140a], D. V. Perepelitsa[29], F. Peri[19], L. Perini[68a,68b], H. Pernegger[36], S. Perrella[69a,69b], K. Peters[46], R. F. Y. Peters[100], B. A. Petersen[36], T. C. Petersen[40], E. Petit[101], A. Petridis[1], C. Petridou[162], P. Petroff[132], M. Petrov[135], F. Petrucci[74a,74b], M. Pettee[183], N. E. Pettersson[102], K. Petukhova[143], A. Peyaud[145], R. Pezoa[147c], L. Pezzotti[70a,70b], T. Pham[104], F. H. Phillips[106], P. W. Phillips[144], M. W. Phipps[173], G. Piacquadio[155], E. Pianori[18], A. Picazio[102], R. H. Pickles[100], R. Piegaia[30], D. Pietreanu[27b], J. E. Pilcher[37], A. D. Pilkington[100], M. Pinamonti[73a,73b], J. L. Pinfold[3], M. Pitt[180], L. Pizzimento[73a,73b], M.-A. Pleier[29], V. Pleskot[143], E. Plotnikova[79], D. Pluth[78], P. Podberezko[121a,121b], R. Poettgen[96], R. Poggi[54], L. Poggioli[132], I. Pogrebnyak[106], D. Pohl[24], I. Pokharel[53], G. Polesello[70a], A. Poley[18], A. Policicchio[72a,72b], R. Polifka[143], A. Polini[23b], C. S. Pollard[46], V. Polychronakos[29], D. Ponomarenko[111], L. Pontecorvo[36], S. Popa[27a], G. A. Popeneciu[27d], D. M. Portillo Quintero[58], S. Pospisil[142], K. Potamianos[46], I. N. Potrap[79], C. J. Potter[32], H. Potti[11], T. Poulsen[96], J. Poveda[36], T. D. Powell[149], G. Pownall[46], M. E. Pozo Astigarraga[36], P. Pralavorio[101], S. Prell[78], D. Price[100], M. Primavera[67a], S. Prince[103], M. L. Proffitt[148], N. Proklova[111], K. Prokofiev[63c], F. Prokoshin[79], S. Protopopescu[29], J. Proudfoot[6], M. Przybycien[83a], D. Pudzha[138], A. Puri[173], P. Puzo[132], J. Qian[105], Y. Qin[100], A. Quadt[53], M. Queitsch-Maitland[46], A. Qureshi[1], P. Rados[104], F. Ragusa[68a,68b], G. Rahal[97], J. A. Raine[54], S. Rajagopalan[29], A. Ramirez Morales[92], K. Ran[15a,15d], T. Rashid[132], S. Raspopov[5], M. G. Ratti[68a,68b], D. M. Rauch[46], F. Rauscher[113], S. Rave[99], B. Ravina[149], I. Ravinovich[180], J. H. Rawling[100], M. Raymond[36], A. L. Read[134], N. P. Readioff[58], M. Reale[67a,67b], D. M. Rebuzzi[70a,70b], A. Redelbach[177], G. Redlinger[29], K. Reeves[43], L. Rehnisch[19], J. Reichert[137], D. Reikher[161], A. Reiss[99], A. Rej[151], C. Rembser[36], M. Renda[27b], M. Rescigno[72a], S. Resconi[68a], E. D. Resseguie[137], S. Rettie[175], E. Reynolds[21], O. L. Rezanova[121a,121b], P. Reznicek[143], E. Ricci[75a,75b], R. Richter[114], S. Richter[46], E. Richter-Was[83b], O. Ricken[24], M. Ridel[136], P. Rieck[114], C. J. Riegel[182], O. Rifki[46], M. Rijssenbeek[155], A. Rimoldi[70a,70b], M. Rimoldi[46], L. Rinaldi[23b], G. Ripellino[154], B. Ristić[89], E. Ritsch[36], I. Riu[14], J. C. Rivera Vergara[176], F. Rizatdinova[129], E. Rizvi[92], C. Rizzi[36], R. T. Roberts[100], S. H. Robertson[103,ag], M. Robin[46], D. Robinson[32], J. E. M. Robinson[46], C. M. Robles Gajardo[147c], A. Robson[57], E. Rocco[99], C. Roda[71a,71b], S. Rodriguez Bosca[174], A. Rodriguez Perez[14], D. Rodriguez Rodriguez[174], A. M. Rodríguez Vera[168b], S. Roe[36], O. Røhne[134], R. Röhrig[114], C. P. A. Roland[65], J. Roloff[59], A. Romaniouk[111], M. Romano[23a,23b], N. Rompotis[90], M. Ronzani[124], L. Roos[136], S. Rosati[72a], K. Rosbach[52], G. Rosin[102], B. J. Rosser[137], E. Rossi[46], E. Rossi[74a,74b], E. Rossi[69a,69b], L. P. Rossi[55b], L. Rossini[68a,68b], R. Rosten[14], M. Rotaru[27b], J. Rothberg[148], D. Rousseau[132], G. Rovelli[70a,70b], A. Roy[11], D. Roy[33c], A. Rozanov[101], Y. Rozen[160], X. Ruan[33c], F. Rubbo[153], F. Rühr[52], A. Ruiz-Martinez[174], A. Rummler[36], Z. Rurikova[52], N. A. Rusakovich[79], H. L. Russell[103], L. Rustige[38,47], J. P. Rutherfoord[7], E. M. Rüttinger[46,l], M. Rybar[39], G. Rybkin[132], A. Ryzhov[123], G. F. Rzehorz[53], P. Sabatini[53], G. Sabato[119], S. Sacerdoti[132], H.F-W. Sadrozinski[146], R. Sadykov[79], F. Safai Tehrani[72a], B. Safarzadeh Samani[156], P. Saha[120], S. Saha[103], M. Sahinsoy[61a], A. Sahu[182], M. Saimpert[46], M. Saito[163], T. Saito[163], H. Sakamoto[163], A. Sakharov[124,aq], D. Salamani[54], G. Salamanna[74a,74b], J. E. Salazar Loyola[147c], P. H. Sales De Bruin[172], A. Salnikov[153], J. Salt[174], D. Salvatore[41a,41b], F. Salvatore[156], A. Salvucci[63a,63b,63c], A. Salzburger[36], J. Samarati[36], D. Sammel[52], D. Sampsonidis[162], D. Sampsonidou[162], J. Sánchez[174], A. Sanchez Pineda[66a,66c], H. Sandaker[134], C. O. Sander[46], I. G. Sanderswood[89], M. Sandhoff[182], C. Sandoval[22], D. P. C. Sankey[144], M. Sannino[55a,55b], Y. Sano[116], A. Sansoni[51], C. Santoni[38], H. Santos[140a,140b], S. N. Santpur[18], A. Santra[174], A. Sapronov[79], J. G. Saraiva[140a,140d], O. Sasaki[81], K. Sato[169], E. Sauvan[5], P. Savard[167,ba], N. Savic[114], R. Sawada[163], C. Sawyer[144], L. Sawyer[95,ao], C. Sbarra[23b], A. Sbrizzi[23a], T. Scanlon[94], J. Schaarschmidt[148], P. Schacht[114], B. M. Schachtner[113], D. Schaefer[37], L. Schaefer[137], J. Schaeffer[99], S. Schaepe[36], U. Schäfer[99], A. C. Schaffer[132], D. Schaile[113], R. D. Schamberger[155], N. Scharmberg[100], V. A. Schegelsky[138], D. Scheirich[143], F. Schenck[19], M. Schernau[171], C. Schiavi[55a,55b], S. Schier[146], L. K. Schildgen[24], Z. M. Schillaci[26], E. J. Schioppa[36], M. Schioppa[41a,41b], K. E. Schleicher[52], S. Schlenker[36], K. R. Schmidt-Sommerfeld[114], K. Schmieden[36], C. Schmitt[99], S. Schmitt[46], S. Schmitz[99], J. C. Schmoeckel[46], U. Schnoor[52], L. Schoeffel[145], A. Schoening[61b], P. G. Scholer[52], E. Schopf[135], M. Schott[99], J. F. P. Schouwenberg[118], J. Schovancova[36], S. Schramm[54],

F. Schroeder[182], A. Schulte[99], H-C. Schultz-Coulon[61a], M. Schumacher[52], B. A. Schumm[146], Ph. Schune[145], A. Schwartzman[153], T. A. Schwarz[105], Ph. Schwemling[145], R. Schwienhorst[106], A. Sciandra[146], G. Sciolla[26], M. Scodeggio[46], M. Scornajenghi[41a,41b], F. Scuri[71a], F. Scutti[104], L. M. Scyboz[114], C. D. Sebastiani[72a,72b], P. Seema[19], S. C. Seidel[117], A. Seiden[146], T. Seiss[37], J. M. Seixas[80b], G. Sekhniaidze[69a], K. Sekhon[105], S. J. Sekula[42], N. Semprini-Cesari[23a,23b], S. Sen[49], S. Senkin[38], C. Serfon[76], L. Serin[132], L. Serkin[66a,66b], M. Sessa[60a], H. Severini[128], T. Šfiligoj[91], F. Sforza[170], A. Sfyrla[54], E. Shabalina[53], J. D. Shahinian[146], N. W. Shaikh[45a,45b], D. Shaked Renous[180], L. Y. Shan[15a], R. Shang[173], J. T. Shank[25], M. Shapiro[18], A. Sharma[135], A. S. Sharma[1], P. B. Shatalov[122], K. Shaw[156], S. M. Shaw[100], A. Shcherbakova[138], Y. Shen[128], N. Sherafati[34], A. D. Sherman[25], P. Sherwood[94], L. Shi[158,aw], S. Shimizu[81], C. O. Shimmin[183], Y. Shimogama[179], M. Shimojima[115], I. P. J. Shipsey[135], S. Shirabe[87], M. Shiyakova[79,ad], J. Shlomi[180], A. Shmeleva[110], M. J. Shochet[37], J. Shojaii[104], D. R. Shope[128], S. Shrestha[126], E. M. Shrif[33c], E. Shulga[180], P. Sicho[141], A. M. Sickles[173], P. E. Sidebo[154], E. Sideras Haddad[33c], O. Sidiropoulou[36], A. Sidoti[23a,23b], F. Siegert[48], Dj. Sijacki[16], M. Jr. Silva[181], M. V. Silva Oliveira[80a], S. B. Silverstein[45a], S. Simion[132], E. Simioni[99], R. Simoniello[99], S. Simsek[12b], P. Sinervo[167], V. Sinetckii[112,110], N. B. Sinev[131], M. Sioli[23a,23b], I. Siral[105], S. Yu. Sivoklokov[112], J. Sjölin[45a,45b], E. Skorda[96], P. Skubic[128], M. Slawinska[84], K. Sliwa[170], R. Slovak[143], V. Smakhtin[180], B. H. Smart[144], J. Smiesko[28a], N. Smirnov[111], S. Yu. Smirnov[111], Y. Smirnov[111], L. N. Smirnova[112,w], O. Smirnova[96], J. W. Smith[53], M. Smizanska[89], K. Smolek[142], A. Smykiewicz[84], A. A. Snesarev[110], H. L. Snoek[119], I. M. Snyder[131], S. Snyder[29], R. Sobie[176,ag], A. M. Soffa[171], A. Soffer[161], A. Søgaard[50], F. Sohns[53], C. A. Solans Sanchez[36], E. Yu. Soldatov[111], U. Soldevila[174], A. A. Solodkov[123], A. Soloshenko[79], O. V. Solovyanov[123], V. Solovyev[138], P. Sommer[149], H. Son[170], W. Song[144], W. Y. Song[168b], A. Sopczak[142], F. Sopkova[28b], C. L. Sotiropoulou[71a,71b], S. Sottocornola[70a,70b], R. Soualah[66a,66c,h], A. M. Soukharev[121a,121b], D. South[46], S. Spagnolo[67a,67b], M. Spalla[114], M. Spangenberg[178], F. Spanò[93], D. Sperlich[52], T. M. Spieker[61a], R. Spighi[23b], G. Spigo[36], M. Spina[156], D. P. Spiteri[57], M. Spousta[143], A. Stabile[68a,68b], B. L. Stamas[120], R. Stamen[61a], M. Stamenkovic[119], E. Stanecka[84], R. W. Stanek[6], B. Stanislaus[135], M. M. Stanitzki[46], M. Stankaityte[135], B. Stapf[119], E. A. Starchenko[123], G. H. Stark[146], J. Stark[58], S. H. Stark[40], P. Staroba[141], P. Starovoitov[61a], S. Stärz[103], R. Staszewski[84], G. Stavropoulos[44], M. Stegler[46], P. Steinberg[29], A. L. Steinhebel[131], B. Stelzer[152], H. J. Stelzer[139], O. Stelzer-Chilton[168a], H. Stenzel[56], T. J. Stevenson[156], G. A. Stewart[36], M. C. Stockton[36], G. Stoicea[27b], M. Stolarski[140a], P. Stolte[53], S. Stonjek[114], A. Straessner[48], J. Strandberg[154], S. Strandberg[45a,45b], M. Strauss[128], P. Strizenec[28b], R. Ströhmer[177], D. M. Strom[131], R. Stroynowski[42], A. Strubig[50], S. A. Stucci[29], B. Stugu[17], J. Stupak[128], N. A. Styles[46], D. Su[153], S. Suchek[61a], V. V. Sulin[110], M. J. Sullivan[90], D. M. S. Sultan[54], S. Sultansoy[4c], T. Sumida[85], S. Sun[105], X. Sun[3], K. Suruliz[156], C. J. E. Suster[157], M. R. Sutton[156], S. Suzuki[81], M. Svatos[141], M. Swiatlowski[37], S. P. Swift[2], T. Swirski[177], A. Sydorenko[99], I. Sykora[28a], M. Sykora[143], T. Sykora[143], D. Ta[99], K. Tackmann[46,ab], J. Taenzer[161], A. Taffard[171], R. Tafirout[168a], H. Takai[29], R. Takashima[86], K. Takeda[82], T. Takeshita[150], E. P. Takeva[50], Y. Takubo[81], M. Talby[101], A. A. Talyshev[121a,121b], N. M. Tamir[161], J. Tanaka[163], M. Tanaka[165], R. Tanaka[132], S. Tapia Araya[173], S. Tapprogge[99], A. Tarek Abouelfadl Mohamed[136], S. Tarem[160], G. Tarna[27b,d], G. F. Tartarelli[68a], P. Tas[143], M. Tasevsky[141], T. Tashiro[85], E. Tassi[41a,41b], A. Tavares Delgado[140a,140b], Y. Tayalati[35e], A. J. Taylor[50], G. N. Taylor[104], W. Taylor[168b], A. S. Tee[89], R. Teixeira De Lima[153], P. Teixeira-Dias[93], H. Ten Kate[36], J. J. Teoh[119], S. Terada[81], K. Terashi[163], J. Terron[98], S. Terzo[14], M. Testa[51], R. J. Teuscher[167,ag], S. J. Thais[183], T. Theveneaux-Pelzer[46], F. Thiele[40], D. W. Thomas[93], J. O. Thomas[42], J. P. Thomas[21], A. S. Thompson[57], P. D. Thompson[21], L. A. Thomsen[183], E. Thomson[137], Y. Tian[39], R. E. Ticse Torres[53], V. O. Tikhomirov[110,as], Yu. A. Tikhonov[121a,121b], S. Timoshenko[111], P. Tipton[183], S. Tisserant[101], K. Todome[23a,23b], S. Todorova-Nova[5], S. Todt[48], J. Tojo[87], S. Tokár[28a], K. Tokushuku[81], E. Tolley[126], K. G. Tomiwa[33c], M. Tomoto[116], L. Tompkins[153,s], B. Tong[59], P. Tornambe[102], E. Torrence[131], H. Torres[48], E. Torró Pastor[148], C. Tosciri[135], J. Toth[101,ae], D. R. Tovey[149], A. Traeet[17], C. J. Treado[124], T. Trefzger[177], F. Tresoldi[156], A. Tricoli[29], I. M. Trigger[168a], S. Trincaz-Duvoid[136], W. Trischuk[167], B. Trocmé[58], A. Trofymov[145], C. Troncon[68a], M. Trovatelli[176], F. Trovato[156], L. Truong[33b], M. Trzebinski[84], A. Trzupek[84], F. Tsai[46], J.C-L. Tseng[135], P. V. Tsiareshka[107,am], A. Tsirigotis[162], N. Tsirintanis[9], V. Tsiskaridze[155], E. G. Tskhadadze[159a], M. Tsopoulou[162], I. I. Tsukerman[122], V. Tsulaia[18], S. Tsuno[81], D. Tsybychev[155], Y. Tu[63b], A. Tudorache[27b], V. Tudorache[27b], T. T. Tulbure[27a], A. N. Tuna[59], S. Turchikhin[79], D. Turgeman[180], I. Turk Cakir[4b,x], R. J. Turner[21], R. T. Turra[68a], P. M. Tuts[39], S. Tzamarias[162], E. Tzovara[99], G. Ucchielli[47], K. Uchida[163], I. Ueda[81], M. Ughetto[45a,45b], F. Ukegawa[169], G. Unal[36], A. Undrus[29], G. Unel[171], F. C. Ungaro[104], Y. Unno[81], K. Uno[163], J. Urban[28b], P. Urquijo[104], G. Usai[8], J. Usui[81], Z. Uysal[12d], L. Vacavant[101], V. Vacek[142], B. Vachon[103], K. O. H. Vadla[134], A. Vaidya[94], C. Valderanis[113], E. Valdes Santurio[45a,45b], M. Valente[54], S. Valentinetti[23a,23b], A. Valero[174], L. Valéry[46], R. A. Vallance[21], A. Vallier[36], J. A. Valls Ferrer[174], T. R. Van Daalen[14], P. Van Gemmeren[6], I. Van Vulpen[119], M. Vanadia[73a,73b], W. Vandelli[36], A. Vaniachine[166], D. Vannicola[72a,72b], R. Vari[72a], E. W. Varnes[7], C. Varni[55a,55b], T. Varol[42], D. Varouchas[132], K. E. Varvell[157], M. E. Vasile[27b], G. A. Vasquez[176], J. G. Vasquez[183], F. Vazeille[38], D. Vazquez Furelos[14], T. Vazquez Schroeder[36],

J. Veatch[53], V. Vecchio[74a,74b], M. J. Veen[119], L. M. Veloce[167], F. Veloso[140a,140c], S. Veneziano[72a], A. Ventura[67a,67b], N. Venturi[36], A. Verbytskyi[114], V. Vercesi[70a], M. Verducci[74a,74b], C. M. Vergel Infante[78], C. Vergis[24], W. Verkerke[119], A. T. Vermeulen[119], J. C. Vermeulen[119], M. C. Vetterli[152,ba], N. Viaux Maira[147c], M. Vicente Barreto Pinto[54], T. Vickey[149], O. E. Vickey Boeriu[149], G. H. A. Viehhauser[135], L. Vigani[135], M. Villa[23a,23b], M. Villaplana Perez[68a,68b], E. Vilucchi[51], M. G. Vincter[34], V. B. Vinogradov[79], A. Vishwakarma[46], C. Vittori[23a,23b], I. Vivarelli[156], M. Vogel[182], P. Vokac[142], S. E. von Buddenbrock[33c], E. Von Toerne[24], V. Vorobel[143], K. Vorobev[111], M. Vos[174], J. H. Vossebeld[90], M. Vozak[100], N. Vranjes[16], M. Vranjes Milosavljevic[16], V. Vrba[142], M. Vreeswijk[119], R. Vuillermet[36], I. Vukotic[37], P. Wagner[24], W. Wagner[182], J. Wagner-Kuhr[113], S. Wahdan[182], H. Wahlberg[88], K. Wakamiya[82], V. M. Walbrecht[114], J. Walder[89], R. Walker[113], S. D. Walker[93], W. Walkowiak[151], V. Wallangen[45a,45b], A. M. Wang[59], C. Wang[60b], F. Wang[181], H. Wang[18], H. Wang[3], J. Wang[157], J. Wang[61b], P. Wang[42], Q. Wang[128], R.-J. Wang[99], R. Wang[60a], R. Wang[6], S. M. Wang[158], W. T. Wang[60a], W. Wang[15c,ah], W. X. Wang[60a,ah], Y. Wang[60a,ap], Z. Wang[60c], C. Wanotayaroj[46], A. Warburton[103], C. P. Ward[32], D. R. Wardrope[94], N. Warrack[57], A. Washbrook[50], A. T. Watson[21], M. F. Watson[21], G. Watts[148], B. M. Waugh[94], A. F. Webb[11], S. Webb[99], C. Weber[183], M. S. Weber[20], S. A. Weber[34], S. M. Weber[61a], A. R. Weidberg[135], J. Weingarten[47], M. Weirich[99], C. Weiser[52], P. S. Wells[36], T. Wenaus[29], T. Wengler[36], S. Wenig[36], N. Wermes[24], M. D. Werner[78], M. Wessels[61a], T. D. Weston[20], K. Whalen[131], N. L. Whallon[148], A. M. Wharton[89], A. S. White[105], A. White[8], M. J. White[1], D. Whiteson[171], B. W. Whitmore[89], F. J. Wickens[144], W. Wiedenmann[181], M. Wielers[144], N. Wieseotte[99], C. Wiglesworth[40], L. A. M. Wiik-Fuchs[52], F. Wilk[100], H. G. Wilkens[36], L. J. Wilkins[93], H. H. Williams[137], S. Williams[32], C. Willis[106], S. Willocq[102], J. A. Wilson[21], I. Wingerter-Seez[5], E. Winkels[156], F. Winklmeier[131], O. J. Winston[156], B. T. Winter[52], M. Wittgen[153], M. Wobisch[95], A. Wolf[99], T. M. H. Wolf[119], R. Wolff[101], R. W. Wölker[135], J. Wollrath[52], M. W. Wolter[84], H. Wolters[140a,140c], V. W. S. Wong[175], N. L. Woods[146], S. D. Worm[21], B. K. Wosiek[84], K. W. Woźniak[84], K. Wraight[57], S. L. Wu[181], X. Wu[54], Y. Wu[60a], T. R. Wyatt[100], B. M. Wynne[50], S. Xella[40], Z. Xi[105], L. Xia[178], D. Xu[15a], H. Xu[60a,d], L. Xu[29], T. Xu[145], W. Xu[105], Z. Xu[60b], Z. Xu[153], B. Yabsley[157], S. Yacoob[33a], K. Yajima[133], D. P. Yallup[94], D. Yamaguchi[165], Y. Yamaguchi[165], A. Yamamoto[81], T. Yamanaka[163], F. Yamane[82], M. Yamatani[163], T. Yamazaki[163], Y. Yamazaki[82], Z. Yan[25], H. J. Yang[60c,60d], H. T. Yang[18], S. Yang[77], X. Yang[58,60b], Y. Yang[163], W-M. Yao[18], Y. C. Yap[46], Y. Yasu[81], E. Yatsenko[60c,60d], J. Ye[42], S. Ye[29], I. Yeletskikh[79], M. R. Yexley[89], E. Yigitbasi[25], K. Yorita[179], K. Yoshihara[137], C. J. S. Young[36], C. Young[153], J. Yu[78], R. Yuan[60b,j], X. Yue[61a], S. P. Y. Yuen[24], B. Zabinski[84], G. Zacharis[10], E. Zaffaroni[54], J. Zahreddine[136], A. M. Zaitsev[123,ar], T. Zakareishvili[159b], N. Zakharchuk[34], S. Zambito[59], D. Zanzi[36], D. R. Zaripovas[57], S. V. Zeißner[47], C. Zeitnitz[182], G. Zemaityte[135], J. C. Zeng[173], O. Zenin[123], T. Ženiš[28a], D. Zerwas[132], M. Zgubič[135], D. F. Zhang[15b], F. Zhang[181], G. Zhang[60a], G. Zhang[15b], H. Zhang[15c], J. Zhang[6], L. Zhang[15c], L. Zhang[60a], M. Zhang[173], R. Zhang[60a], R. Zhang[24], X. Zhang[60b], Y. Zhang[15a,15d], Z. Zhang[63a], Z. Zhang[132], P. Zhao[49], Y. Zhao[60b], Z. Zhao[60a], A. Zhemchugov[79], Z. Zheng[105], D. Zhong[173], B. Zhou[105], C. Zhou[181], M. S. Zhou[15a,15d], M. Zhou[155], N. Zhou[60c], Y. Zhou[7], C. G. Zhu[60b], H. L. Zhu[60a], H. Zhu[15a], J. Zhu[105], Y. Zhu[60a], X. Zhuang[15a], K. Zhukov[110], V. Zhulanov[121a,121b], D. Zieminska[65], N. I. Zimine[79], S. Zimmermann[52], Z. Zinonos[114], M. Ziolkowski[151], L. Živković[16], G. Zobernig[181], A. Zoccoli[23a,23b], K. Zoch[53], T. G. Zorbas[149], R. Zou[37], L. Zwalinski[36]

[1] Department of Physics, University of Adelaide, Adelaide, Australia

[2] Physics Department, SUNY Albany, Albany, NY, USA

[3] Department of Physics, University of Alberta, Edmonton, AB, Canada

[4] (a)Department of Physics, Ankara University, Ankara, Turkey; (b)Istanbul Aydin University, Istanbul, Turkey; (c)Division of Physics, TOBB University of Economics and Technology, Ankara, Turkey

[5] LAPP, Université Grenoble Alpes, Université Savoie Mont Blanc, CNRS/IN2P3, Annecy, France

[6] High Energy Physics Division, Argonne National Laboratory, Argonne, IL, USA

[7] Department of Physics, University of Arizona, Tucson, AZ, USA

[8] Department of Physics, University of Texas at Arlington, Arlington, TX, USA

[9] Physics Department, National and Kapodistrian University of Athens, Athens, Greece

[10] Physics Department, National Technical University of Athens, Zografou, Greece

[11] Department of Physics, University of Texas at Austin, Austin, TX, USA

[12] (a)Bahcesehir University, Faculty of Engineering and Natural Sciences, Istanbul, Turkey; (b)Istanbul Bilgi University, Faculty of Engineering and Natural Sciences, Istanbul, Turkey; (c)Department of Physics, Bogazici University, Istanbul, Turkey; (d)Department of Physics Engineering, Gaziantep University, Gaziantep, Turkey

[13] Institute of Physics, Azerbaijan Academy of Sciences, Baku, Azerbaijan

[14] Institut de Física d'Altes Energies (IFAE), Barcelona Institute of Science and Technology, Barcelona, Spain

15 (a)Institute of High Energy Physics, Chinese Academy of Sciences, Beijing, China; (b)Physics Department, Tsinghua University, Beijing, China; (c)Department of Physics, Nanjing University, Nanjing, China; (d)University of Chinese Academy of Science (UCAS), Beijing, China

16 Institute of Physics, University of Belgrade, Belgrade, Serbia

17 Department for Physics and Technology, University of Bergen, Bergen, Norway

18 Physics Division, Lawrence Berkeley National Laboratory and University of California, Berkeley, CA, USA

19 Institut für Physik, Humboldt Universität zu Berlin, Berlin, Germany

20 Albert Einstein Center for Fundamental Physics and Laboratory for High Energy Physics, University of Bern, Bern, Switzerland

21 School of Physics and Astronomy, University of Birmingham, Birmingham, UK

22 Facultad de Ciencias y Centro de Investigaciónes, Universidad Antonio Nariño, Bogotá, Colombia

23 (a)Dipartimento di Fisica, INFN Bologna and Universita' di Bologna, Bologna, Italy; (b)INFN Sezione di Bologna, Bologna, Italy

24 Physikalisches Institut, Universität Bonn, Bonn, Germany

25 Department of Physics, Boston University, Boston, MA, USA

26 Department of Physics, Brandeis University, Waltham, MA, USA

27 (a)Transilvania University of Brasov, Brasov, Romania; (b)Horia Hulubei National Institute of Physics and Nuclear Engineering, Bucharest, Romania; (c)Department of Physics, Alexandru Ioan Cuza University of Iasi, Iasi, Romania; (d)National Institute for Research and Development of Isotopic and Molecular Technologies, Physics Department, Cluj Napoca, Romania; (e)University Politehnica Bucharest, Bucharest, Romania; (f)West University in Timisoara, Timisoara, Romania

28 (a)Faculty of Mathematics, Physics and Informatics, Comenius University, Bratislava, Slovak Republic; (b)Department of Subnuclear Physics, Institute of Experimental Physics of the Slovak Academy of Sciences, Kosice, Slovak Republic

29 Physics Department, Brookhaven National Laboratory, Upton, NY, USA

30 Departamento de Física, Universidad de Buenos Aires, Buenos Aires, Argentina

31 California State University, California, CA, USA

32 Cavendish Laboratory, University of Cambridge, Cambridge, UK

33 (a)Department of Physics, University of Cape Town, Cape Town, South Africa; (b)Department of Mechanical Engineering Science, University of Johannesburg, Johannesburg, South Africa; (c)School of Physics, University of the Witwatersrand, Johannesburg, South Africa

34 Department of Physics, Carleton University, Ottawa, ON, Canada

35 (a)Faculté des Sciences Ain Chock, Réseau Universitaire de Physique des Hautes Energies - Université Hassan II, Casablanca, Morocco; (b)Faculté des Sciences, Université Ibn-Tofail, Kénitra, Morocco; (c)Faculté des Sciences Semlalia, Université Cadi Ayyad, LPHEA-Marrakech, Morocco; (d)Faculté des Sciences, Université Mohamed Premier and LPTPM, Oujda, Morocco; (e)Faculté des sciences, Université Mohammed V, Rabat, Morocco

36 CERN, Geneva, Switzerland

37 Enrico Fermi Institute, University of Chicago, Chicago, IL, USA

38 LPC, Université Clermont Auvergne, CNRS/IN2P3, Clermont-Ferrand, France

39 Nevis Laboratory, Columbia University, Irvington, NY, USA

40 Niels Bohr Institute, University of Copenhagen, Copenhagen, Denmark

41 (a)Dipartimento di Fisica, Università della Calabria, Rende, Italy; (b)INFN Gruppo Collegato di Cosenza, Laboratori Nazionali di Frascati, Frascati, Italy

42 Physics Department, Southern Methodist University, Dallas, TX, USA

43 Physics Department, University of Texas at Dallas, Richardson, TX, USA

44 National Centre for Scientific Research "Demokritos", Agia Paraskevi, Greece

45 (a)Department of Physics, Stockholm University, Stockholm, Sweden; (b)Oskar Klein Centre, Stockholm, Sweden

46 Deutsches Elektronen-Synchrotron DESY, Hamburg and Zeuthen, Germany

47 Lehrstuhl für Experimentelle Physik IV, Technische Universität Dortmund, Dortmund, Germany

48 Institut für Kern- und Teilchenphysik, Technische Universität Dresden, Dresden, Germany

49 Department of Physics, Duke University, Durham, NC, USA

50 SUPA - School of Physics and Astronomy, University of Edinburgh, Edinburgh, UK

51 INFN e Laboratori Nazionali di Frascati, Frascati, Italy

52 Physikalisches Institut, Albert-Ludwigs-Universität Freiburg, Freiburg, Germany

[53] II. Physikalisches Institut, Georg-August-Universität Göttingen, Göttingen, Germany

[54] Département de Physique Nucléaire et Corpusculaire, Université de Genève, Geneva, Switzerland

[55] (a)Dipartimento di Fisica, Università di Genova, Genoa, Italy; (b)INFN Sezione di Genova, Genoa, Italy

[56] II. Physikalisches Institut, Justus-Liebig-Universität Giessen, Giessen, Germany

[57] SUPA - School of Physics and Astronomy, University of Glasgow, Glasgow, UK

[58] LPSC, Université Grenoble Alpes, CNRS/IN2P3, Grenoble INP, Grenoble, France

[59] Laboratory for Particle Physics and Cosmology, Harvard University, Cambridge, MA, USA

[60] (a)Department of Modern Physics and State Key Laboratory of Particle Detection and Electronics, University of Science and Technology of China, Hefei, China; (b)Institute of Frontier and Interdisciplinary Science and Key Laboratory of Particle Physics and Particle Irradiation (MOE), Shandong University, Qingdao, China; (c)School of Physics and Astronomy, Shanghai Jiao Tong University, KLPPAC-MoE, SKLPPC, Shanghai, China; (d)Tsung-Dao Lee Institute, Shanghai, China

[61] (a)Kirchhoff-Institut für Physik, Ruprecht-Karls-Universität Heidelberg, Heidelberg, Germany; (b)Physikalisches Institut, Ruprecht-Karls-Universität Heidelberg, Heidelberg, Germany

[62] Faculty of Applied Information Science, Hiroshima Institute of Technology, Hiroshima, Japan

[63] (a)Department of Physics, Chinese University of Hong Kong, Shatin, N.T., Hong Kong, China; (b)Department of Physics, University of Hong Kong, Hong Kong, China; (c)Department of Physics and Institute for Advanced Study, Hong Kong University of Science and Technology, Clear Water Bay, Kowloon, Hong Kong, China

[64] Department of Physics, National Tsing Hua University, Hsinchu, Taiwan

[65] Department of Physics, Indiana University, Bloomington, IN, USA

[66] (a)INFN Gruppo Collegato di Udine, Sezione di Trieste, Udine, Italy; (b)ICTP, Trieste, Italy; (c)Dipartimento Politecnico di Ingegneria e Architettura, Università di Udine, Udine, Italy

[67] (a)INFN Sezione di Lecce, Lecce, Italy; (b)Dipartimento di Matematica e Fisica, Università del Salento, Lecce, Italy

[68] (a)INFN Sezione di Milano, Milan, Italy; (b)Dipartimento di Fisica, Università di Milano, Milan, Italy

[69] (a)INFN Sezione di Napoli, Naples, Italy; (b)Dipartimento di Fisica, Università di Napoli, Naples, Italy

[70] (a)INFN Sezione di Pavia, Pavia, Italy; (b)Dipartimento di Fisica, Università di Pavia, Pavia, Italy

[71] (a)INFN Sezione di Pisa, Pisa, Italy; (b)Dipartimento di Fisica E. Fermi, Università di Pisa, Pisa, Italy

[72] (a)INFN Sezione di Roma, Rome, Italy; (b)Dipartimento di Fisica, Sapienza Università di Roma, Rome, Italy

[73] (a)INFN Sezione di Roma Tor Vergata, Rome, Italy; (b)Dipartimento di Fisica, Università di Roma Tor Vergata, Rome, Italy

[74] (a)INFN Sezione di Roma Tre, Rome, Italy; (b)Dipartimento di Matematica e Fisica, Università Roma Tre, Rome, Italy

[75] (a)INFN-TIFPA, Trento, Italy; (b)Università degli Studi di Trento, Trento, Italy

[76] Institut für Astro- und Teilchenphysik, Leopold-Franzens-Universität, Innsbruck, Austria

[77] University of Iowa, Iowa City, IA, USA

[78] Department of Physics and Astronomy, Iowa State University, Ames, IA, USA

[79] Joint Institute for Nuclear Research, Dubna, Russia

[80] (a)Departamento de Engenharia Elétrica, Universidade Federal de Juiz de Fora (UFJF), Juiz de Fora, Brazil; (b)Universidade Federal do Rio De Janeiro COPPE/EE/IF, Rio de Janeiro, Brazil; (c)Universidade Federal de São João del Rei (UFSJ), São João del Rei, Brazil; (d)Instituto de Física, Universidade de São Paulo, São Paulo, Brazil

[81] KEK, High Energy Accelerator Research Organization, Tsukuba, Japan

[82] Graduate School of Science, Kobe University, Kobe, Japan

[83] (a)AGH University of Science and Technology, Faculty of Physics and Applied Computer Science, Kraków, Poland; (b)Marian Smoluchowski Institute of Physics, Jagiellonian University, Kraków, Poland

[84] Institute of Nuclear Physics Polish Academy of Sciences, Kraków, Poland

[85] Faculty of Science, Kyoto University, Kyoto, Japan

[86] Kyoto University of Education, Kyoto, Japan

[87] Research Center for Advanced Particle Physics and Department of Physics, Kyushu University, Fukuoka , Japan

[88] Instituto de Física La Plata, Universidad Nacional de La Plata and CONICET, La Plata, Argentina

[89] Physics Department, Lancaster University, Lancaster, UK

[90] Oliver Lodge Laboratory, University of Liverpool, Liverpool, UK

[91] Department of Experimental Particle Physics, Jožef Stefan Institute and Department of Physics, University of Ljubljana, Ljubljana, Slovenia

[92] School of Physics and Astronomy, Queen Mary University of London, London, UK

[93] Department of Physics, Royal Holloway University of London, Egham, UK

[94] Department of Physics and Astronomy, University College London, London, UK

[95] Louisiana Tech University, Ruston, LA, USA

[96] Fysiska institutionen, Lunds universitet, Lund, Sweden

[97] Centre de Calcul de l'Institut National de Physique Nucléaire et de Physique des Particules (IN2P3), Villeurbanne, France

[98] Departamento de Física Teorica C-15 and CIAFF, Universidad Autónoma de Madrid, Madrid, Spain

[99] Institut für Physik, Universität Mainz, Mainz, Germany

[100] School of Physics and Astronomy, University of Manchester, Manchester, UK

[101] CPPM, Aix-Marseille Université, CNRS/IN2P3, Marseille, France

[102] Department of Physics, University of Massachusetts, Amherst, MA, USA

[103] Department of Physics, McGill University, Montreal, QC, Canada

[104] School of Physics, University of Melbourne, Victoria, Australia

[105] Department of Physics, University of Michigan, Ann Arbor, MI, USA

[106] Department of Physics and Astronomy, Michigan State University, East Lansing, MI, USA

[107] B.I. Stepanov Institute of Physics, National Academy of Sciences of Belarus, Minsk, Belarus

[108] Research Institute for Nuclear Problems of Byelorussian State University, Minsk, Belarus

[109] Group of Particle Physics, University of Montreal, Montreal, QC, Canada

[110] P.N. Lebedev Physical Institute of the Russian Academy of Sciences, Moscow, Russia

[111] National Research Nuclear University MEPhI, Moscow, Russia

[112] D.V. Skobeltsyn Institute of Nuclear Physics, M.V. Lomonosov Moscow State University, Moscow, Russia

[113] Fakultät für Physik, Ludwig-Maximilians-Universität München, Munich, Germany

[114] Max-Planck-Institut für Physik (Werner-Heisenberg-Institut), Munich, Germany

[115] Nagasaki Institute of Applied Science, Nagasaki, Japan

[116] Graduate School of Science and Kobayashi-Maskawa Institute, Nagoya University, Nagoya, Japan

[117] Department of Physics and Astronomy, University of New Mexico, Albuquerque, NM, USA

[118] Institute for Mathematics, Astrophysics and Particle Physics, Radboud University Nijmegen/Nikhef, Nijmegen, The Netherlands

[119] Nikhef National Institute for Subatomic Physics and University of Amsterdam, Amsterdam, The Netherlands

[120] Department of Physics, Northern Illinois University, DeKalb, IL, USA

[121] [a]Budker Institute of Nuclear Physics and NSU, SB RAS, Novosibirsk, Russia; [b]Novosibirsk State University, Novosibirsk, Russia

[122] Institute for Theoretical and Experimental Physics named by A.I. Alikhanov of National Research Centre "Kurchatov Institute", Moscow, Russia

[123] Institute for High Energy Physics of the National Research Centre Kurchatov Institute, Protvino, Russia

[124] Department of Physics, New York University, New York, NY, USA

[125] Ochanomizu University, Otsuka, Bunkyo-ku, Tokyo, Japan

[126] Ohio State University, Columbus, OH, USA

[127] Faculty of Science, Okayama University, Okayama, Japan

[128] Homer L. Dodge Department of Physics and Astronomy, University of Oklahoma, Norman, OK, USA

[129] Department of Physics, Oklahoma State University, Stillwater, OK, USA

[130] Palacký University, RCPTM, Joint Laboratory of Optics, Olomouc, Czech Republic

[131] Center for High Energy Physics, University of Oregon, Eugene, OR, USA

[132] LAL, Université Paris-Sud, CNRS/IN2P3, Université Paris-Saclay, Orsay, France

[133] Graduate School of Science, Osaka University, Osaka, Japan

[134] Department of Physics, University of Oslo, Oslo, Norway

[135] Department of Physics, Oxford University, Oxford, UK

[136] LPNHE, Sorbonne Université, Université de Paris, CNRS/IN2P3, Paris, France

[137] Department of Physics, University of Pennsylvania, Philadelphia, PA, USA

[138] Konstantinov Nuclear Physics Institute of National Research Centre "Kurchatov Institute", PNPI, St. Petersburg, Russia

[139] Department of Physics and Astronomy, University of Pittsburgh, Pittsburgh, PA, USA

[140] [a]Laboratório de Instrumentação e Física Experimental de Partículas - LIP, Lisbon, Portugal; [b]Departamento de Física, Faculdade de Ciências, Universidade de Lisboa, Lisbon, Portugal; [c]Departamento de Física, Universidade de Coimbra,

Coimbra, Portugal; [d]Centro de Física Nuclear da Universidade de Lisboa, Lisbon, Portugal; [e]Departamento de Física, Universidade do Minho, Braga, Portugal; [f]Universidad de Granada, Granada, Spain; [g]Dep Física and CEFITEC of Faculdade de Ciências e Tecnologia, Universidade Nova de Lisboa, Caparica, Portugal; [h]Instituto Superior Técnico, Universidade de Lisboa, Lisbon, Portugal

141 Institute of Physics of the Czech Academy of Sciences, Prague, Czech Republic

142 Czech Technical University in Prague, Prague, Czech Republic

143 Charles University, Faculty of Mathematics and Physics, Prague, Czech Republic

144 Particle Physics Department, Rutherford Appleton Laboratory, Didcot, UK

145 IRFU, CEA, Université Paris-Saclay, Gif-sur-Yvette, France

146 Santa Cruz Institute for Particle Physics, University of California Santa Cruz, Santa Cruz, CA, USA

147 [a]Departamento de Física, Pontificia Universidad Católica de Chile, Santiago, Chile; [b]Universidad Andres Bello, Department of Physics, Santiago, Chile; [c]Departamento de Física, Universidad Técnica Federico Santa María, Valparaíso, Chile

148 Department of Physics, University of Washington, Seattle, WA, USA

149 Department of Physics and Astronomy, University of Sheffield, Sheffield, UK

150 Department of Physics, Shinshu University, Nagano, Japan

151 Department Physik, Universität Siegen, Siegen, Germany

152 Department of Physics, Simon Fraser University, Burnaby, BC, Canada

153 SLAC National Accelerator Laboratory, Stanford, CA, USA

154 Physics Department, Royal Institute of Technology, Stockholm, Sweden

155 Departments of Physics and Astronomy, Stony Brook University, Stony Brook, NY, USA

156 Department of Physics and Astronomy, University of Sussex, Brighton, UK

157 School of Physics, University of Sydney, Sydney, Australia

158 Institute of Physics, Academia Sinica, Taipei, Taiwan

159 [a]E. Andronikashvili Institute of Physics, Iv. Javakhishvili Tbilisi State University, Tbilisi, Georgia; [b]High Energy Physics Institute, Tbilisi State University, Tbilisi, Georgia

160 Department of Physics, Technion, Israel Institute of Technology, Haifa, Israel

161 Raymond and Beverly Sackler School of Physics and Astronomy, Tel Aviv University, Tel Aviv, Israel

162 Department of Physics, Aristotle University of Thessaloniki, Thessaloniki, Greece

163 International Center for Elementary Particle Physics and Department of Physics, University of Tokyo, Tokyo, Japan

164 Graduate School of Science and Technology, Tokyo Metropolitan University, Tokyo, Japan

165 Department of Physics, Tokyo Institute of Technology, Tokyo, Japan

166 Tomsk State University, Tomsk, Russia

167 Department of Physics, University of Toronto, Toronto, ON, Canada

168 [a]TRIUMF, Vancouver, BC, Canada; [b]Department of Physics and Astronomy, York University, Toronto, ON, Canada

169 Division of Physics and Tomonaga Center for the History of the Universe, Faculty of Pure and Applied Sciences, University of Tsukuba, Tsukuba, Japan

170 Department of Physics and Astronomy, Tufts University, Medford, MA, USA

171 Department of Physics and Astronomy, University of California Irvine, Irvine, CA, USA

172 Department of Physics and Astronomy, University of Uppsala, Uppsala, Sweden

173 Department of Physics, University of Illinois, Urbana, IL, USA

174 Instituto de Física Corpuscular (IFIC), Centro Mixto Universidad de Valencia - CSIC, Valencia, Spain

175 Department of Physics, University of British Columbia, Vancouver, BC, Canada

176 Department of Physics and Astronomy, University of Victoria, Victoria, BC, Canada

177 Fakultät für Physik und Astronomie, Julius-Maximilians-Universität Würzburg, Würzburg, Germany

178 Department of Physics, University of Warwick, Coventry, UK

179 Waseda University, Tokyo, Japan

180 Department of Particle Physics, Weizmann Institute of Science, Rehovot, Israel

181 Department of Physics, University of Wisconsin, Madison, WI, USA

182 Fakultät für Mathematik und Naturwissenschaften, Fachgruppe Physik, Bergische Universität Wuppertal, Wuppertal, Germany

183 Department of Physics, Yale University, New Haven, CT, USA

184 Yerevan Physics Institute, Yerevan, Armenia

[a] Also at Borough of Manhattan Community College, City University of New York, New York NY, USA

[b] Also at Centre for High Performance Computing, CSIR Campus, Rosebank, Cape Town, South Africa

[c] Also at CERN, Geneva, Switzerland

[d] Also at CPPM, Aix-Marseille Université, CNRS/IN2P3, Marseille, France

[e] Also at Département de Physique Nucléaire et Corpusculaire, Université de Genéve, Geneva, Switzerland

[f] Also at Departament de Fisica de la Universitat Autonoma de Barcelona, Barcelona, Spain

[g] Also at Departamento de Física, Instituto Superior Técnico, Universidade de Lisboa, Lisbon, Portugal

[h] Also at Department of Applied Physics and Astronomy, University of Sharjah, Sharjah, United Arab Emirates

[i] Also at Department of Financial and Management Engineering, University of the Aegean, Chios, Greece

[j] Also at Department of Physics and Astronomy, Michigan State University, East Lansing MI, USA

[k] Also at Department of Physics and Astronomy, University of Louisville, Louisville, KY, USA

[l] Also at Department of Physics and Astronomy, University of Sheffield, Sheffield, UK

[m] Also at Department of Physics, Ben Gurion University of the Negev, Beer Sheva, Israel

[n] Also at Department of Physics, California State University, East Bay, USA

[o] Also at Department of Physics, California State University, Fresno, USA

[p] Also at Department of Physics, California State University, Sacramento, USA

[q] Also at Department of Physics, King's College London, London, UK

[r] Also at Department of Physics, St. Petersburg State Polytechnical University, St. Petersburg, Russia

[s] Also at Department of Physics, Stanford University, Stanford CA, USA

[t] Also at Department of Physics, University of Adelaide, Adelaide, Australia

[u] Also at Department of Physics, University of Fribourg, Fribourg, Switzerland

[v] Also at Department of Physics, University of Michigan, Ann Arbor MI, USA

[w] Also at Faculty of Physics, M.V. Lomonosov Moscow State University, Moscow, Russia

[x] Also at Giresun University, Faculty of Engineering, Giresun, Turkey

[y] Also at Graduate School of Science, Osaka University, Osaka, Japan

[z] Also at Hellenic Open University, Patras, Greece

[aa] Also at Institucio Catalana de Recerca i Estudis Avancats, ICREA, Barcelona, Spain

[ab] Also at Institut für Experimentalphysik, Universität Hamburg, Hamburg, Germany

[ac] Also at Institute for Mathematics, Astrophysics and Particle Physics, Radboud University Nijmegen/Nikhef, Nijmegen, The Netherlands

[ad] Also at Institute for Nuclear Research and Nuclear Energy (INRNE) of the Bulgarian Academy of Sciences, Sofia, Bulgaria

[ae] Also at Institute for Particle and Nuclear Physics, Wigner Research Centre for Physics, Budapest, Hungary

[af] Also at Institute of High Energy Physics, Chinese Academy of Sciences, Beijing, China

[ag] Also at Institute of Particle Physics (IPP), Vancouver, Canada

[ah] Also at Institute of Physics, Academia Sinica, Taipei, Taiwan

[ai] Also at Institute of Physics, Azerbaijan Academy of Sciences, Baku, Azerbaijan

[aj] Also at Institute of Theoretical Physics, Ilia State University, Tbilisi, Georgia

[ak] Also at Instituto de Fisica Teorica, IFT-UAM/CSIC, Madrid, Spain

[al] Also at Istanbul University, Dept. of Physics, Istanbul, Turkey

[am] Also at Joint Institute for Nuclear Research, Dubna, Russia

[an] Also at LAL, Université Paris-Sud, CNRS/IN2P3, Université Paris-Saclay, Orsay, France

[ao] Also at Louisiana Tech University, Ruston LA, USA

[ap] Also at LPNHE, Sorbonne Université, Université de Paris, CNRS/IN2P3, Paris, France

[aq] Also at Manhattan College, New York NY, USA

[ar] Also at Moscow Institute of Physics and Technology State University, Dolgoprudny, Russia

[as] Also at National Research Nuclear University MEPhI, Moscow, Russia

[at] Also at Physics Department, An-Najah National University, Nablus, Palestine

[au] Also at Physics Dept, University of South Africa, Pretoria, South Africa

[av] Also at Physikalisches Institut, Albert-Ludwigs-Universität Freiburg, Freiburg, Germany

[aw] Also at School of Physics, Sun Yat-sen University, Guangzhou, China

[ax] Also at The City College of New York, New York NY, USA

[ay] Also at The Collaborative Innovation Center of Quantum Matter (CICQM), Beijing, China

[az] Also at Tomsk State University, Tomsk, and Moscow Institute of Physics and Technology State University, Dolgoprudny, Russia

[ba] Also at TRIUMF, Vancouver BC, Canada

[bb] Also at Universita di Napoli Parthenope, Naples, Italy

*Deceased